Durham E-Theses

Direct extraction of (_MS) from e(^+)e jet observables

Burby, Stephen J.

How to cite:

Burby, Stephen J. (2000) *Direct extraction of (_MS) from e(^+)e jet observables*, Durham theses, Durham University. Available at Durham E-Theses Online: http://etheses.dur.ac.uk/4348/

Use policy

The full-text may be used and/or reproduced, and given to third parties in any format or medium, without prior permission or charge, for personal research or study, educational, or not-for-profit purposes provided that:

- a full bibliographic reference is made to the original source
- a link is made to the metadata record in Durham E-Theses
- the full-text is not changed in any way

The full-text must not be sold in any format or medium without the formal permission of the copyright holders.

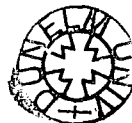Please consult the full Durham E-Theses policy for further details.

Direct Extraction of $\Lambda_{\overline{MS}}$ from e^+e^- Jet Observables

A thesis presented for the degree of
Doctor of Philosophy
by

Stephen J. Burby

Physics Department
University of Durham
September 2000

Abstract

We demonstrate a renormalisation group improved formulation of QCD perturbation theory. At next-to-leading order (NLO) and beyond this permits a direct extraction of the QCD dimensional transmutation parameter, $\Lambda_{\overline{MS}}$ that typifies the one parameter freedom of the theory in the limit of massless quarks. We apply this to a variety of experimental data on e^+e^- jet observables at NLO. We take into consideration data from PETRA, PEP, TRISTAN, SLC and LEP 1 and 2. In this procedure there is no need to mention, let alone to arbitrarily vary, the unphysical renormalization scale μ, and one avoids the spurious and meaningless "theoretical error" associated with standard α_s determinations. An attempt is made to estimate the importance of uncalculated next-to-NLO and higher order perturbative corrections, and power corrections, by studying the scatter in the values of $\Lambda_{\overline{MS}}$ obtained for different observables.

We also consider large infrared logarithm resummations in these jet observables and present results for the particular cases of the four-jet rate to a next-to-leading logarithm approximation and the distributions for the four-jet variables, "light hemisphere mass" and "narrow jet broadening" to a next-to-next-to-leading logarithm approximation in the perturbative expansion. We apply a simple power correction to these variables and obtain remarkably good fits to the data.

To Mum, Dad, Dawn and Shigeko.

Acknowledgements

First and foremost, I would like to thank Chris Maxwell for his supervision and all the help he has provided over my three years in Durham. Thanks for introducing me to the controversial world of renormalisation scale/scheme dependence and showing me the right way to go!

Secondly, special thanks must go to Nigel Glover for all of his help and advice in all matters physics-related. It takes a courageous person to have an office right in the heart of enemy (aka student) territory.

To all the staff and postgrads, past and present, for making such an interesting and friendly atmosphere. Never a dull moment. Well, maybe during summer! To my office-mates Pawel, Babis, Abolfazl, Ricardo and Thanos for putting up with me over the years. Babis, in particular for the in-depth physics discussions at all hours of the day and night.

To my various house-mates, Alejandra, Diego, Mike and Fil, thanks for providing a safe haven away from "the Department". I am grateful to Jeppe for managing to be a friend, house-mate, computer expert and fellow physicist.

There are numerous others I should rightfully thank, but as always I am running out of time and must stop somewhere. :)

So finally I would like to thank all of those who helped in any way during the "weeks" of writing up.

Declaration

I declare that I have previously submitted no material in this thesis for a degree at this or any other university.

The research presented in this thesis has been carried out in collaboration with E.W.N. Glover and C.J. Maxwell. Aspects of Chapters 2-4 are based on the following publications:

- S. J. Burby and C. J. Maxwell,

  'Direct Extraction of QCD $\Lambda_{\overline{MS}}$ from e^+e^- Jet Observables',

  In preparation.

- S. J. Burby,

  'The four-jet rate in e^+e^- annihilation'

  Phys. Lett. **B453** (1999) 54 [hep-ph/9902305]

- S. J. Burby and E. W, N. Glover,

  'Resumming the Light Hemisphere Mass and Narrow Jet Broadening distributions in e^+e^- annihilation',

  In preparation.

© The copyright of this thesis rests with the author.

Contents

Preface

Quantum Chromodynamics (QCD) is now well established as the theory of the strong interaction. It was formulated nearly three decades ago to describe the empirical properties of the parton constituents of hadrons. The pioneering experiments at the Stanford Linear Accelerator Center (SLAC) investigated the deeply inelastic electron-proton scattering. Here evidence was found for a scaling property proposed by Bjorken [1]. This scaling behaviour could be explained by the counterintuitive idea of partons becoming almost free at large momentum transfers. This *asymptotic freedom* at large energy was then a fundamental requirement for any theory proposing to describe the dynamics of the partons. The only successful candidate was the quantised non-Abelian gauge field theory, QCD. The fundamental matter fields (quarks) were then associated with the parton constituents of hadrons. Applying the gauge principle to QCD in a manner analogous to that of the theory of Quantum Electrodynamics (QED), eight *charged* gauge bosons (gluons) arise due to its non-Abelian nature. The gluons may then self-interact, providing a rich and complex structure. As with QED, it is necessary to renormalise the Lagrangian, but in this case, the addition of terms arising due to gluon self-interactions causes the running coupling to decrease with increasing energy. This is the crucial property of asymptotic freedom. A consequence of this is the opportunity to apply a perturbative expansion in the coupling, and obtain a reliable approximation at high enough energies. Unfortunately the very procedure of renormalisation, that introduces the scaling behaviour, gives rise to an unphysical parameter, μ, and an inherent ambiguity in the perturbative series order by order.

Furthermore, this perturbative expansion can only be considered for observable quantities away from the low-energy (long distance) regime. This forbids any attempts to probe the "infrared" physics where a complete description of QCD is required. We may tentatively describe quantities that draw a distinct line between

the two regimes as long as care is taken in approaching the boundary. Typically these will be subject to "large infrared logarithms" that enhance the coupling at all orders of perturbation theory and require resumming to regain control over the approximation.

In this thesis we shall consider both of these aspects of perturbative QCD within the framework of electron-positron (e^+e^-) annihilation.

Chapter 1

Introduction to QCD

1.1 Introduction

Quantum Chromodynamics (QCD) is the theory of the strong interaction. It is a quantised non-Abelian gauge field theory built upon the powerful gauge principle and renormalisability. It describes the dynamics of quarks, the constituents of hadrons, and gluons, the force mediators. When taken with the Electroweak (EW) theory of Glashow, Salam and Weinberg it comprises the SU(3) × SU(2) × U(1) Standard Model of elementary particles. There are many parallels between QCD and quantum electrodynamics (QED), the U(1) subgroup describing the interactions of electrically charged fermions with photons. In fact the Lagrangian of each theory is constructed following exactly the same principles. What separates them is the underlying gauge group. Where QED obeys an Abelian U(1) invariance, QCD abides by a non-Abelian SU(3) invariance. We shall see how this non-commutative algebra gives rise to eight colour charged gauge bosons that can self interact in contrast to the solitary neutral photon. The apparent artificial manner in which QCD is combined with EW theory enables us to treat QCD completely separately. The only complication arises in the mass terms of fermion fields. Formally these will break global gauge invariance of the Standard Model due to the left and right handed components having different gauge quantum numbers. This can be rectified through coupling to the Higgs field. In treating QCD separately we are justified in neglecting these subtleties and can insert a Dirac mass term [1]

We shall begin by giving a brief introduction to QCD, considering the La-

---

[1] Even this shall turn out to be surplus to our needs and typically we shall take the massless approximation.

1

grangian[2] and the origin of each of its terms and Feynman rules. After motivating the perturbative expansion we shall move on to the divergences that arise at each order. In particular we shall explore the ideas of renormalisation that will be the main focus of this thesis. For a detailed treatment of field theory and in particular QCD, see [2, 3, 4].

1.2 Overview of Quantum Chromodynamics

1.2.1 The Underlying Gauge Group, SU(3)

As stated in the previous section, QCD is a quantised gauge field theory based on the SU(3) group. It describes the interactions of spin $\frac{1}{2}$ fermion matter fields (quarks) with spin 1 gauge bosons (gluons) by ascribing the property of colour charge. Experimentally these quantum numbers were required to explain the spin statistics of various hadrons [5]. Furthermore there are six *flavours* of quark, namely up (u), down (d), charm (c), strange (s), top (t) and bottom (b) observed in nature. It suffices to say that within the context of QCD the only difference between them is their mass. We indicate approximately these masses in Table 1.1 quoted from [6]

Quark	Mass/GeV
u	~ 0.003
d	~ 0.006
s	~ 0.12
c	~ 1.5
b	~ 4.2
t	~ 175

Table 1.1: Quark masses

In QCD there are three different possible charges and for practical purposes these are chosen to take the values of the primary colours (red, green and blue). Each quark is then typically ascribed one of three colours.

A transformation in colour space is then given by

$$q_a \rightarrow q_a' = U_{ab}\, q_b, \qquad\qquad a, b = 1, 2, 3, \qquad\qquad (1.1)$$

---

[2]More precisely the Lagrangian density

where U_{ab} is a group element of SU(3) and the q_a represent Dirac spinors where we have suppressed the spinor indices for clarity. The label a runs over the colour degrees of freedom $1, 2, 3$ corresponding to red, green and blue. It is straightforward to extend the analysis to a general number of colours, N_c, by considering the group $SU(N_c)$. The generators of the Lie algebra, T^A satisfy the commutation relation

$$\left[T^A, T^B\right] = if^{ABC}T^C, \qquad\qquad A, B, C = 1, 2, \ldots, N_c^2 - 1, \qquad (1.2)$$

which define f^{ABC}, the structure constants characterising the algebra. The labels, A, B, C go from $1, \ldots, n$, n being the dimension of the Lie algebra (in this case $n = 8$). We can then perform a general unitary local gauge transformation via

$$U = \exp\left(-iT^A\theta^A(x)\right), \qquad\qquad (1.3)$$

where $\theta^A(x)$ is a coordinate dependent parameter. The *local* gauge principle demands that the theory is invariant under the gauge transformation of Equation (1.3). In particular when composing the dynamic terms of the matter and gauge fields, local gauge invariance must be satisfied.

1.2.2   The QCD Lagrangian

Building upon gauge invariance and utilising Lorentz invariance we obtain the QCD Lagrangian which we may break down as follows,

$$\mathcal{L}_{\text{QCD}} = \mathcal{L}_{\text{quark}} + \mathcal{L}_{\text{gluon}} + \mathcal{L}_{\text{gauge-fixing}} + \mathcal{L}_{\text{ghost}}. \qquad (1.4)$$

Creating a dynamic quark term that satisfies gauge invariance we obtain

$$\mathcal{L}_{\text{quark}} = \sum_{f=1}^{N_f} \left(\overline{q}_a(i\gamma_\mu D^\mu - m)_{ab}\, q_b\right)_f. \qquad (1.5)$$

with N_f copies corresponding to each quark flavour. The gamma matrices are defined in the usual way and satisfy the Clifford algebra ($\{\gamma^\mu, \gamma^\nu\} = 2g^{\mu\nu}$). To preserve gauge invariance we are required to define a covariant derivative D_μ in exactly the same way as QED,

$$D_\mu = \partial_\mu + igT^A\mathcal{A}_\mu^A, \qquad\qquad (1.6)$$

which can be written in component form as

$$(D_\mu)_{ab} = \partial_\mu \delta_{ab} + ig \, T^A_{ab} \, \mathcal{A}^A_\mu. \tag{1.7}$$

In doing so we have necessarily introduced *eight* gauge fields, $\mathcal{A}^A_\mu$ that correspond to the gluons. Since the quarks *live* in the fundamental representation, we have additionally introduced the corresponding generators, T^A_{ab}.

Analogous to QED the dynamics of the gauge bosons are incorporated through the gauge field strength term,

$$\mathcal{L}_{\text{gluon}} = -\frac{1}{4} F^{\mu\nu}_A F^A_{\mu\nu}, \tag{1.8}$$

where

$$F^A_{\mu\nu} = \partial_\mu \mathcal{A}^A_\nu - \partial_\nu \mathcal{A}^A_\mu - g f^{ABC} \mathcal{A}^B_\mu \mathcal{A}^C_\nu. \tag{1.9}$$

A crucial aspect of non-Abelian gauge theories is the presence of the last term in Equation (1.9) that will give rise to gluon self interactions. Later we shall see how as a consequence of this, we obtain the desirable property of asymptotic freedom. We also note that from gauge invariance requirements the coupling strength is universal, i.e. there is only one coupling (g) needed to describe all QCD interactions. This would now seem to be adequate to describe the strong interaction but as with QED we are forced to include a gauge fixing term. This is needed to eliminate two unphysical degrees of freedom of the gauge boson. In imposing gauge invariance the gluon fields attain the full freedom of the gauge transformation, thereby needing additional constraints to be placed upon it before the free gluon Green's function can be inverted to give the propagator,

$$\mathcal{L}_{\text{gauge-fixing}} = -\frac{1}{2\xi} (\partial^\mu \mathcal{A}^A_\mu)^2. \tag{1.10}$$

This form of gauge fixing defines a *covariant* gauge. It has the benefit of preserving Lorentz invariance at the expense of needing unphysical *ghost* fields. This is most easily seen within the Fadeev-Popov quantisation of gauge fields by application of the path integral formalism. In composing the generating functional for the gluon field we are required to fix the gauge and in doing so introduce a change in the invariant measure. According to the exact choice of gauge fixing method this can introduce a term that looks like the gluon field (spin 1) but anti-commutes. This

then restores gauge invariance and unitarity at every order of the coupling by clearly unphysical fields. ξ represents the gauge parameter which can be defined arbitrarily since all physical quantities must not depend upon it. Two popular choices are the Feynman gauge ($\xi = 1$) and Landau gauge ($\xi = 0$). It is also possible to perform axial gauge fixing whereby rather than specifying the derivative of the gluon field, the product with an arbitrary four vector is taken. As such it manifestly breaks Lorentz invariance but has the benefit of being able to quantise the gluon field without the need for ghosts. This class of *physical gauges* are particularly useful for resummation calculations enabling a direct interpretation of parton probabilities [7]. Since we choose to work in a covariant gauge we must include the ghost term,

$$\mathcal{L}_{\text{ghost}} = \overline{\eta}^A(-\partial^\mu D_\mu^{AB})\eta^B. \tag{1.11}$$

where the η^A are the ghost fields and the covariant derivative now includes the representation of T^A in the adjoint representation, $(T^A)^{BC} = -if^{ABC}$.

Throughout perturbative QCD calculations, the generators, T_A appear in various combinations. We will find it beneficial to define the group invariants or Casimirs, T_F, C_F and C_A. We begin by normalising the trace

$$\text{tr}(T^A T^B) = T_F \delta^{AB} \tag{1.12}$$

where T_F is commonly taken to be $1/2$. This then gives for the fundamental representation

$$C_F N_c \equiv \text{tr}\left(\sum_{A=1}^{N_c^2-1} T^A T^A\right) \quad \Rightarrow \quad C_F = \frac{N_c^2 - 1}{2N_c} \tag{1.13}$$

and for the adjoint representation

$$C_A \delta^{CD} \equiv f^{ABC} f^{ABD} \quad \Rightarrow \quad C_A = N_c \tag{1.14}$$

1.2.3 The Feynman Rules

With the Lagrangian defined we can calculate the Green's functions of QCD and hence obtain the Feynman rules. We begin by separating the Lagrangian into a free term from field bilinears and an interaction term from the rest. The free term is exactly solvable giving the propagators of the theory. Working in momentum space

(i.e. $\partial_\alpha = -ip_\alpha$) we can consider the one particle irreducible (1PI) Green's function, $\Gamma^{(n_A, n_F)}(p)$ where $n_A(n_F)$ is the number of external gluons(quarks). We find for the leading term to the quark 2-point function,

$$\Gamma^{(0,2)}_{ab}(p) = -i\delta_{ab}(\slashed{p} - m),\qquad (1.15)$$

where the slash notation denotes contraction of a four vector with a gamma matrix, $\slashed{p} = \gamma_\mu p^\mu$. Inverting this we obtain the free quark propagator $\Delta^{ab}(p)$,

$$\Delta^{ab}(p) = \frac{i}{\slashed{p} - m + i\epsilon}\,\delta^{ab},\qquad (1.16)$$

Here we have used the $i\epsilon$ prescription to ensure causality. It enforces the correct time ordering of fields in integrals over p^0.

Similarly we can obtain the gluon and ghost propagators by inverting the corresponding 2-point functions. The interactions are obtained by expanding the interaction term perturbatively in the coupling. This will be permissible *on condition that* the coupling is a reasonably small number. We can now extend this to the analysis of a particular transition amplitude by breaking it down into a combination of freely propagating particles, interaction vertices and external legs. In this way we can generate a perturbative expansion of the transition matrix element for any given process bearing in mind the time ordering of fields, etc. [2]. Fortunately there exists a shorthand manner to incorporate all necessary conditions via the application of *Feynman diagrams* and *rules*. These are given below.

1. Draw all topologically distinct diagrams corresponding to the required initial and final state to a given order of the coupling.

2. Assign a factor to each vertex, propagator and external leg as given in Tables 1.2 and 1.3

3. Write down the factors in order of the flow of colour charge.

4. Multiply by -1 for every fermion or ghost loop.

5. Multiply by -1 for every anti-fermion connected from initial through final state

6. Ensure momentum is conserved at every vertex

7. Integrate over all loop momenta with a measure of $\int d^4\ell/(2\pi)^4$

8. Multiply by a factor of $1/n!$ for a loop of n identical gluons

The external fermion legs (straight lines) are given by Dirac spinors $(u(p), \overline{u}(p), v(p), \overline{v}(p))$ and external gluons (springy lines) by their polarisation vectors $(\epsilon^{\mu(*)})$. Ghosts are represented by the dashed lines. In most cases we can take the simplification of zero quark masses. This is permissible away from quark mass thresholds by the decoupling theorem [8]. We therefore only need be concerned with the number of active flavours at a given scale.
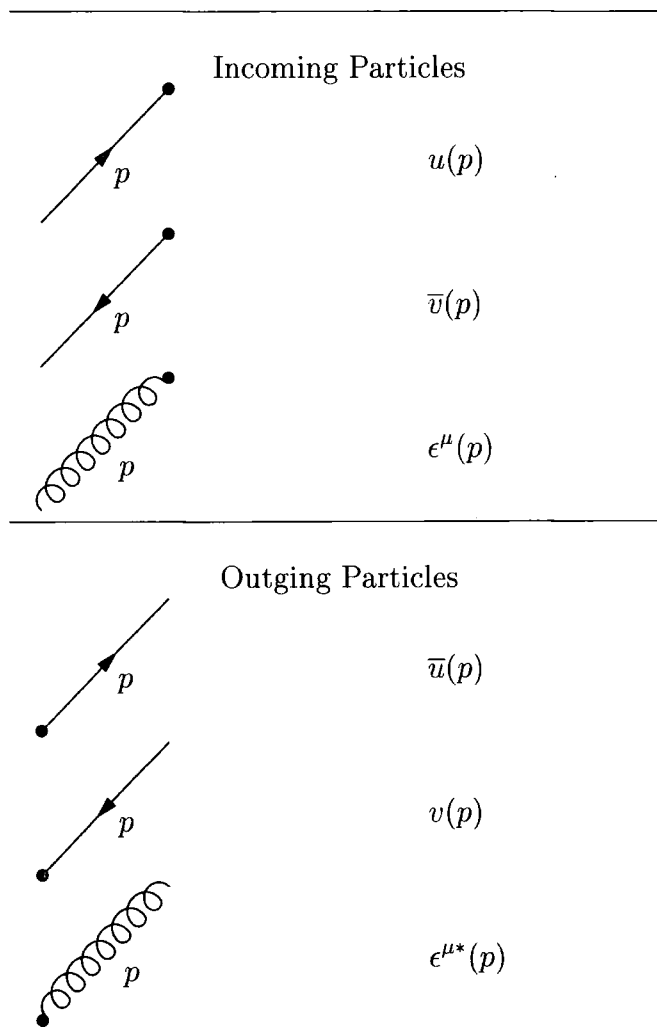
Table 1.2: The QCD Feynman rules in momentum space for incoming and outgoing particles. All particles are assumed to have momentum p going from left to right and color charge flows in the direction of the arrow.

Propagators

$i \xrightarrow{\quad p \quad} j$ $\qquad\qquad \dfrac{i(\not{p}+m)}{p^2 - m^2 + i\epsilon}\delta^{ab}$

$A,\mu\, \text{〰〰〰}\, B,\nu$ $\qquad \dfrac{i}{p^2+i\epsilon}\left(-g^{\mu\nu}+(1-\xi)\dfrac{p^\mu p^\nu}{p^2+i\epsilon}\right)\delta^{AB}$

$A \cdots\blacktriangleright\cdots B$ $\qquad\qquad \dfrac{i}{p^2+i\epsilon}\delta^{AB}$

Vertex Factors

$-ig\gamma^\mu T_{ij}^A$

$-gf^{ABC}\;\;[(p_1-p_2)^\rho g^{\mu\nu}$
$+(p_2-p_3)^\mu g^{\nu\rho}$
$+ (p_3-p_1)^\nu g^{\rho\mu}]$

$(\text{where}\quad p_1+p_2+p_3=0)$

$gf^{ABC}p^\mu$

$-ig^2\;\;[f^{ACE}f^{BDE}[g^{\mu\nu}g^{\rho\sigma}-g^{\mu\sigma}g^{\nu\rho}]$
$+f^{ADE}f^{BCE}[g^{\mu\nu}g^{\rho\sigma}-g^{\mu\rho}g^{\nu\sigma}]$
$+ f^{ABE}f^{CDE}[g^{\mu\rho}g^{\nu\sigma}-g^{\mu\sigma}g^{\nu\rho}]]$

Table 1.3: The propagator and vertex factors for Feynman rules in momentum space. All particles are assumed to have momentum p and the flow of charge is indicated by the arrow

1.3   Renormalisation

In this section we shall address the problems of divergences in the theory. There are two distinct kinds that arise when performing a calculation within perturbative QCD, namely the infrared (IR) and ultraviolet (UV) divergences. We will be particularly interested in the latter which necessitate the procedure of *renormalisation* and give rise to some of the problems this thesis attempts to address. We shall commence though with a consideration of IR divergences.

1.3.1   Infrared Divergences

This form of divergence arises in the presence of massless gauge fields. It enters into perturbative QCD calculations when a radiated gluon becomes either soft or collinear with the emitting parton. Furthermore, when taking the massless approximation for quarks we must consider additional collinear singularities from a gluon splitting into a $q\bar{q}$ pair. Perturbative treatment fails to describe this low energy behaviour. Cancellations of this divergence from real gluon emission occur at every order of perturbation theory for inclusive quantities by incorporating virtual gluon corrections. This is because in the infrared limit these states are indistinguishable. The infrared divergences are therefore intimately linked with the integration of the matrix elements over the phase space. The theorem of Kinoshita, Lee and Nauenberg [9], ensures that these IR divergences cancel out in the physical cross sections if the degeneracy of the states is introduced. This safeguards fully inclusive observables, but semi-inclusive and exclusive observables have a restricted phase space. As such it is of paramount importance to ensure that the quantity is *infrared safe*. i.e. it is unchanged by the inclusion of an extra parton in the limit that it becomes soft and/or collinear. This can be formulated for an observable, λ that depends on an arbitrary number of external particles with three-momentum, $\mathbf{p}$ as

$$\lambda(\dots,\mathbf{p_i},\dots) \underset{\text{IR limit}}{=} \lambda(\dots,\mathbf{p_j}+\mathbf{p_k},\dots) \qquad (1.17)$$

where a particle with momentum $\mathbf{p_i}$ has branched into two with momenta $\mathbf{p_j}$ and $\mathbf{p_k}$. The IR limit is when one or both of the collinear condition ($\mathbf{p_j} \parallel \mathbf{p_k}$) and soft condition ($|\mathbf{p_j}|, |\mathbf{p_k}| \to \mathbf{0}$) holds. Clearly this requires the definition of the observable to be linear in the three-momentum. In restricting the phase space, we
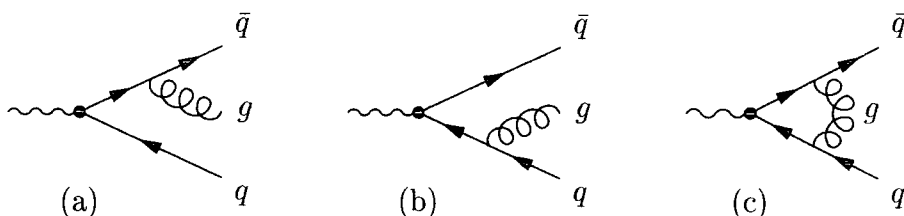
Figure 1.1: (a) and (b) represent IR divergent contributions to the LO total cross section from real gluon emission and (c) represents the IR diverent conrtibution to the LO total cross section from a virtual gluon

become sensitive to the cancellation of the IR divergences. This manifests itself as logarithms of the cut in phase space. We shall see later how this gives rise to the problem of large kinematic logarithms in perturbation theory which requires the use of resummation techniques to be overcome.

A simple illustration of the cancellation of IR divergences is that occurring in $e^+e^- \rightarrow$ hadrons at order α_s. The diagrams with IR divergences are given in Figure 1.1. In order to cancel the IR divergences we must integrate each separate matrix element over the correct phase space. We find that the $q\bar{q}g$ partons' matrix element becomes singular as the emitted gluon becomes soft, and then additionally as it becomes collinear with the direction of the quark emitter. These singular terms exactly cancel with the divergence that arises when integrating over the loop momentum in the virtual contribution in Figure 1.1(c). Therefore when taking the sum of

$$\sigma_{hadrons} = \sigma_0 \left(\int d\Omega_2 |\mathcal{M}_{q\bar{q}}|^2 + \int d\Omega_3 |\mathcal{M}_{q\bar{q}g}|^2 \right), \tag{1.18}$$

the result is finite. To actually perform the calculation we need to regulate the singularity in a precise manner. There are a number of different regularisation procedures, each with their own benefits. Before considering them we shall explore the UV divergences.

1.3.2 Ultraviolet Divergences

Ultraviolet divergences go straight to the heart of the theory and therefore can threaten its very existence. Treating these divergences requires the procedure of renormalisation without which a theory is of limited use. Proof of the renormalisability of gauge theories [10] has enabled physical calculations to be performed in perturbation theory. Problems first arise at the one loop level when the loop momenta is taken to infinity. Unlike with the infrared case there are no cancellations of
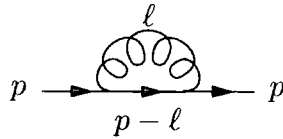
Figure 1.2: The quark self energy part, $\Sigma(p)$

these divergences. The crucial step is in realising that these divergences correspond exactly to shifts in the parameters of the action and hence Lagrangian. Realising that these parameters are not physical we trade their finiteness for that of the one loop contribution by shifting them by the amount needed to remove the UV divergence. This procedure can be repeated for all orders in perturbation theory. It is best illustrated with an example. We consider the most simple diagram containing an UV divergence, the quark self energy part obtained from the amputated 2-point quark Green's function by the relation $\Gamma_{ab}^{(0,2)}(p) = -i\delta_{ab}(\not{p} - m + i\not{p}\Sigma(p))$

Using the Feynman rules and taking the massless quark limit we find

$$\Sigma(p) = 2g^2 C_F \int \frac{d^4 l}{(2\pi)^4} \frac{1}{(p+\ell)^2 \ell^2}. \tag{1.19}$$

For large momentum this can be rewritten as

$$\int \frac{d^4 l}{(2\pi)^4} \frac{1}{(p+\ell)^2 \ell^2} \underset{|\ell|\to\infty}{=} \int d\Omega \int d\ell \frac{\ell^3}{\ell^4}. \tag{1.20}$$

This is clearly logarithmically divergent but to know by how much to shift the Lagrangian parameters requires, once again, a procedure for regularisation.

1.3.3 Regularisation

The aim of regularisation is to control the divergence of integrals in a mathematically precise manner such that the nature of the singularity is parameterised. There are numerous ways of regularising the divergence. Each one has its own merits but must somehow break a symmetry of the Lagrangian.

The simplest method (*cut off*) is to impose a large momentum cutoff by hand. This contravenes both translational and gauge invariance, rendering it useless for gauge theories.

A more sophisticated method is that of *Pauli Villars*. Here a fictitious mass is introduced to alter the propagator by $\frac{1}{m^2 - k^2} \to \frac{1}{m^2 - k^2} - \frac{1}{M^2 - k^2}$, isolating the

divergence as $M \to \infty$. This respects Lorentz and translational invariance and to a certain degree gauge invariance, only breaking down in massive Yang Mills theories.

It is also possible to regulate the integrals by discretising space-time and placing it on a lattice. Now divergences are controlled by the lattice spacing which corresponds to a momentum cut off. This breaks Lorentz and translational invariance although it is the only method to permit a non-perturbative treatment.

Lastly we shall consider *dimensional regularisation*. This has the desirable properties of maintaining Lorentz and gauge invariance in addition to regulating the IR divergences mentioned earlier. It treats the number of dimensions as a parameter ($D = 4 - 2\epsilon$) and thus enables the integral to become finite by reducing the number, i.e. $\epsilon > 0$. Then by analytical continuation back to 4 dimensions, all divergences are isolated by the parameter ϵ. Based on these properties we shall consider this method.

A subtlety occurs when we consider the dimensionality of the Lagrangian. In order to keep the correct dimension of the fields and a dimensionless coupling, we are forced to put a massive constant, μ, in by hand giving,

$$g^2 \frac{\mathrm{d}^4 k}{(2\pi)^4} \to g^2 \mu^{2\epsilon} \frac{\mathrm{d}^{4-2\epsilon} k}{(2\pi)^{4-2\epsilon}}, \qquad (1.21)$$

in order to maintain a dimensionless coupling, g.

Going back to the example of the quark self energy part we obtain,

$$\Sigma(p) = -\frac{g^2}{(4\pi)^2} C_F \left(\frac{1}{\epsilon} - \gamma_E + \ln(4\pi) + 1 - \ln\left(\frac{-p^2}{\mu^2} \right) + \mathcal{O}(\epsilon) \right), \qquad (1.22)$$

where $\gamma_E = 0.57721\ldots$ is the Euler-Mascheroni constant. The divergence is now parameterised as a pole in ϵ and we must investigate ways of eliminating it.

1.3.4   Renormalisation

We stated earlier that one loop divergences are essentially equivalent to a shift in the Lagrangian parameters. Therefore to renormalise the theory we can introduce counterterms in the Lagrangian that generate contributions of equal divergence but opposite sign. This is performed by a redefinition of the fields

$$q_B = Z_2^{1/2} q, \quad \mathcal{A}_B^\mu = Z_3^{1/2} \mathcal{A}^\mu, \quad \eta_B = \tilde{Z}_3^{1/2} \eta, \qquad (1.23)$$

and parameters

$$g_B = Z_g \, \mu^\epsilon \, g, \quad \xi_B = Z_3 \, \xi, \quad m_B = Z_m m, \qquad (1.24)$$

within the Lagrangian. The $Z_2, Z_3, \tilde{Z}_3, Z_g$ and Z_m[3] multiply the *physical* fields and parameters to give the *bare* quantities (subscript B) found in the Lagrangian. The divergences will then be isolated through the Z renormalisation constants. We note that a theory is termed renormalisable if all UV divergences can be removed by the introduction of a finite number of renormalisation constants. By substituting for bare terms in the Lagrangian we can generate the appropriate counterterms. For example the quark term becomes

$$
\begin{aligned}
\bar{q}_B \left(i\gamma^\mu \partial_\mu + i g \gamma^\mu T^A \mathcal{A}^A_{\mu B} \right) q_B &= \bar{q}(i\slashed{p})q \qquad\qquad (1.25)\\
&+ (Z_2 - 1)\,\bar{q}\,(i\slashed{\partial})\,q \\
&+ (\mu^\epsilon Z_g Z_2 Z_3^{1/2} - 1)\,g\,\bar{q}\,T^A \gamma^\mu \mathcal{A}^A_\mu\,q.
\end{aligned}
$$

The first term is exactly the same as in the unrenormalised Lagrangian but now we see two extra *counterterms* arising. Proceeding in a similar manner all propagators and interaction vertices will acquire similar terms.

Returning to the quark self energy part, we can see that the relevant counterterm is $(Z_2 - 1)\,\bar{q}\,(i\slashed{\partial})\,q$, resulting in $\Sigma(p) = \Sigma(p)_B + (Z_2 - 1)$.

We are now free to subtract off the divergence in the bare self energy with Z_2. Exactly how much to subtract off is not dictated, merely that the divergence is removed. We are at liberty to choose the finite part as we wish. In addition, the parameter μ, required to give the correct dimensionality, is also completely arbitrary. A prescription for how much of the finite part is to be removed in addition to a choice for μ is termed the renormalisation scheme (RS). We shall explore the problems associated with this in the next chapter,

1.3.5   The Renormalisation Group Equation

It is clear that the multiplicative renormalisation procedure above can be applied directly to any amputated 1PI Green's function such as the quark self energy part,

---

[3]For the sake of conformity, we have adopted the usual conventions for labelling the Z's

$\Sigma(p)$. In doing so we obtain a renormalised version that will in general depend on a particular value of μ and the chosen finite subtraction. Since we are free to choose these values we can obtain an answer using two different schemes (unbarred and barred),

$$\Sigma(p) = Z_\Sigma \, \Sigma(p)_B, \quad \overline{\Sigma}(p) = Z_{\overline{\Sigma}} \, \Sigma(p)_B. \tag{1.26}$$

As the renormalisation constants will contain exactly the same divergences we can relate $\Sigma(p)$ to $\overline{\Sigma}(p)$ by a *finite* renormalisation,

$$\Sigma(p) = z \, \overline{\Sigma}(p). \tag{1.27}$$

Here z is finite in the limit $\epsilon \to 0$. This constitutes what is known as the *renormalisation group*. The strength of this extends beyond perturbation theory, holding as an exact property of the theory. This can be expressed analytically in terms of the *renormalisation group equation* (RGE), utilising the independence of the bare 1PI Green's function on the choice of renormalisation scheme,

$$\mu \frac{\mathrm{d}\Gamma_B^{(n_A, n_F)}}{\mathrm{d}\mu} = 0. \tag{1.28}$$

Yet again ignoring quark masses and working in the Feynman gauge we obtain,

$$\Gamma_B^{(n_A, n_F)}(k_i, p_j, \xi, \mathrm{g}) = (Z_3)^{-n_A/2} \, (Z_2)^{-n_F/2} \, \Gamma^{(n_A, n_F)}(k_i, p_j, \xi(\mu), \mathrm{g}(\mu), \mu), \tag{1.29}$$

for n_A gluons with momenta k_i and n_F quarks with momenta p_j. Differentiating with respect to μ we get

$$\left(\mu \frac{\partial}{\partial \mu} + \beta(\mathrm{g}) \frac{\partial}{\partial \mathrm{g}} - n_A \gamma_A(\mathrm{g}) - n_F \gamma_F(\mathrm{g}) + \delta(\mathrm{g}) \frac{\partial}{\partial \xi} \right) \Gamma^{(n_A, n_F)}(k_i, p_j, \xi(\mu), \mathrm{g}(\mu), \mu) = 0, \tag{1.30}$$

where

$$\beta(\mathrm{g}) = \mu \frac{\partial \mathrm{g}}{\partial \mu} \bigg|_{\mathrm{g}, \xi}, \quad \gamma_A(\mathrm{g}) = -\frac{\mu}{2Z_3} \frac{\partial Z_3}{\partial \mu} \bigg|_{\mathrm{g}, \xi}, \quad \gamma_F(\mathrm{g}) = -\frac{\mu}{2Z_2} \frac{\partial Z_2}{\partial \mu} \bigg|_{\mathrm{g}, \xi}, \quad \delta(\mathrm{g}) = \mu \frac{\partial \xi}{\partial \mu} \bigg|_{\mathrm{g}, \xi}. \tag{1.31}$$

Now we shall see a very important property due to the renormalisation group, namely that of a running coupling in Green's functions. For simplicity we consider

a dimensionless Green's function with no external legs, $G(p_i, g(\mu), \mu)$, and suppress the dependence on the gauge parameter. Equation (1.30) then gives

$$\left(\mu \frac{\partial}{\partial \mu} + \beta(\mathrm{g}) \frac{\partial}{\partial \mathrm{g}} \right) G(e^t p_i, \mathrm{g}(\mu), \mu) = 0, \tag{1.32}$$

where we have introduced a dimensionless scaling parameter t. Since G is dimensionless we may write

$$G(p_i e^t, g(\mu), \mu) = \mathcal{F} \left(\frac{p_i \cdot p_j}{\mu^2} e^{2t}, g(\mu) \right), \tag{1.33}$$

$$G(p_i, g(\mu e^{-t}), \mu e^{-t}) = \mathcal{F} \left(\frac{p_i \cdot p_j}{\mu^2} e^{2t}, g(\mu) \right). \tag{1.34}$$

Changing variable $\lambda = \mu e^{-t}$ and utilising the equality of Equations (1.33) and (1.34) we can write

$$\frac{\mathrm{d}}{\mathrm{d}t} G(p_i e^t, g(\mu), \mu) = \left(\lambda \frac{\partial}{\partial \lambda} + \mu \frac{\partial}{\partial \mu} \right) G(p_i e^t, g(\mu), \mu) = 0. \tag{1.35}$$

Combining with Equation (1.32) to eliminate the $\partial / \partial \mu$ term we arrive at

$$\left(-\lambda \frac{\partial}{\partial \lambda} + \beta(\mathrm{g}) \frac{\partial}{\partial \mathrm{g}} \right) G(p_i e^t, g(\mu), \mu) = 0. \tag{1.36}$$

This is an homogeneous partial differential equation of order one and may be solved by introducing the *running coupling constant* $\bar{\mathrm{g}}(\lambda)$ defined at a renormalisation scale λ,

$$\lambda \frac{\partial \bar{\mathrm{g}}}{\partial \lambda} = \beta(\bar{\mathrm{g}}(\lambda)), \quad \bar{\mathrm{g}}(\lambda = 0) = \mathrm{g}. \tag{1.37}$$

This result holds true when we go to a dimensionful Green's function and demonstrates that the dependence of the coupling on μ can be freely interchanged with the energy scale λ. In this way a dimensionless observable inherits all of its energy dependence from the coupling through the RGE. We shall discuss this in more detail in Chapter 2.

1.3.6 The Running Coupling, β-Function Equation and Asymptotic Freedom

We have just seen how the coupling constant is really a running parameter dependent on the energy as dictated by the QCD β-function . In practical calculations it has become usual to define the strong coupling constant

$$\alpha_s = \frac{\mathrm{g}^2}{4\pi}, \tag{1.38}$$

and as a result we obtain a slightly altered β-function

$$\mu^2 \frac{\partial \alpha_s(\mu^2)}{\partial \mu^2} = \beta(\alpha_s) = -\beta_0\,\alpha_s^2 - \beta_1\,\alpha_s^3 - \beta_2\,\alpha_s^4 + \dots, \qquad (1.39)$$

where

$$\beta_0 = \frac{11C_A - 2N_f}{12\pi}, \quad \beta_1 = \frac{17C_A{}^2 - 5C_A N_f - 3C_F N_f}{24\pi^2}, \dots. \qquad (1.40)$$

In fact there are numerous conventions in defining the β-function of QCD with coefficients differing by factors of 2 and π depending on whether the coupling is differentiated with respect to μ^2 or μ or whether to include factors of π with the coupling. Regardless of these, the most important aspect of this is the sign of the leading term. For QCD, we see that providing $N_f \leq 16$ the coupling will *decrease* with increasing energy. This is the much desired property of asymptotic freedom and turns out to be a feature of all non-Abelian gauge theories. Furthermore the first two coefficients of the β-function given in Equation (1.40) are universal regardless of the choice of renormalisation scheme. In contrast all higher β-function coefficients are scheme dependent and we note in passing that the next two have been calculated to the $\overline{\text{MS}}$ scheme (see Section 2.2.1).

Since we will be dealing with the β-function extensively, we shall use a definition of Stevenson [11] that simplifies the analysis. Noting that α_s always appears with a factor of π we define the *couplant*, $a(\mu) = \alpha_s(\mu)/\pi$ with corresponding β-function

$$\mu \frac{\partial a(\mu)}{\partial \mu} = -ba^2(1 + ca + c_2\,a^2 + c_3\,a^3 + \dots), \qquad (1.41)$$

where now

$$b = 2\pi\beta_0 = \frac{11C_A - 2N_f}{6}, \quad c = \frac{\pi\beta_1}{\beta_0}, \dots. \qquad (1.42)$$

Truncating to one-loop order and integrating up we obtain,

$$-b \int_{Q_0}^{Q_1} \frac{d\mu}{\mu} = \int_{a(Q_0)}^{a(Q_1)} \frac{da}{a^2} \qquad (1.43)$$

which can be separated as

$$\frac{1}{a(Q_0)} - b \ln Q_0 = \frac{1}{a(Q_1)} - b \ln Q_1 \equiv -b \ln \Lambda, \qquad (1.44)$$

to define a universal massive constant, Λ. It can be naïvely interpreted as the scale at which the renormalised coupling becomes infinite *when extrapolated beyond its domain of applicability*. We shall give a more sophisticated discussion of Λ in the next chapter.

1.4 Experimental Tests of QCD

To ascertain whether QCD really does describe the strong interaction we must look to its theoretical predictions and attempt to test the extent to which it describes observed phenomena. Since we are not able to give an exact solution to QCD, we are forced into looking at the high energy regime where we have just seen the renormalised coupling constant decreases in magnitude and we are able to apply perturbation theory. At first sight we still encounter the problem of hadronisation affecting any result. We know empirically that the complete spectrum of observed hadrons are colour-singlet (colourless) combinations of quarks. The most simple solution to this is to calculate completely inclusive observables such as the total cross section for $e^+e^- \to$ hadrons that proceeds through the basic mechanism of $e^+e^- \to \gamma^*, Z^* \to q\bar{q}$ with the final state quarks turning into hadrons with unit probability. Typically instead of the cross section, the $R_{e^+e^-}$ ratio is used where

$$R_{e^+e^-}(Q) \equiv \frac{\sigma(e^+e^- \to \text{hadrons})}{\sigma(e^+e^- \to \mu^+\mu^-)} = \left(\sum_{f=1}^{N_f} Q_f^2 \right) N_c \left(1 + \sum_{n \geq 1} K_n \left(\frac{\alpha_s(Q)}{\pi} \right)^n \right)$$

(1.45)

These fully inclusive variables are unaffected by hadronisation because the probability of going from a partonic state to hadrons is unity.

There are numerous other interactions one could study but probably the most clean is that of electron-positron annihilation. In this process the initial state is completely free of strong interactions and can be factorised out as in the R ratio. This leaves us free to treat the QCD corrections to the final state in isolation. As a result there have been a number of collider experiments taking advantage of this process (see Section 1.4.1).

The next level of calculational sophistication requires a less inclusive quantity. We would like, for example, a measure of the angular distribution of the final state particles regardless of the actual hadronic state. Considering a perturbative expansion we see that to a leading approximation all events will be back-to-back from the emission of a quark-antiquark pair. This is verified by experiment. Furthermore, including the first QCD radiative correction we are able to emit a *hard* gluon which can take away a significant fraction of the momentum thus giving a well separated three parton event. There is of course no guarantee that the subsequent emission of

partons will not diffuse this effect during the process of hadronisation. Fortunately the hypothesis of local parton-hadron duality comes to the rescue (see for example [12]). This proposes that not only is hadronisation a local effect but furthermore the deviation of the momentum flow and quantum numbers is not significant enough to destroy the underlying characteristics of the hard partons. This is remarkably verified by experiment where exactly the *jet* structure predicted by perturbation theory is witnessed. How exactly to quantify a jet remains debatable provided its definition is infrared safe. We will explore the different jet definitions in Chapter 3.

With a specific choice of jet definition it is then possible to calculate the n-jet fraction,

$$R_n = \frac{\sigma(e^+e^- \to n \text{ jets})}{\sigma(e^+e^- \to \text{hadrons})} \tag{1.46}$$

where R_n begins of order α_s^{n-2} ($n \geq 2$). Providing a jet algorithm that does not induce correlations between the *hadronic jets*[4] is chosen, the n-jet rate can be calculated completely within the framework of perturbative QCD.

There are two further classes of less inclusive quantities that are typically studied. Firstly there are the *event shapes* that describe the hadronic structure of an event by defining measures to reflect certain qualities. Common examples of these describe the broadness and mass of the final state jets. Secondly there are the energy correlations between pairs of particles/jets. As with the jet rates, these observables must satisfy some important properties. Of primary importance is the requirement of infrared safety. Without this, its distribution would not be calculable in perturbation theory. Furthermore we would like to keep hadronisation effects to a minimum by not inducing spurious correlations. Ultimately it goes without saying that it must be experimentally determinable. Under these circumstances, these quantities too can be calculated within the context of perturbative QCD and have been used extensively in determination of the strong coupling constant. These quantities will be examined in greater detail in Chapter 3.

---

[4]By hadronic jets we mean jets defined such that the hadronisation effects are localised within. Unfortunately without an exact treatment of hadronisation we can only attempt to minimise this empirically

1.4.1 e^+e^- Annihilation Experiments

Since the inception of QCD, there have been numerous experiments putting it to the test. Of these, e^+e^- colliders have proved popular, providing a clean environment within which to extract the single free parameter of massless QCD. Starting from 1982, the PETRA e^+e^- collider at DESY was the first to measure the jet fractions with centre-of-mass energies ranging from $\sqrt{s} = 12$ to 46.6 GeV, closely followed by the PEP collider (29 GeV) at SLAC and the TRISTAN collider at KEK (up to 70 GeV). It was not until the end of the decade that the two dominating e^+e^- accelerators of their generation came online. The LEP experiment at CERN (1989) and the SLC at SLAC (1991) began taking data at a centre-of-mass energy of 91 GeV equal to the mass of the Z_0 boson. Together, they have provided a vast number of events orders of magnitude in excess of any other energy scale. This has provided the ideal test bed for precision measurements in QCD and has given rise to the popularity of quoting $\alpha_s(M_Z)$ as the free parameter of the theory. The LEP experiment has since been superceded by LEPII that came online in 1995 operating at centre-of-mass energies from just above the Z^0 mass to 200 GeV. Unfortunately the event statistics are far less at these energies.

1.5 Summary

In this chapter we have introduced some of the key aspects behind perturbative QCD. After examining the Lagrangian and its subsequent Feynman rules, we broached the subject of renormalisation that underlies the theme of this thesis. The necessity to renormalise the QCD Lagrangian introduced the concept of an asymptotically free, running coupling "constant", α_s. This provided the ingredient so crucial to any theory attempting to describe the observed scaling behaviour in deeply inelastic electron-hadron scattering. We then considered some of the experimental measurements that could be used to test the theory. We shall return to these observables later in the thesis for a more detailed analysis, but for now we proceed with a discussion of the issues arising during renormalisation.

Chapter 2

Renormalisation Scheme Dependence

2.1 Introduction

We saw in the previous chapter the necessity to renormalise the fields and the parameters of the Lagrangian in order to make physical sense of perturbative calculations. Even if we could solve QCD exactly, we would still need to perform this renormalisation. It was also stated that the process of renormalisation is not unique. In considering the Lagrangian, the process of renormalisation has the effect of separating infinite[1] counterterms from the original bare ones but where exactly to draw the line remained undetermined. Expanding perturbatively this freedom manifests itself at every order of the coupling. In subtracting each UV divergence we are at liberty to choose the finite remainder, providing we remove the infinity in a consistent manner.

It is obvious that any physically measurable quantity must be independent of how we perform the renormalisation and hence any dependence must cancel on including all orders of perturbation theory. We shall see however that termination of the series at any given order will result in a residual dependence being picked up. There will be a dependency on the renormalisation scale, μ, (i.e. the scale at which the theory is renormalised) in addition to the finite subtraction dependence Together these constitute what is known as a *renormalisation scheme (RS)*. Clearly this problem will plague *any* perturbative calculation. The most common resolution of this is to choose a specific scheme that is convenient for the calculation and

---

[1] Infinite in magnitude not in number

quote the answer in that scheme. For the majority of calculations this corresponds to the $\overline{\text{MS}}$ scheme (see Section 2.2.1). Ideally we would like to disentangle the universal scheme dependence from the process dependent contributions. Fortunately the independence of the observable on the renormalisation scheme constrains the subtraction parameters via the renormalisation group in the same manner as the scale. With a parameterisation of these, we are then able to show the explicit dependence on the RS arising order by order.

In this chapter we shall address a variety of aspects relating to renormalisation schemes. We shall consider a description of the most common schemes (Section 2.2), how to parameterise this dependence formally (Section 2.3) and details of various attempts made at resolving the inherent ambiguities (Section 2.4). We shall ultimately consider the importance of the asymptotic behaviour of observables to remedy the renormalisation scale ambiguity (Section 2.5) before summarising the chapter (Section 2.9).

2.2 Renormalisation Schemes

In QED the renormalisation scheme dependence problem is to a certain extent irrelevant since the expansion parameter is small at accessible energies and the variation in the renormalisation scale negligible. In contrast, the relatively large QCD expansion parameter and the considerable effect of scale variation suggest careful treatment of the RS dependence is necessary. In limiting the analysis to physical observables in the massless quark approximation the renormalisation scheme enters purely through the renormalised coupling. The effects of renormalising the other Lagrangian parameters and fields will cancel order by order in expressions for physical observables. A renormalisation scheme therefore constitutes a prescription for

1. how much of the finite piece to subtract from the UV divergence order by order and

2. a choice of renormalisation scale, μ.

For the purposes of clarity we shall refer to these throughout as the subtraction parameters (SP) and the renormalisation scale, respectively. This is best illustrated with a practical example. Once again we return to the one-loop quark self-energy

part, $\Sigma(p)$. The aim of renormalisation was to make the 2-point quark Green's function finite. This was performed via the inclusion of the counterterm, Z_2. We can see from Equation (1.22) that we must define Z_2 up to $\mathcal{O}(g^2)$ in order to subtract the divergent $\frac{1}{\epsilon}$ pole. We consider two of the most common classes of schemes.

2.2.1 The Class of Minimal Subtraction Schemes

This class of schemes is intimately linked with the method of dimensional regularisation. As we have seen, regularising the integrals in this way isolates the divergences in ϵ poles. The minimal subtraction (MS) scheme simply removes this term [13]. A further variation is the hugely popular modified minimal subtraction ($\overline{\text{MS}}$) [14] scheme where it is recognised that every $\frac{1}{\epsilon}$ terms comes with a $\ln(4\pi) - \gamma_E$ due to the purely mathematical procedure of regularising through variation of space-time dimension. Therefore the $\overline{\text{MS}}$ scheme subtracts off these additional constant pieces. We obtain

$$Z_2^{\text{MS}} = 1 + \frac{(g_{\text{MS}})^2}{(4\pi)^2} C_F \frac{1}{\epsilon} + \mathcal{O}(g^4), \tag{2.1}$$

$$Z_2^{\overline{\text{MS}}} = 1 + \frac{(g_{\overline{\text{MS}}})^2}{(4\pi)^2} C_F \left(\frac{1}{\epsilon} - \gamma_E + \ln(4\pi)\right) + \mathcal{O}(g^4). \tag{2.2}$$

Through the use of dimensional regularisation and subsequent minimal subtraction no physical meaning is attributed to the renormalisation scale, μ, leaving it an entirely free, although artificial, parameter. Its algebraic simplicity and ease of implementation have resulted in the widespread use of the $\overline{\text{MS}}$ renormalisation scheme in perturbative QCD calculations.

2.2.2 The Class of Momentum Subtraction Schemes

The class of momentum subtraction (MOM) schemes attempt to extend the ideas of QED techniques to QCD. The scheme focuses on a particular interaction vertex and includes all radiative corrections within its definition. Within the context of QED this has the benefit that an *on mass shell* definition can be given to the electron-electron-photon vertex. The coupling constant can then be defined as the coupling strength between an electron and a zero energy photon and hence can be related to the classical measurement of low energy Compton scattering. Extending this to QCD

we immediately face the problem of taking the quark on mass shell[2]. An extension to this is the off-shell momentum subtraction scheme where a *characteristic* scale is used in the definition[15, 16]. The aim here is to specify desirable properties for the renormalised Green's function and define the renormalisation constants such that these are realised. In the case of the quark self-energy part, we require the full propagator to be of the form of the free massless propagator at a given off shell energy scale, $-\nu^2 < 0$. This gives rise to the more complicated counterterm,

$$Z_2^{\text{MOM}} = 1 + \frac{g_{\text{MOM}}^2}{(4\pi)^2} C_F \left(\frac{1}{\epsilon} - \gamma_E + \ln 4\pi + 1 - \ln \frac{\nu^2}{\mu^2} \right) + \mathcal{O}(g^4). \quad (2.3)$$

A further ambiguity lies in the choice of which vertex to take in the definition of the coupling (for example we could have taken the triple gluon vertex). Lastly we note that due to the structure of Z_g in all MOM schemes, the β-function is gauge dependent. As a result of these aspects, not least of which is the complexity of the counterterms, the MOM schemes are not commonly used in perturbative calculations.

2.3 Parameterising the Dependence on the Renormalisation Scheme

Now that we have seen how the one loop subtraction of UV divergences gives rise to a scheme dependence we would like to parameterise this in a precise and consistent manner.

For all further discussions we shall now consider a generic, dimensionless, QCD, single scale observable, denoted $\mathcal{R}(Q)$ with a perturbative expansion

$$\mathcal{R}(Q) = a + r_1 a^2 + r_2 a^3 + \ldots + r_n a^{n+1} + \ldots . \quad (2.4)$$

It is always possible to obtain this form from any such observable by means of algebraic manipulation (e.g. subtracting leading constants, dividing by tree level coefficients, etc.). The RG-improved couplant is defined by the β-function of Equation (1.41).

A priori we have two strong constraints that shall prove crucial in later analysis. Firstly we know that $\mathcal{R}(Q)$ is a scheme independent quantity when defined to all

---

[2]Note that we are still taking the massless approximation.

orders. Secondly we know that as it can be related to the Green's functions of the theory, it too will also satisfy a renormalisation group equation. This reiterates the point that for dimensionless quantities, the energy dependence comes purely from the RGE and hence the running coupling.

We therefore concentrate for the time being on the renormalisation scheme dependence of the coupling. Strictly the renormalised couplant is a function of both the renormalisation scale *and* the subtraction parameters and can always be related between two different schemes via a *finite renormalisation*. The couplant renormalised in two different schemes, barred and unbarred,

$$a = Z_a a_B, \quad \bar{a} = Z_{\bar{a}} a_B \tag{2.5}$$

will obey

$$a(\mu) = z\bar{a}(\mu) = \bar{a}(\mu)(1 + \nu_1 \bar{a}(\mu) + \nu_2 \bar{a}(\mu)^2 + \dots), \tag{2.6}$$

where z can be expanded in the renormalised couplant[3] and hence the ν_n parameters each describe the finite subtractions at every order. We stress that even though the actual values of the renormalisation scales are the same, the meaning in each RS may be different. Even though these parameters have the correct degrees of freedom to label the scheme, we shall find it advantageous to exchange them for a different set. Rewriting the relationship of Equation (2.6) equivalently using the β-functions defined in each RS we get

$$\beta(a) = \frac{\mathrm{d}a}{\mathrm{d}\bar{a}} \bar{\beta}(\bar{a}). \tag{2.7}$$

Clearly the β-function has a scheme dependent expansion but remarkably the first two coefficients are universal. The subsequent c_n β-function coefficients can then each be exchanged for the corresponding ν_n to label the scheme. They have the property that they are all independent, have a unique correspondence to a particular scheme and hence can be used to define a basis for parameterisation of the scheme dependence (see Stevenson [11]).

For a fixed order calculation of $\mathcal{R}(Q)$ up to order $r_n a^{n+1}$, we are required to match the accuracy in the definition of the couplant by including terms up to and including

---

[3]while the $Z_{[a,\bar{a}]}$ are separately divergent the ratio is finite in the $\epsilon \to 0$ limit

$c_n a^{n+2}$, giving $a = a(\mu, c_2, c_3, \ldots, c_n)$. Returning to our generic observable, self-consistency requires the r_n coefficients to be increasingly dependent on the scheme parameters, i.e. $r_1(\mu), r_2(\mu, c_2), r_3(\mu, c_2, c_3), \ldots, r_n(\mu, c_2, \ldots, c_n)$. Finally we arrive at a complete parameterisation of the nth order truncated approximant,

$$
\begin{aligned}
\mathcal{R}^{(n)}(\mu, c_2, \ldots, c_n) &= a(\mu, c_2, \ldots, c_n) \\
&+ r_1(\mu) a(\mu, c_2, \ldots, c_n)^2 \\
&+ \ldots \\
&+ r_n(\mu, c_2, \ldots, c_n) \, a(\mu, c_2, \ldots, c_n)^{n+1}.
\end{aligned}
\tag{2.8}
$$

The scheme dependence will cancel completely on including all orders giving a formally RS-independent result. An artifact of the consistency of perturbation theory, order by order, is the relation between two n^{th} order approximants in different RS's,

$$
\mathcal{R}^{(n)}(\mu, c_2, \ldots, c_n) - \bar{R}^{(n)}(\bar{\mu}, \bar{c}_2, \ldots, \bar{c}_n) = \mathcal{O}(a^{n+2}).
\tag{2.9}
$$

That is, if we truncate a calculation at $\mathcal{O}(a^{n+1})$, a change of scheme will only affect terms of one order higher.

2.3.1   Scheme Dependence at Next-to-Leading Order

We now consider the case of a next-to-leading order (NLO) approximation since it is the simplest case to exhibit RS dependence. Immediately we encounter one of the most important aspects featuring in all renormalised gauge theories, namely that of *dimensional transmutation*. We first saw this tacitly when we integrated up the one-loop β-function and a dimensionful scale, Λ entered to parameterise the missing boundary condition. We shall come back to this in greater detail in Section 2.5. For the time being we shall adopt a further notation of Stevenson to define, $\tau = b \ln(\mu/\tilde{\Lambda})$ where $\tilde{\Lambda}$ is dependent on the chosen RS but is μ independent. The tilde over Λ is to distinguish it from the traditional definition of Buras et al. [14, 17] which is based on an expansion of a in inverse powers of $\ln(\mu^2/\Lambda^2)$. The two can be easily related via the exact relation

$$
\tilde{\Lambda} = \left(\frac{2c}{b} \right)^{-\frac{c}{b}} \Lambda.
\tag{2.10}
$$

We can now trade all μ dependence for τ in the definition of the β-function and $\mathcal{R}(Q)$, to include this extra boundary information. At NLO we have

$$\mathcal{R}^{(1)}(\tau) = a(\tau) + r_1(\tau)a(\tau)^2, \tag{2.11}$$

where $a(\tau)$ is defined by integrating up the NLO truncated β-function,

$$\frac{\mathrm{d}a}{\mathrm{d}\tau} = -a^2(1 + ca). \tag{2.12}$$

Taking the boundary condition of $a(\tau = 0) = \infty$ we obtain

$$\tau = \frac{1}{a(\tau)} + c\ln\left(\frac{ca(\tau)}{1 + ca(\tau)}\right) \equiv F(a), \tag{2.13}$$

where we have specified the function $F(x)$ for later convenience. This equation defines the coupling to next-to-leading order. It is possible to invert this [18, 19] using the Lambert W function [20] to obtain an expression for the coupling,

$$a(\tau) = \frac{-1}{c(1 + W(z(\tau)))}, \quad z(\tau) \equiv -\exp\left(-\frac{\tau}{c} - 1\right). \tag{2.14}$$

The Lambert W function is the inverse of the function $w \mapsto we^w$. As such it has many branches, only two of which are real; $W_0(x)$ in the range $\frac{-1}{e} \leq x < \infty$ and $W_{-1}(x)$ in the range $\frac{-1}{e} \leq x \leq 0$. The requirement that the coupling is real and positive in the perturbative domain is sufficient to determine the branch to be $W_{-1}(x)$ [18]. Subsequently, the use of this branch is implicit and we shall drop the -1 notation.

To determine the dependence of r_1 on τ (i.e. the scheme dependence to NLO), we first relate two r_1 values from different schemes via substitution of Equation (2.6) into Equation (2.11) and equating coefficients, to get

$$r_1 = \bar{r}_1 + \nu_1. \tag{2.15}$$

Similarly we can use Equation (2.6) to find the difference of two τ's in different schemes

$$\tau - \bar{\tau} = \frac{1}{a} + c\ln\left(\frac{ca}{1 + ca}\right) + \ldots - \frac{1}{\bar{a}} - c\ln\left(\frac{c\bar{a}}{1 + c\bar{a}}\right) + \ldots, \tag{2.16}$$

where the ellipses denotes terms that enter beyond NLO in the β-function. Since this should hold for all values of μ we can take the $\mu \to \infty$ limit, and utilising asymptotic freedom ($a(\mu = \infty) = 0$) we reach

$$\tau - \bar{\tau} = \nu_1. \tag{2.17}$$

Eliminating ν_1 between Equation (2.15) and Equation (2.17) gives

$$\tau - r_1(\tau) = \bar{\tau} - \bar{r}_1(\bar{\tau}) \equiv \rho_0, \tag{2.18}$$

where it is clear that the combination on the LHS is independent of τ and hence is a renormalisation scheme invariant, ρ_0 [11]. Since $\mathcal{R}(Q)$ is a function of a single scale, Q, we can write this as

$$\rho_0(Q) = \tau - r_1(\tau) \equiv b \ln \frac{Q}{\Lambda_{\mathcal{R}}}, \tag{2.19}$$

where to maintain dimensionality we have defined an observable dependent but RS invariant quantity, $\Lambda_{\mathcal{R}}$. Later we shall see the importance of this quantity in the asymptotic behaviour of the observable. Equation (2.19) specifies precisely how the NLO coefficient depends on the scale. We notice two important points. Firstly that at NLO we need μ *and* $\tilde{\Lambda}_{\mathrm{RS}}$ to specify the scheme and secondly r_1 can itself be traded for τ to describe the renormalisation scale as a result of their combination being RS invariant.

Reconsidering $\Lambda_{\mathcal{R}}$, we note that it is also possible to relate this observable dependent quantity with the dimensional transmutation parameter $\tilde{\Lambda}_{\mathrm{RS}}$ that is universal but RS dependent by rearranging Equation (2.19),

$$\Lambda_{\mathcal{R}} = \tilde{\Lambda}_{\mathrm{RS}} \exp\left(\frac{r_1^{\mathrm{RS}}(\mu = Q)}{b}\right). \tag{2.20}$$

In fact utilising the same formula we see that it is possible to relate *any* two lambdas exactly via a one-loop calculation, otherwise known as the Celmaster-Gonsalves relation [15].

2.4   Proposed Solutions to the Scheme Dependence Problem

Due to the strong dependence of the QCD coupling on the renormalisation scheme, there have been a number of attempts made to resolve the ambiguities inherent in these perturbative calculations. To date, most state-of-the-art calculations are at NLO and as a result the scheme dependence problem is commonly viewed as an exercise in choosing the optimum scale for μ. In this section we shall review a number of these proposals.

2.4.1   The Physical Scale

Nearly universally accepted as the de facto method at NLO, the physical scale attempts to minimise higher order contributions by choosing a value of μ in the vicinity of Q, the physical scale. The reasoning behind this is the recognition of terms in an nth order coefficient of the form

$$r_n = \sum_{m=0}^{n} \mathcal{K}_{nm} \left(b \ln \frac{\mu}{Q} \right)^m , \qquad (2.21)$$

purely due to one-loop running of the coupling. The $\mathcal{K}_{nm}$ denote scheme-dependent coefficients. On the surface choosing $\mu \approx Q$ would appear to reduce these contributions to higher order coefficients. Careful consideration demonstrates that this is not completely true and in fact we obtain

$$r_n = \sum_{m=0}^{n} \tilde{\mathcal{K}}_{nm} \left(b \ln \frac{\mu}{Q} + r_1^{\mathrm{RS}}(\mu = Q) \right)^m , \qquad (2.22)$$

using renormalisation group arguments where the $\tilde{\mathcal{K}}_{nm}$ represent RS-*invariant* coefficients. We shall demonstrate this explicitly in Section 2.5.4. In light of this, applying the motivation behind the physical scale would suggest using a value of $\mu = \exp(-r_1^{\mathrm{RS}}(\mu = Q)/b)$ which we shall see coincides with the method of Effective Charges.

2.4.2   The Principle of Minimal Sensitivity (PMS)

Proposed by Stevenson [11], the principle of minimal sensitivity (PMS) approach attempts to resolve the renormalisation scheme dependence problem by relying on the renormalisation group invariance of physical quantities. The idea is that since the exact all-orders result is independent of the RS parameters, one should choose the nth-order approximation to mimic this property and to be as insensitive as possible to chosen value of these unphysical parameters. That is, one arranges that

$$\left. \frac{\mathrm{d}\mathcal{R}^{(n)}}{\mathrm{d}(\mathrm{RS})} \right|_{\mathrm{RS}=Optimal\ \mathrm{RS}} = 0. \qquad (2.23)$$

Associating the β-function coefficients with the scheme parameters we can rewrite this as

$$\left. \frac{\partial \mathcal{R}^{(n)}}{\partial \tau} \right|_{\tau=\bar{\tau}} = \left. \frac{\partial \mathcal{R}^{(n)}}{\partial c_2} \right|_{c_2=\bar{c}_2} = \ldots = \left. \frac{\partial \mathcal{R}^{(n)}}{\partial c_n} \right|_{c_3=\bar{c}_n} = 0. \qquad (2.24)$$

The PMS scheme is then specified by the parameters $\bar{\tau}, \bar{c}_2, \ldots, \bar{c}_n$. At NLO this corresponds to minimising the τ dependence. This gives

$$\left.\frac{\partial \mathcal{R}^{(1)}}{\partial \tau}\right|_{\tau=\bar{\tau}} = \bar{a}^2 \left.\frac{\partial r_1}{\partial \tau}\right|_{\tau=\bar{\tau}} - \bar{a}(1+c\bar{a})(1+2\bar{r}_1\bar{a}) = 0, \qquad (2.25)$$

where the barred quantities are evaluated with the PMS NLO scheme parameter, $\tau = \bar{\tau}$. Self consistency enforces Equation (2.19) with $\frac{\partial r_1}{\partial \tau} = 1$. This leaves

$$r_1(\bar{\tau}) = -\frac{c}{2(1+c\bar{a})}, \qquad (2.26)$$

giving

$$\mathcal{R}^{(2)} = \bar{a}\frac{1+\frac{1}{2}c\bar{a}}{1+c\bar{a}}, \qquad (2.27)$$

for the NLO PMS expression for a NLO approximant. It now remains to evaluate $\bar{a} = a(\bar{\tau})$. Substituting Equation (2.26) into Equation (2.19) we are left with

$$\frac{2+3c\bar{a}}{2(1+c\bar{a})\bar{a}} + c\ln\left(\frac{c\bar{a}}{1+c\bar{a}}\right) = b\ln\left(\frac{Q}{\Lambda_{\mathcal{R}}}\right). \qquad (2.28)$$

Solving this transcendental equation gives the PMS coupling which can then be used with Equation (2.27) to give the NLO estimate for $\mathcal{R}$. In favour of this methodology is the scheme invariance of the approximant. The only possible scheme dependence entering $\mathcal{R}^{(1)}(\bar{a})$ is through the couplant, and from Equation (2.28) we can see that the couplant is defined only through renormalisation scheme invariants. Furthermore it optimises the combination of μ and $\tilde{\Lambda}_{\mathrm{RS}}$ both of which are required at NLO.

Against the method of PMS is the complex nature of the coupled equations needed to solve for the scheme parameters. If $\mathcal{R}^{(n)}(a)$ and subsequent n derivatives of Equation (2.24) are monotonic then we are faced with a difficulty in even defining the PMS scheme parameters.

2.4.3 BLM Scale Setting

Brodsky, Lepage and Mackenzie (BLM) proposed to resolve the renormalisation scale ambiguity by providing a prescription for process dependent scale fixing [21]. Strongly motivated by QED where the photon self-energy corrections are absorbed into the coupling constant by an appropriate choice of scale, BLM attempts to reproduce the key ideas within the context of QCD. Its primary assumptions are

that there exists an optimal scale for μ at every order and that there is such a thing as a *good* RS to work in. The need for a good RS is due to the lack of boundary condition value for α_s in contrast to the low energy value of $\alpha_{\text{QED}} = 1/137.036\ldots$. If there is no gluon-gluon interaction at this order, the optimal scale is obtained by the requirement that all light quark vacuum polarisation corrections are absorbed within it. At NLO this gives

$$\mathcal{R} = a(\mu) + r_1 a(\mu)^2 \xrightarrow{\text{BLM}} \bar{\mathcal{R}} = a(\bar{\mu}) + \bar{r}_1 a(\bar{\mu})^2, \qquad (2.29)$$

where the barred quantities are fixed via BLM. We can separate out the N_f dependent part of r_1 and the first β-function coefficient, b, such that

$$r_1 = r_1^0 + r_1^1 N_f, \qquad (2.30)$$

$$b = b^0 + b^1 N_f, \qquad (2.31)$$

we can fix perform the BLM scale setting by rescaling b such that the magnitudes of b^1 and r_1^1 coincide and then completely subtracting it from r_1. Formally this amounts to expanding the one-loop running of the couplant and substituting it into Equation (2.29) to obtain

$$r_1^0 + r_1^1 N_f = \bar{r}_1 - (b^0 + b^1 N_f) \ln \frac{\bar{\mu}}{\mu}. \qquad (2.32)$$

Equating N_f independent and dependent parts we obtain

$$\bar{\mu} \quad = \mu \exp\left(\frac{-r_1^1}{b^1}\right) \quad = \mu \exp(-3r_1^1), \qquad (2.33)$$

$$\bar{r}_1 \quad = r_1^0 - b^0 \ln \frac{\bar{\mu}}{\mu} \quad = r_1^0 - \frac{33}{2} r_1^1. \qquad (2.34)$$

Throughout this procedure we have only specified the scale. The underlying scheme (i.e. subtraction parameters) have been implicitly assumed to be good. A major problem will now arise when we change scheme to one with different subtraction parameters and end up getting completely different results. This is precisely due to the fact that μ by itself does not specify the RS, one needs in addition a $\tilde{\Lambda}_{\text{RS}}$ parameter. Some effort to resolve this has been recently [22] by use of commensurate scale relations that give the relationship between two physical observables. By using these relationships, it is proposed that all renormalisation *scheme* dependence is removed, giving a completely unambiguous prediction. It requires that the running coupling effects can be cleanly separated from the conformal part of the perturbative expansion of a generic physical quantity. This is currently unproven.

2.4.4   Effective Charges (EC)

In this section we shall consider the method of *Effective Charges* (EC's) first proposed by Grunberg [23, 24] as a way of resolving the renormalisation scheme ambiguity. The motivation behind this method is the recognition that for a dimensionless observable the energy scale dependence arises purely from the renormalised coupling. Thus by specifying an observable of the form $\mathcal{R}$ in Equation (2.4) proportional to the coupling and defined to all orders, we obtain an *effective charge* and as such we can apply the same renormalisation group equation as satisfied by the coupling. Furthermore since $\mathcal{R}$ is a physical observable we can differentiate with respect to the actual hard scale, Q to examine how it scales. We can write this mathematically as

$$\frac{\mathrm{d}\mathcal{R}}{\mathrm{d}\ln Q} \equiv B(\mathcal{R}) \tag{2.35}$$

where $B(\mathcal{R})$ takes the rôle of the β-function. Crucially, the physical nature of these quantities means the EC β-function is itself a physical observable given measurements of $\mathcal{R}$ at a variety of centre-of-mass energies. As such the function $B(\mathcal{R})$ permits a non-perturbative definition and we shall see later how it is possible to model such non-perturbative effects.

Returning to our expansion of $\mathcal{R}$, we see that it is possible to choose the scheme parameters such that all higher order coefficients are zero ($r_n = 0$) giving an all orders exact coupling equal to the observable,

$$\mathcal{R}(Q) = a \quad \text{where} \quad r_1 = 0 = r_2 = \ldots = r_n = \ldots . \tag{2.36}$$

We shall refer to this as the EC scheme. This will have a value of $\tau = \rho_0$ from Equation (2.18) and scheme parameters obtained via Equation (2.7). At NLO, the scheme dependence is equivalent to specifying a value for τ. In the EC formalism this is simply

$$\tilde{\tau} = \rho_0 \equiv b \ln\left(\frac{Q}{\Lambda_R}\right) \tag{2.37}$$

with the coupling given by

$$\frac{1}{a(\tilde{\tau})} + c \ln\left(\frac{ca(\tilde{\tau})}{1 + ca(\tilde{\tau})}\right) = b \ln\left(\frac{Q}{\Lambda_R}\right) \tag{2.38}$$

We see that, as with the PMS prescription, the EC gives an RS invariant approximant, $R^{(1)} = a(\tilde{\tau})$. Once again this occurs at every order in perturbation theory.

Comparing with the PMS NLO result, we find that the EC result is very similar since $\tilde{\tau} = \rho_0$ for the EC and $\bar{\tau} \simeq \rho_0 + \frac{c}{2}$ with the PMS. Even at NNLO it has been shown that they remain close to each other [25, 26]. Since the EC is equivalent to choosing the scale such that the higher order coefficients vanish, it is sometimes referred to in the literature as the Fastest Apparent Convergence (FAC) scheme [11].

We maintain that the EC approach is fundamentally correct although, rather than claim it provides a solution to the whole renormalisation scheme dependence ambiguity, we suggest that it can only motivate the appropriate scale dependence. Beyond this, it provides an RS-invariant formulation based on the assumption that higher order terms vanish. We discuss these issues in the next section.

2.5 RS Invariant Formulations of Perturbation Theory

We saw in the previous section a number of proposed solutions to the renormalisation scale/scheme dependence problem. We stressed that at NLO we must specify *two* parameters, μ and $\tilde{\Lambda}_{RS}$, to obtain an unambiguous answer (c.f. BLM scale setting). Two proposals, namely the PMS and method of EC's, treated this correctly and in this section we shall reconsider that of the effective charges. We begin with a closer look at how a dimensionful scale enters the theory via dimensional transmutation.

2.5.1 Dimensional Transmutation

This analysis owes much to the original discussion of Stevenson [27] on utilising dimensional arguments in RG analysis and closely follows that of [28, 29]. We start, once again with a dimensionless generic QCD observable $\mathcal{R}(Q)$, dependent on a single dimensionful (energy) scale Q. Quark masses will be taken to be zero throughout our discussion, the extension to the massive case has been considered in [30]. Since $\mathcal{R}(Q)$ is dimensionless, dimensional analysis clearly demands that

$$\mathcal{R}(Q) = \Phi\left(\frac{Q}{\Lambda}\right) , \tag{2.39}$$

where Λ is a dimensionful scale, which will turn out to be related to the dimensional transmutation parameter. There is an extra trivial possibility that $\mathcal{R}(Q) = C$, where C is a dimensionless *constant* implying there is no energy dependence. This

trivial Q-dependence would be the case if the bare coupling of QCD was finite, since the QCD Lagrangian (with massless quarks) contains no massive parameters. Of course, in fact, the bare coupling is infinite, and an infinite renormalisation must be performed, leading to a functional relation as given in Equation (2.39). The appearance of a dimensionful parameter such as Λ is due to the non-uniqueness of the theory. In QCD this is because the bare Lagrangian corresponds to an infinite set of theories, each with a different Λ. Determination of the value of Λ, the one free parameter, can only be performed by experimental measurement. To fix the theory up to a one parameter degree of freedom we can specify that the derivative of $\mathcal{R}(Q)$ with respect to Q is given. The free parameter is now contained in the boundary condition. Going back to our formula for $\mathcal{R}(Q)$, an obvious proposal is to invert this to obtain

$$\frac{Q}{\Lambda} = \Phi^{-1}(\mathcal{R}(Q)), \tag{2.40}$$

where Φ^{-1} is the inverse function. This is indeed the basic motivation for Grunberg's method of Effective Charges [24]. To obtain the form of Φ^{-1} we apply the above reasoning of specifying the derivative of $\mathcal{R}(Q)$ which must clearly behave as

$$\frac{\mathrm{d}\mathcal{R}(Q)}{\mathrm{d}Q} = \frac{B(\mathcal{R}(Q))}{Q} , \tag{2.41}$$

where $B(\mathcal{R}(Q))$ is a dimensionless function of $\mathcal{R}$. This can be rearranged to obtain,

$$\frac{\mathrm{d}\mathcal{R}(Q)}{\mathrm{d}\ln Q} = B(\mathcal{R}(Q)) . \tag{2.42}$$

This is a separable first-order differential equation. In order to solve it we will need to impose the boundary condition, and know something of the behaviour of $B(\mathcal{R})$. We shall assume that $\mathcal{R}$ has the prototypical perturbative expansion,

$$\mathcal{R} = a\left(1 + \sum_{n>0} r_n a^n\right) , \tag{2.43}$$

as previously given in Equation (2.4) where $a \equiv \alpha_s(\mu)/\pi$ is the RG-improved coupling. The required boundary condition will be given by asymptotic freedom, that is $\mathcal{R}(\infty) = 0$. Integrating Equation (2.42) one then obtains

$$\ln\frac{Q}{\Lambda_\mathcal{R}} = \int_0^{\mathcal{R}(Q)} \frac{\mathrm{d}x}{B(x)} + \kappa . \tag{2.44}$$

The constant of integration has been split into $\ln\Lambda_{\mathcal{R}} + \kappa$, where $\Lambda_{\mathcal{R}}$ is a finite dimensionful scale specific to the observable $\mathcal{R}$, and κ is a universal infinite constant needed to implement $\mathcal{R}(\infty) = 0$. To determine κ we need to know the behaviour of $B(x)$ around $x = 0$.

Returning to the perturbative series of Equation (2.43) we recall that the couplant a satisfies the β-function equation,

$$\frac{\partial a}{\partial \ln \mu} = \beta(a) = -ba^2 \left(1 + ca + \sum_{n>1} c_n a^n \right), \qquad (2.45)$$

If we set $\mu = Q$ in Equation (2.43), and differentiate with respect to $\ln Q$ term-by-term using the β-function equation of the couplant (Equation (2.45)), we can obtain $B(\mathcal{R}(a))$ as a power series in a,

$$\begin{aligned} B(\mathcal{R}) &= \frac{\mathrm{d}\mathcal{R}}{\mathrm{d}\ln Q} \\ &= \frac{\partial a(Q)}{\partial \ln Q} + 2r_1(\mu{=}Q)\, a\, \frac{\partial a(Q)}{\partial \ln Q} + \ldots + nr_n(\mu{=}Q)\, a^{n-1} \frac{\partial a(Q)}{\partial \ln Q} + \ldots. \end{aligned}$$
$$(2.46)$$

Inverting the series $\mathcal{R}(a)$ in Equation (2.43) to obtain $a(\mathcal{R})$ as a power series in $\mathcal{R}$, we can obtain $B(\mathcal{R})$ as a power series in $\mathcal{R}$,

$$\frac{\mathrm{d}\mathcal{R}}{\mathrm{d}\ln Q} = -b\,\mathcal{R}^2(1 + c\mathcal{R} + \rho_2\mathcal{R}^2 + \rho_3\mathcal{R}^3 + \ldots), \qquad (2.47)$$

giving $B(x)$ around $x = 0$,

$$B(x) = -bx^2 \left(1 + cx + \sum_{n>1} \rho_n x^n \right). \qquad (2.48)$$

The first two coefficients b and c, are the universal β-function coefficients. The higher terms $\rho_i, (i > 1)$ are renormalisation scheme (RS)-invariant, and Q-independent, combinations of the r_i and c_i. The first two are [11, 24, 28]

$$\begin{aligned} \rho_2 &= c_2 + r_2 - r_1 c - r_1^2 \\ \rho_3 &= c_3 + 2r_3 - 4r_1 r_2 - 2r_1 \rho_2 - r_1^2 c + 2r_1^3. \end{aligned} \qquad (2.49)$$

Knowledge of ρ_n requires a complete N^nLO perturbative calculation, that is a calculation of the r_i for $i = 1, 2, \ldots, n$ and the c_i for $i = 2, 3, \ldots, n$, in any given renormalisation scheme, for instance $\overline{\text{MS}}$. The fact that Equation (2.48) has the

same form as the β-function equation given in Equation (2.45) follows from the fact that there exists an RS in which $\mathcal{R} = a$, i.e. $r_i = 0$, $i > 0$, and in this scheme the non-universal β-function coefficients are $c_i = \rho_i$, $i > 1$. The existence of this Effective Charge scheme [24] is underwritten by the algebraic steps above from which Equation (2.48) can be directly derived. Armed with knowledge of the form of $B(x)$ around $x = 0$ we see that the infinite constant of integration κ will be of the form

$$\kappa = -\int_0^C \frac{\mathrm{d}x}{K(x)}, \tag{2.50}$$

where $K(x)$ must be such that the singularity of $1/B(x)$ at $x = 0$ in Equation (2.44) is canceled. This implies from Equation (2.48) that

$$K(x) = -bx^2(1 + cx + \Delta(x)), \tag{2.51}$$

where $\Delta(x)$ is only constrained by the requirement that $\Delta(x)/x^2$ is finite as $x \to 0$. Different choices of the upper limit of integration, C, and the function $\Delta(x)$, can be absorbed into the dimensionful constant $\Lambda_\mathcal{R}$. Convenient choices are $C = \infty$ and $\Delta(x) = 0$. With these choices Equation (2.44) can be re-written as,

$$b \ln \frac{Q}{\Lambda_\mathcal{R}} = \int_{\mathcal{R}(Q)}^\infty \frac{\mathrm{d}x}{x^2(1 + cx)} + \int_0^{\mathcal{R}(Q)} \mathrm{d}x \left[\frac{b}{B(x)} + \frac{1}{x^2(1 + cx)} \right] . \tag{2.52}$$

The first integral on the r.h.s. of Equation (2.52) gives the now familiar

$$F(\mathcal{R}) \equiv \frac{1}{\mathcal{R}} + c \ln \left[\frac{c\mathcal{R}}{1 + c\mathcal{R}} \right] . \tag{2.53}$$

Denoting the second integral by $G(\mathcal{R})$ we have

$$b \ln \frac{Q}{\Lambda_\mathcal{R}} = F(\mathcal{R}) + G(\mathcal{R}) . \tag{2.54}$$

The desired inverse function Φ^{-1} of Equation (2.40) can then be obtained by exponentiating Equation (2.54), which gives

$$\mathcal{F}(\mathcal{R}(Q))\mathcal{G}(\mathcal{R}(Q)) = \frac{\Lambda_\mathcal{R}}{Q} \tag{2.55}$$

where $\mathcal{F}$ is the universal function

$$\mathcal{F}(\mathcal{R}) \equiv e^{-F(\mathcal{R})/b} = e^{-1/b\mathcal{R}}(1 + 1/c\mathcal{R})^{c/b} , \tag{2.56}$$

and

$$\mathcal{G}(\mathcal{R}) \equiv e^{-G(\mathcal{R})/b} = \exp\left[-\int_0^{\mathcal{R}(Q)} dx \left(\frac{1}{B(x)} + \frac{1}{bx^2(1+cx)}\right)\right] . \qquad (2.57)$$

If only a NLO perturbative calculation has been completed then our state of knowledge of $B(x)$ is $B(x) = -bx^2(1+cx)$ since the NNLO and higher RS invariants $\rho_2, \rho_3, \ldots$ of Equation (2.48) will be unknown. From Equation (2.57) we then have $\mathcal{G}(\mathcal{R}) = 1$.

2.5.2 Relating the Observable Dependent $\Lambda_{\mathcal{R}}$ to the Universal Λ_{RS}

We finally need to relate the observable-dependent constant of integration $\Lambda_{\mathcal{R}}$ which arose on integrating Equation (2.42), to the *universal* dimensional transmutation constant which depends only on the subtraction procedure used to remove the ultraviolet divergences, $\Lambda_{\overline{\mathrm{MS}}}$ for instance. We have already encountered the celebrated Celmaster and Gonsalves relation [15] enabling the transition from one Λ parameter to another exactly via a one-loop (NLO) perturbative calculation of the observable (Equation (2.20)). We shall now demonstrate this relationship from a different perspective to clarify the connection between scheme independent but observable dependent Λ's and a universal but scheme dependent Λ_{RS}.

To see this we begin by noting that on rearranging Equation (2.54) and taking the limit as $Q \to \infty$, we obtain an operational definition of $\Lambda_{\mathcal{R}}$,

$$\Lambda_{\mathcal{R}} = \lim_{Q \to \infty} Q \exp(-F(\mathcal{R}(Q))/b) . \qquad (2.58)$$

This property was denoted "Asymptotic Scaling" by Maxwell [31]. We have used the fact that $G(0) = 0$ together with asymptotic freedom. If we denote by $a(Q)$ the $\overline{\mathrm{MS}}$ coupling with $\mu = Q$ we see that it will satisfy the β-function equation Equation (2.45), of the same form as Equation (2.42) for $\mathcal{R}$, with $\beta_{\overline{\mathrm{MS}}}(a)$ replacing $B(\mathcal{R})$. This may be integrated following the same steps as above. The constant of integration $\Lambda_{\mathcal{R}}$ will be replaced by $\tilde{\Lambda}_{\overline{\mathrm{MS}}}$, and the coefficients ρ_i by the $\overline{\mathrm{MS}}$ β-function coefficients $c_i^{\overline{\mathrm{MS}}}$. Again choosing $C = \infty$ and $\Delta(x) = 0$, we arrive at

$$\tilde{\Lambda}_{\overline{\mathrm{MS}}} = \lim_{Q \to \infty} Q \exp(-F(a(Q))/b) . \qquad (2.59)$$

From the perturbative expansion of $\mathcal{R}$ in Equation (2.43) we will have

$$\mathcal{R}(Q) = a(Q) + r(a(Q))^2 + \dots , \tag{2.60}$$

where we have defined for convenience $r \equiv r_1^{\overline{MS}}(\mu = Q)$, as the notation suggests r is Q-independent. It is then straightforward to show that as $Q \to \infty$

$$F(\mathcal{R}) \approx F(a) - r + \dots , \tag{2.61}$$

where the ellipsis denotes terms which vanish as $Q \to \infty$. Inserting this result into Equation (2.58), and comparing with Equation (2.59), one finally finds (c.f. the Celmaster Gonsalves relation of Equation (2.20)

$$\Lambda_{\mathcal{R}} = e^{r/b} \tilde{\Lambda}_{\overline{MS}} = \left(\frac{2c}{b} \right)^{-c/b} \Lambda_{\overline{MS}} , \tag{2.62}$$

for the promised exact relation between the observable-dependent and universal Λ's. The tilde over Λ is once again present to draw attention to the fact that the above choice of infinite integration constant κ does not accord with the standard choice [17]. This definition corresponds to translating κ by the finite shift $c \ln(b/2c)$. Finally assembling all this we arrive at the desired relation between the universal dimensional transmutation parameter $\Lambda_{\overline{MS}}$ and the QCD observable $\mathcal{R}$,

$$\Lambda_{\overline{MS}} = Q \, \mathcal{F}(\mathcal{R}(Q)) \, \mathcal{G}(\mathcal{R}(Q)) \, e^{-r/b} \left(\frac{2c}{b} \right)^{c/b} . \tag{2.63}$$

Notice that all dependence on the subtraction convention chosen to remove ultraviolet divergences reside in the single factor $e^{-r/b}$, the remainder of the expression being independent of this choice.

2.5.3   Practical Application

As noted above, if only a NLO calculation has been performed then the state of our knowledge of the function $B(\mathcal{R})$ in (4) is $B(\mathcal{R}) = -b\mathcal{R}^2(1 + c\mathcal{R})$, and then from Equation (2.57) $\mathcal{G}(\mathcal{R}) = 1$. So at NLO the *best* we can do in extracting $\Lambda_{\overline{MS}}$ from the data is

$$\Lambda_{\overline{MS}} = Q\mathcal{F}(\mathcal{R}(Q)) e^{-r/b} (2c/b)^{c/b} . \tag{2.64}$$

If two-loop (NNLO) and higher-order perturbative calculations are available then $\mathcal{G}(\mathcal{R})$ will differ from unity by calculable corrections. One can expand $\mathcal{G}(\mathcal{R})$ as a power series in $\mathcal{R}$,

$$\mathcal{G}(\mathcal{R}) = 1 - \frac{\rho_2}{b}\mathcal{R} + O(\mathcal{R}^2) + \ldots, \tag{2.65}$$

where ρ_2 is the NNLO RS-invariant defined in Equation (2.49). Alternatively $G(\mathcal{R})$ can be expanded in the exponent as a power series in $\mathcal{R}$ by expanding the integrand in Equation (2.57), to give

$$\mathcal{G}(\mathcal{R}) = \exp[(-\rho_2\mathcal{R} + O(\mathcal{R}^2) + \ldots)/b]. \tag{2.66}$$

One could also evaluate the integral in Equation (2.57) numerically with $B(x)$ truncated , so that at NNLO for instance $B(x) = -bx^2(1 + cx + \rho_2 x^2)$.

Focusing now on the NLO case where $\mathcal{G} = 1$ we note that Equation (2.64) can be inverted to give

$$\begin{aligned} \mathcal{R}(Q) &= -\frac{1}{c[1 + W(z(Q))]}, \\ z(Q) &\equiv -\frac{1}{e}\left(\frac{Q}{\Lambda_{\mathcal{R}}}\right)^{-b/c}, \end{aligned} \tag{2.67}$$

where W is the -1 branch of the Lambert W-function. Equation (2.67) is equivalent to the two-loop $\overline{\text{MS}}$ coupling with scale $\mu = e^{-r/b}Q$, and in this scheme $r_1 = 0$. This scheme is sometimes referred to as the "Fastest Apparent Convergence" (FAC) scheme [11], and is equivalent to Grunberg's Effective Charge approach at NLO [23, 24]. Crucially, we have derived Equation (2.67) without having to argue for a specific choice of scale. Starting from the form of Q-dependence of $\mathcal{R}$ implied by dimensional analysis in Equation (2.41), we simply solved this differential equation applying asymptotic freedom as a boundary condition. To define the required infinite constant of integration we needed to know the series expansion of $B(x)$ around $x = 0$, Equation (2.48), whose form is completely scheme-independent, and we arrived at Equation (2.54). The constant of integration $\Lambda_{\mathcal{R}}$ could then be exactly related to the universal dimensional transmutation parameter $\Lambda_{\overline{\text{MS}}}$ associated with use of $\overline{\text{MS}}$ subtraction to remove ultraviolet divergences, given a NLO calculation of r, as in Equation (2.62). In all of this the renormalised coupling a only ever appeared in intermediate steps, playing, as neatly expressed in [27], "the rôle of a conjuror's

handkerchief- now you see it, now you don't !". This, of course, begs the question as to what is special about the Effective Charge (FAC) scheme, and why other choices of scale μ do not provide equally valid predictions for $\mathcal{R}$. The key is to identify the way in which the Q-dependence of $\mathcal{R}(Q)$ arises. In the construction above, it is built automatically by integration of Equation (2.41), but how does it arise from the perturbation series in Equation (2.43) ? For this purpose it will be more illuminating to consider an alternative formulation by Maxwell [32, 33] termed Complete Renormalisation Group Improvement (CORGI). This procedure treats the renormalisation scale, μ completely independent of the energy scale Q. This different perspective turns out to be entirely equivalent to that detailed above.

2.5.4 Complete Renormalisation Group Improvement (CORGI)

We have now seen that the correct manner to deal with the unphysical μ dependence is to look to how the physical observable scales with energy. In this section we shall consider this from a different point of view proposed by Maxwell in [32, 33, 34]. It demonstrates a variation on the effective charge methodology, namely that of complete renormalisation group improvement (CORGI). The benefits are not least of which a greater transparency in analysing the issues of scheme dependence and the ability to implement higher order corrections through simple algebraic manipulation without sacrificing the paramount correct treatment of scale dependence. We start as always with an expansion for $\mathcal{R}$ as given in Equation (2.4). We have already seen that we may use (τ, c_n) as a complete parameterisation of the scheme. Furthermore we demonstrated that we are free to trade τ for r_1 to describe the scale dependence.

Using the self consistency of perturbation theory we know that an nth order approximant will be unchanged by RS variation to one order higher in the coupling,

$$\frac{\mathrm{d}\mathcal{R}^{(n)}}{\mathrm{d}(\mathrm{RS})} = \mathcal{O}(a^{n+2}). \tag{2.68}$$

This can be used to derive expressions for partial derivatives of the r_n with respect

to the scheme parameters. Applied at NNLO we find

$$\frac{\partial \mathcal{R}^{(2)}}{\partial r_1} = \frac{\partial a}{\partial r_1} + a^2 + 2r_1 a \frac{\partial a}{\partial r_1} + \frac{\partial r_2}{\partial r_1} a^3 + 3r_2 a \frac{\partial a}{\partial r_1} + \dots , \qquad (2.69)$$

$$\frac{\partial \mathcal{R}^{(2)}}{\partial c_2} = \frac{\partial a}{\partial c_2} + 2r_1 a \frac{\partial a}{\partial c_2} + \frac{\partial r_2}{\partial c_2} a^3 + 3r_2 a \frac{\partial a}{\partial c_2} + \dots , \qquad (2.70)$$

$$\frac{\partial \mathcal{R}^{(2)}}{\partial c_3} = \dots . \qquad (2.71)$$

where the ellipses denotes terms that start at $\mathcal{O}(a^4)$. Enforcing self consistency requirements requires each lower order of the couplant to vanish independently. This leaves us with

$$\frac{\partial r_2}{\partial r_1} = 2r_1 + c, \quad \frac{\partial r_2}{\partial c_2} = -1, \quad \frac{\partial r_2}{\partial c_3} = 0. \qquad (2.72)$$

Since the only scheme parameters that r_2 will depend on are r_1 and c_2 we can integrate Equations (2.72) to obtain the most general form. Applying this formalism to each order of perturbation theory we arrive at

$$r_2(r_1, c_2) = r_1^2 + cr_1 + X_2 - c_2, \qquad (2.73)$$

$$r_3(r_1, c_2, c_3) = r_1^3 + \tfrac{5}{2}cr_1^2 + (3X_2 - 2c_2)r_1 + X_3 - \tfrac{1}{2}c_3, \qquad (2.74)$$

$$\vdots \ = \ \vdots . \qquad (2.75)$$

The X_n are the constants of integration and are clearly unpredictable within renormalisation group arguments. As such they will be RS-invariant and Q-independent[4]. Comparing the X_n with the ρ_n of the EC formalism we find that they are closely related [32],

$$\begin{aligned} X_2 &= \rho_2, \\ X_3 &= \rho_3/2, \\ X_4 &= \rho_4/3 + c\,\rho_3/6 + 2\rho_2^2, \\ \vdots &= \vdots \end{aligned} \qquad (2.76)$$

At NNLO in the $\overline{\text{MS}}$ scheme we can obtain X_2 by setting $\mu = Q$,

$$X_2 = r_2^{\overline{\text{MS}}}(\mu = Q) - (r_1^{\overline{\text{MS}}}(\mu = Q))^2 - cr_1^{\overline{\text{MS}}}(\mu = Q) + c_2^{\overline{\text{MS}}}. \qquad (2.77)$$

---

[4]This is because any scheme or scale dependence will obey the RGE and hence contribute through the scheme parameters.

We stress that this is a RS invariant combination and would be the same regardless of the choice of scheme.

Labelling the higher order coefficients in this way, the contributions from renormalisation are apparent. Rewriting Equation (2.4) in light of this we obtain

$$
\begin{aligned}
\mathcal{R}(Q) &= a + r_1 a^2 + (r_1^2 + c r_1 + X_2 - c_2)a^3 \\
&+ (r_1^3 + \tfrac{5}{2}c r_1^2 + (3X_2 - 2c_2)r_1 + X_3 - \tfrac{1}{2}c_3)a^4 + \dots .
\end{aligned}
\tag{2.78}
$$

At this stage the CORGI proposal is to include *all* the renormalisation group predictable terms to all orders leaving only the purely unpredictable X_n that can only be obtained via explicit higher order calculations. We define the complete subset of RG-terms as

$$
a_0 \equiv a + r_1 a^2 + (r_1^2 + c r_1 - c_2)a^3 + (r_1^3 + \tfrac{5}{2}c r_1^2 - 2c_2 r_1 - \tfrac{1}{2})a^4 + \dots .
\tag{2.79}
$$

At NLO this will be the entirety of known terms and can be evaluated by realising that a_0 is a RS-invariant quantity. This can be understood by noting that the sum of Equation (2.78) is RS-invariant and that the elimination of the X_n terms cannot affect this. Now since the combination is completely invariant under a variation in scheme parameters, we are at liberty to choose any suitable values as this will be compensated in the sum total. Choosing $r_1 = 0, c_2 = 0, \dots, c_n = 0, \dots$ we see that since beyond the first term, every coefficient is polynomial in the scheme parameters, we are left with the task of evaluating the couplant in the scheme $a = a(r_1 = 0, c_2 = 0, c_3 = 0, \dots)$ which corresponds to the so called 't Hooft scheme [13] with $r_1 = 0$. Once again we stress that even though we are specifying a set of scheme parameters, the quantity a_0 is RS-invariant. To obtain the couplant we must solve the β-function equation. In light of our definition of $\Lambda_{\mathcal{R}}$ we may write this now as

$$
\frac{1}{a} + c \ln\left(\frac{ca}{1+ca}\right) = \tau - \int_0^a dx \left(-\frac{1}{B(x)} + \frac{1}{x^2(1+cx)}\right),
\tag{2.80}
$$

where now $B(x) = x^2(1 + cx + c_2 x^2 + \dots)$. To obtain a_0 we may set the c_n equal to zero giving,

$$
\frac{1}{a_0} + c \ln\left(\frac{ca_0}{1+ca_0}\right) = b \ln\left(\frac{Q}{\Lambda_{\mathcal{R}}}\right).
\tag{2.81}
$$

This may now be extended beyond NLO by recognising that the combination of terms proportional to X_n are equivalent to a_0^{n+1} resulting in

$$\mathcal{R}(Q) = a_0 + X_2 a_0^3 + X_3 a_0^4 + \dots, \tag{2.82}$$

which is simply the perturbation series in the RS with $r_1 = c_2 = c_3 = \dots = c_n = \dots = 0$ as can be seen by setting all scheme parameters to zero in Equation (2.78).

Concentrating on the NLO result we see that in evaluating a_0, we are really resumming all the r_1 dependence to all orders. This effectively resums all the $\ln \mu / \tilde{\Lambda}_{\mathrm{RS}}$ terms as has traditionally been advocated in renormalisation group improvement with the additional $\ln Q / \Lambda_{\mathcal{R}}$ terms that necessarily appear as previously indicated. This is highlighted by rewriting Equation (2.19) as

$$r_1(\mu) = b\ln\frac{\mu}{\tilde{\Lambda}_{\mathrm{RS}}} - b\ln\frac{Q}{\Lambda_{\mathcal{R}}}, \tag{2.83}$$

where μ is taken to be the scale defined in the renormalisation scheme "RS". The crucial observation is that r_1 is a difference of a scheme-dependent logarithm involving μ and a "physical" scheme-independent ultraviolet logarithm involving Q. For clarity we temporarily set $c = 0$ and at NLO can set $c_n = 0$. The couplant, $a(\mu)$ is then

$$a(\mu) = \frac{1}{b \ln \mu / \tilde{\Lambda}_{\mathrm{RS}}}, \tag{2.84}$$

with the RG-improved expression for $\mathcal{R}(Q)$ at NLO given from Equation (2.78) by

$$\mathcal{R}(Q) \approx a(\mu) + r_1(\mu)a^2(\mu) + r_1^2(\mu)a^3(\mu) + \dots. \tag{2.85}$$

Substituting Equation (2.83) for $r_1(\mu)$ and summing the geometric series one obtains,

$$\mathcal{R}(Q) = a(\mu) / \left[1 - \left(b\ln\frac{\mu}{\tilde{\Lambda}_{\mathrm{RS}}} - b\ln\frac{Q}{\Lambda_{\mathcal{R}}} \right) a(\mu) \right] = \frac{1}{b\ln(Q/\Lambda_{\mathcal{R}})}, \tag{2.86}$$

in which the unphysical μ-dependence has cancelled between $a(\mu)$ and the μ-dependent logarithms contained in $r_1(\mu)$. In the realistic case with nonzero c and c_n, the simple logarithm of $Q/\Lambda_{\mathcal{R}}$ is replaced by the expression involving the Lambert W-function of Equation (2.67). The key point is that the all-orders CORGI improvement can be carried out with *any* choice of μ to yield a μ-independent result. One has therefore directly traded unphysical μ-dependence for the physical Q-dependence.

In contrast standard NLO fixed-order perturbation theory is then manifestly inapplicable, since one has

$$\mathcal{R}_{\text{NLO}} = a(\mu) + \left(b\ln\frac{\mu}{\tilde{\Lambda}_{\overline{\text{MS}}}} - b\ln\frac{Q}{\Lambda_{\mathcal{R}}} \right) (a(\mu))^2 \ . \tag{2.87}$$

With μ constant, asymptotic freedom only arises if *all* the RG-predictable UV logarithms are resummed to *all-orders.*

2.5.5   Tainted Results from Using the "Physical" Scale

To further emphasise the connection of the suggested direct extraction of $\Lambda_{\overline{\text{MS}}}$ with the standard approach we can consider the following result for $\Lambda_{\overline{\text{MS}}}(r_1, \mathcal{R})$, which we define to be the value of $\Lambda_{\overline{\text{MS}}}$ obtained by fitting a NLO order perturbative calculation in a scheme corresponding to the NLO coefficient r_1, to the data $\mathcal{R}$. Notice that r_1 completely labels the scheme at NLO. We can directly convert r_1 into the $\overline{\text{MS}}$ scale μ since from Equations (2.83) we have

$$r_1 = r + b\ln\frac{\mu}{Q} \ . \tag{2.88}$$

It is then straightforward to derive the result [28]

$$\Lambda_{\overline{\text{MS}}}(r_1, \mathcal{R}) = \frac{\exp[f(r_1, \mathcal{R})/b]}{\mathcal{G}(\mathcal{R})} \Lambda_{\overline{\text{MS}}} , \tag{2.89}$$

where $f(r_1, \mathcal{R})$ is given by

$$f(r_1, \mathcal{R}) \equiv F(\mathcal{R}) - F\left(\frac{-1 + \sqrt{1 + 4r_1\mathcal{R}}}{2r_1} \right) + r_1 \ . \tag{2.90}$$

In the CORGI approach $r_1 = 0$ and we have $f(0, \mathcal{R}) = 0$, so that the value of $\Lambda_{\overline{\text{MS}}}$ obtained is $\Lambda_{\overline{\text{MS}}}/\mathcal{G}(\mathcal{R})$, as expected comparing Equations (2.63) and (2.64). Thus to the extent that $\mathcal{G}(\mathcal{R}){\approx}1$ we obtain the *actual* value of $\Lambda_{\overline{\text{MS}}}$. As we have argued that the estimate $\mathcal{G}(\mathcal{R}){\approx}1$ is the *best* we can do given only a NLO calculation since we are in complete ignorance of the deviations of $\mathcal{G}$ from unity, which will depend on the NNLO RS-invariant ρ_2 of Equation (2.49). Another way of saying this is that at asymptotic values of Q, Equation (2.64) will hold, and that the deviation of $\mathcal{G}(\mathcal{R})$ from unity provides an operational definition of how far from asymptotia we are, at $Q = M_Z$, say. The scatter of the $\Lambda_{\overline{\text{MS}}}$ values for different observables obtained from Equation (2.64) thus provides unambiguous information about the size of sub-asymptotic effects (uncalculated NNLO and higher perturbative corrections and

power corrections). Variation of the renormalisation scale taking $\mu = xQ$ with the "physical scale" $x = 1$ to give a central value, merely serves to confuse matters. For instance taking $r = 10$ and $\mathcal{R} = 0.05$, values typical of jet observables at $Q = M_Z$, we find $\exp[f(10, 0.05)/b] = 2.44$, and so using the "physical scale" the value of $\Lambda_{\overline{MS}}$ extracted will be $2.44\Lambda_{\overline{MS}}/\mathcal{G}(\mathcal{R})$. This will accurately determine $\Lambda_{\overline{MS}}$ if it fortuitously happens that $\mathcal{G}(\mathcal{R}) \approx 2.44$. We have, of course, no reason to suppose that $\mathcal{G}$ differs from unity to such a drastic extent, or correspondingly that the effect of uncalculated NNLO and higher-order perturbative corrections, and possible power corrections should be so large. Varying the scale simply introduces an extra *known* factor into the determination of $\Lambda_{\overline{MS}}$, which, *other things being equal*, i.e. if $\mathcal{G} \approx 1$, will give values very different from the true one.

2.6   RS-Invariance Beyond NLO

We have seen how the method of Effective Charges and Complete Renormalisation Group Improvement have provided a resolution to the renormalisation scale ambiguity by appealing to the asymptotic behaviour of physical observables. Yet beyond NLO we are faced with the additional scheme parameters entering and in these cases the EC and CORGI approaches differ. Both provide an RS-invariant treatment but are based on different assumptions. In this section we will address the problems inherent in tackling the scheme dependence at higher orders.

2.6.1   How Can Scheme Parameters be Scheme Invariants?

We begin by tackling the seemingly paradoxical question "**How can scheme parameters be scheme invariants?**". Within the EC formalism the scheme parameters c_n become those of the EC, namely ρ_n. We noted earlier that these ρ_n were actually scheme invariant quantities. How can a parameter that defines a choice of scheme not depend on the choice of scheme? If we consider the following argument we see that if they exist, they *must* be scheme invariant. We begin by considering any two RS's and in general these will result in different values of the r_n coefficients. We can then insist on the coupling to be all orders exact, i.e. there is a choice of scheme whereby this is possible. Since the coupling is now all orders exact it must be scheme invariant, after all it has become a physical observable. In making the

transition from *any* scheme to the unique one in which the coupling is the observable requires the c_n subtraction parameters to be defined such that no matter what the scheme and hence r_n coefficients, the c_n must take this into account in order to cancel them. Hence even though they are scheme parameters themselves, they comprise of a scheme invariant combination.

This is best illustrated by considering what happens explicitly to the scheme parameters in going to the EC scheme. We begin with a general (τ^A, c_n^A) set of parameters that *define a particular scheme, A.* We could likewise have renormalised in a completely different scheme, B with parameters (τ^B, c_n^B). At NLO we are required to fix a value for τ. As stressed earlier this means setting the *two* parameters, μ and $\tilde{\Lambda}_{RS}$. Specifying the renormalisation scheme A (or B) fixes the value of $\tilde{\Lambda}_{RS}$. It then remains to fix τ through μ^5 via three possibilities

1. Setting $\mu = xQ$ where x is a constant (Figure 2.1)

2. Setting $\mu = x\exp(-r_1(\mu = Q)/b)Q$ where x is a constant (Figure 2.2)

3. Setting μ to be any other function (Figure 2.3)

The first possibility corresponds to the standard physical scale setting. If $\mu = Q$ is chosen, two different schemes will clearly give two different estimates. In the other two cases, we see that the only possibility to get a scheme invariant result is by choosing $\mu = x\exp(-r_1(\mu = Q)/b)Q$. The reason for this is due to the additional factor of $\tilde{\Lambda}_{RS}$. The $e^{-r/b}$ factor is then needed to cancel the scheme dependence appearing from initially working in a particular scheme and hence, choice of $\tilde{\Lambda}_{RS}$. The x-factor is present to illustrate that there is an infinite set of RS-invariant possibilities. Crucially, with the specific case of τ we have the asymptotic nature of a physical observable at our disposal. This precisely defines a renormalisation scale of μ to be $\exp(-r_1(\mu=Q)/b)Q$. Beyond NLO, we have no such aid and are required to make further assumptions to specify how to incorporate such contributions. Here lies the difference between the EC and CORGI approaches.

---

[5] We note that even if we resum all μ dependence such that its value is irrelevant, there will be a specific value of μ that reproduces this behaviour at NLO
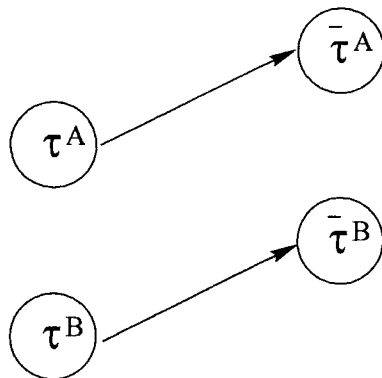
Figure 2.1: Pictorial representation of the mapping of τ, given in two different schemes A and B, to a particular value $\bar{\tau}$ by specification of μ. Choosing $\mu = xQ$ gives a constant shift equivalent to selecting the physical scale. This clearly gives differing results between schemes
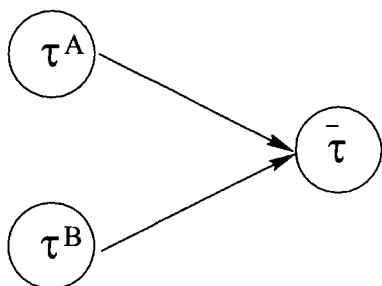
Figure 2.2: Fixing $\bar{\tau}$ by choosing $\mu = x \exp(-r_1(\mu = Q)/b)Q$ gives the same result regardless of the initial renormalisation scheme.
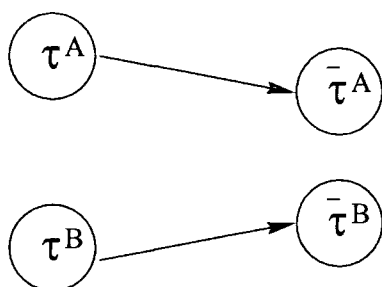
Figure 2.3: Fixing $\bar{\tau}$ by choosing $\mu = x\phi(Q)$ where $\phi(Q)$ differs from $e^{-r/b}Q$ gives differing results between schemes.

2.6.2 Differences between RS-Invariant Formulations Beyond NLO

We have just seen how formulating a RG-invariant approach to perturbation theory does not remove the *scheme* ambiguity. The renormalisation scale has special

significance and permits a unique specification. In contrast no plausible argument exists for dealing with the subtraction parameters. Any method that proposes to resolve the *scheme* dependence must make a further assumption in how to deal with the higher order contributions. For the EC formalism this corresponds to making an assumption that the optimal solution is the one in which all higher order corrections vanish. While seemingly innocuous this statement is not necessarily true. This is because given a N^nNLO calculation, we know absolutely nothing about the magnitude of higher order terms. Arranging the perturbation series such that all lower order coefficients are zero will not necessarily give an approximant closer to the all orders value. We could conversely have specified that we wish to include all renormalisation group predictable information akin to the CORGI philosophy. Even this does not specify unique criteria beyond NLO [33]. It suffices to say that the methods of Effective Charges and CORGI incorporate the correct Q dependence and beyond this we are required to make further assumptions upon the behaviour of QCD.

2.7 Power Correction

In this section we consider how to include power corrections in the EC formalism. It is widely accepted that physical observables in general will be subject to "non-perturbative" power-like corrections in the hard interaction scale, Q. That is to say, there will be terms contributing to cross-sections that cannot be expanded out in the typical perturbative manner arising from expressions of the form

$$\left(\frac{\Lambda}{Q}\right)^k = \exp\left(\frac{-k}{b\,\alpha_s}\right). \tag{2.91}$$

Perturbative techniques cannot describe these terms accurately but have made attempts at predicting the leading behaviour to the power corrections via renormalon-inspired analysis [35, 36] and dispersive techniques [37]. Taking the generic form of these power corrections, we can alter our perturbative expansion for a dimensionless observable $\mathcal{R}$,

$$\mathcal{R} = a + r_1 a^2 + r_2 a^3 + \ldots + \frac{\lambda_0}{Q}(1 + \lambda_1 a + \lambda_2 a^2 + \lambda_3 a^3 + \ldots), \tag{2.92}$$

where we have assumed a leading power correction with exponent 1 (i.e. $\frac{1}{Q}$). To include these term in the EC analysis, we must take the derivative with respect to Q.

We may then rewrite our expression for the EC β-function equation incorporating this effect as

$$
\begin{aligned}
\frac{\mathrm{d}\mathcal{R}}{\mathrm{d}\ln Q} &= -b\mathcal{R}^2(1 + c\mathcal{R} + \rho_2\mathcal{R}^2 + \rho_3\mathcal{R}^3 + \dots) \\
&\quad + \kappa_0\mathcal{R}^{-c/b}e^{-1/b\mathcal{R}}(1 + \kappa_1\mathcal{R} + \dots) + \dots,
\end{aligned}
\tag{2.93}
$$

where the κ_n can be related to the λ_n. For example, the leading power correction coefficient gives a $-\lambda_0/Q$ contribution to the β-function. Using Equation (2.52) to get Q in the leading approximation of $\mathcal{R}$ we find,

$$
Q \approx \Lambda_{\mathcal{R}} e^{1/b\mathcal{R}}(c\mathcal{R})^{c/b}.
\tag{2.94}
$$

Substituting this back in we obtain

$$
\lambda = -\kappa_0 e^{r_1(\mu=Q)/b}\left(\frac{b}{2}\right)^{c/b}\Lambda_{\overline{\mathrm{MS}}},
\tag{2.95}
$$

where we have converted Λ_R to $\Lambda_{\overline{\mathrm{MS}}}$. Having made the connection between κ_0 and λ_0 we may incorporate the power correction term into Equation (2.63) via the $\mathcal{G}(\mathcal{R}(Q))$ function given in Equation (2.57). Expanding out $\mathcal{G}(\mathcal{R}(Q))$ to the accuracy of NNLO and leading power correction gives

$$
\mathcal{G}(\mathcal{R}(Q)) \simeq 1 - \frac{\rho_2}{b}\mathcal{R} + \frac{\kappa_0}{b}\frac{e^{-1/b\mathcal{R}}}{\mathcal{R}^2}\mathcal{R}^{-c/b}.
\tag{2.96}
$$

Substituting this back into Equation (2.63) we finally obtain

$$
\Lambda_{\overline{\mathrm{MS}}} = Q\,\mathcal{F}(\mathcal{R}(Q))\left(1 - \frac{\rho_2}{b}\mathcal{R} + \frac{\kappa_0}{b}\frac{e^{-1/b\mathcal{R}}}{\mathcal{R}^2}\mathcal{R}^{-c/b}\right)e^{-r/b}\left(\frac{2c}{b}\right)^{c/b}.
\tag{2.97}
$$

Given a value for $\Lambda_{\overline{\mathrm{MS}}}$ we are now in a position to make a direct extraction of the leading power correction benefiting from the correct scale dependence of the EC formalism.

2.8   Applying Renormalisation Group Improvement to Experimental Data

In the preceding sections we have demonstrated how one can avoid the renormalisation scale ambiguity. This requires at least a NLO calculation to incorporate the proper *asymptotic scaling* behaviour. There now exists a wide variety of e^+e^- jet

observables at sufficient accuracy to warrant a detailed investigation. In applying the RG-improved treatment we would expect to remove the further confusion induced by not summing all the μ logarithms as occurs with the physical scale. At NLO we can test QCD by attempting to extract the single free parameter, namely $\Lambda_{\overline{MS}}$, using Equation (2.64)[6]. Deviations from a constant value between different observables can then safely be attributed to higher orders and power corrections (to the extent that these hold true). Turning this statement on its head we can accept that there will be a constant scale Λ of the theory and attempt to extract the magnitude of these higher orders contributions and power corrections. In the leading approximation these will be parameterised by ρ_2 and K_0. Setting a value for Λ then permits an extraction of these two quantities.

In the forthcoming section we shall apply this formalism to the large number of three and four-jet event shape variables measured at the LEP and SLC accelerators. Furthermore we concentrate on the thrust distribution for which experimental data exists at a wide range of centre-of-mass energies permitting the investigation of higher order contributions and power corrections.

We note that in all this discussion we have considered strictly massless quarks. In reality the dimensional transmutation parameter has a dependence on the number of active quark flavours, N_f, so really we have $\Lambda_{\overline{MS}}^{(N_f)}$. The NLO correction r and the universal β-function coefficients b and c, in Equations (2.63) and (2.64) also depend on N_f. Transformation between $\Lambda_{\overline{MS}}^{(N_f)}$ for different values of N_f can be effected using the standard apparatus of the decoupling theorem augmented with a matching condition [38]. The matching condition has now been computed to the three-loop level [39]. For all of our analysis $N_f = 5$ will be the active number of flavours, and we shall be extracting $\Lambda_{\overline{MS}}^{(5)}$.

2.9 Summary

In this chapter we investigated the ambiguities arising as a result of renormalising the parameters and fields of the Lagrangian. In particular we saw that for physical observables, the renormalised coupling introduces an unphysical dependence on the renormalisation scheme when a perturbative calculation is truncated at a finite

---

[6]Of course we could have chosen any universal scheme dependent Λ

order. After illustrating the common schemes, we demonstrated how to parameterise this dependence through the non-universal β-function coefficients, c_n. We then examined the various proposals for remedying this dependence indicating the negative aspects of applying the popular physical scale and the importance of specifying two parameters (μ and $\tilde{\Lambda}_{\mathrm{RS}}$) at NLO to give an unambiguous answer. The approaches of the PMS and EC illustrated this requirement and in particular that of the EC highlighted the benefits of concentrating on the energy dependence of physical observables.

Drawing upon the fact that all physical quantities gain their scale dependence purely through the renormalised coupling, we were able to demonstrate a procedure for treating the renormalisation scale dependence by requiring observables to have the correct asymptotic $Q \to \infty$ limit. This was then demonstrated to be entirely equivalent to complete resummation of the ultraviolet logarithms to all orders. Subsequently we highlighted the difficulties beyond NLO where the freedom to choose subtraction parameters is manifest. In this analysis we restrict ourselves to the more conservative claim of resolving the renormalisation *scale* ambiguity and providing a RS invariant prescription for beyond NLO corrections.

Finally we explored the possibility of incorporating power-like corrections to the RG-improved formalism. We demonstrated how to include the leading term in a consistent manner with the energy dependence, providing a means of investigating the magnitude of such contributions .

Chapter 3

Observables

3.1 Introduction

In Chapter 1 we saw how QCD perturbation theory was able to make definite pre-
dictions about the final state of the process $e^+e^- \to$ hadrons. Specifically we would
expect to see the majority of events occurring as back-to-back jets with the frac-
tion of well separated three-jet-like events suppressed by an order of α_s due to the
emission of a hard gluon. In fact the observation of three-jet events by the TASSO
collaboration at the PETRA collider at DESY [40] is taken as experimental evidence
for the very existence of gluons. Before any definite measurements can be made, it
is necessary to clarify what we mean by a jet. Qualitatively, a jet can be understood
with reference to a *hard* parton emitting soft and collinear radiation and undergoing
hadronisation. We would therefore like to impose a *jet measure* that respects these
qualities by being infrared safe and relatively insensitive to the non-perturbative
fragmentation of the partons. From a theoretical perspective, this corresponds to
imposing an infrared cut-off in phase space, specifying the number of "hard" partons
calculated in perturbation theory. Experimentally we can make contact with this
prediction by applying a jet-clustering algorithms that groups together final state
hadrons into some semblance of the underlying hard partons. In order to implement
these ideas, we require a precise definition of the resolution cut and a procedure for
recombining the final state particles. We shall discuss the various possibilities in the
next section.

Complementary to the idea of jets are the event shape variables. These typify
the hadronic structure in much the same way as a jet clustering algorithm would,
except rather than specify the number of jets according to a resolution parameter,

they describe the physical characteristics of the final state hadrons. Nevertheless an event shape variable may still be categorised as n-jet-like according to when its distribution becomes non-zero for n final state hard partons and above. In e^+e^- annihilation this corresponds to perturbative coefficients becoming non-zero at order α_s^{n-2}.

In this chapter we shall explore the consequences of applying the RG-improved perturbation theory to these e^+e^- jet observables. We have already seen that this requires at least a NLO calculation to treat the scale dependence correctly. This permits an analysis of the wide range of *three* and *four*-jet observables. The three-jet variables have a long history with NLO coefficients first calculated in 1981 for the three-jet cross section [41] and extended to numerous event shape distributions by [42]. In contrast, the NLO coefficients for the four-jet observables have only recently become available via four separate general purpose Monte Carlo programs: MENLO PARC [43], DEBRECEN [44] and MERCUTIO [45] employing the one-loop helicity amplitudes for $e^+e^- \rightarrow 4$ partons [46, 47] and EERAD2 [48] based on the interference of the one-loop matrix element with tree level [49, 50].

We shall commence by defining the set of jet variables (three and four-jet like) that we shall be considering in this analysis (Section 3.2) and how to extract a value for $\Lambda_{\overline{MS}}$ across the kinematic range (Section 3.3). This will be followed by an investigation of the three-jet like case with extraction of $\Lambda_{\overline{MS}}$ at NLO (Section 3.4) and a discussion of the results (Section 3.5). We shall then repeat the procedure for four-jet like variables (Sections 3.6–3.7).

Finally we shall consider the energy dependence of event shape distributions in the special case of 1-thrust, with the possibility of fitting a generic power correction (Section 3.8) before summarising the whole chapter (Section 3.9).

3.2   Definitions of the Jet Observables

We restrict ourselves throughout to infrared safe observables and make all definitions in the centre-of-mass frame, with all sums running over N final state particles. We begin with the various jet definitions.

3.2.1   Jet Rates

As mentioned earlier there are a number of different possibilities for clustering particles to form jets. Given a particular jet measure, y_{ij} the following algorithm is common to all,

1. Define a resolution parameter, y_{cut}.

2. For every pair of hadrons, h_i and h_j, evaluate the jet measure, y_{ij}.

3. If the smallest occurrence of this quantity is less than the resolution parameter (i.e. $\min(y_{ij}) < y_{cut}$) combine the corresponding hadron momenta, p_i and p_j into that of a pseudo-particle, p_{ij} according to a recombination prescription.

4. Repeat steps 2–4 until all hadrons and pseudo-hadrons have jet measures greater than the resolution parameter. What remains are then denoted *jets*.

By introducing a jet resolution parameter, y_{cut}, we have made our definition of a jet intrinsically infrared safe. Increasing its value permits a greater number of clusterings and thus few jet events are identified. Likewise, decreasing its value finally results in all final state hadrons being assigned to separate jets. Within the theoretical framework, such small values probe deeply into the infrared region and thus require a thorough treatment of hadronisation. Jet measures are typically normalised by the total visible energy of the hadronic event, E_{vis}, to give a dimensionless quantity.

For a description of the multitude of different algorithms with their merits see [51]. For this analysis we shall restrict ourselves to the *JADE, Durham* and *Geneva* jet finding measures applied by the various experimental collaborations.

The JADE Algorithm

The first jet measure to be proposed was by the **JADE** collaboration [52] and simply uses,

$$y_{ij}^J = \frac{2E_i E_j (1 - \cos\theta_{ij})}{E_{\text{vis}}^2} \approx \frac{M_{ij}^2}{E_{\text{vis}}^2}, \tag{3.1}$$

where E_l denotes the energy of a hadron, l in the centre-of-mass frame and θ_{lm} is the opening angle of the pair under consideration. In the massless limit this measure

corresponds to their invariant mass, M_{ij}^2. Having defined the jet measure we are still at liberty to define the procedure for recombining two hadrons into a pseudo-hadron. There are four immediately obvious possibilities, denoted the E, $E0$, P and $P0$ schemes. In all cases the subscript k denotes the pseudo-particle created by particles i and j.

E scheme:

In the E scheme, we combine two particles according to their four-momenta,

$$p_k = p_i + p_j. \qquad (3.2)$$

Energy and momentum are explicitly conserved in this scheme.

E0 scheme:

In this scheme the three-momenta of the pseudo-particle is rescaled to give it zero invariant mass,

$$E_k = E_i + E_j, \qquad (3.3)$$

$$\mathbf{p}_k = \frac{E_k}{|\mathbf{p}_i + \mathbf{p}_j|}(\mathbf{p}_i + \mathbf{p}_j). \qquad (3.4)$$

As a result the total momentum sum of the event is not conserved.

P scheme:

Conversely we may conserve the total momentum of the event at the expense of the total energy conservation using

$$\mathbf{p}_k = \mathbf{p}_i + \mathbf{p}_j, \qquad (3.5)$$

$$E_k = |\mathbf{p_k}|. \qquad (3.6)$$

P0 scheme:

Lastly we introduce a variation of the P scheme by altering the jet measure such that after recombination, the total visible energy is changed such that,

$$E_{\text{vis}} = \sum_k E_k. \qquad (3.7)$$

Unfortunately the JADE jet measure turns out to introduce spurious clusterings in certain circumstances whereby a resultant jet is formed in a direction lacking any approximately collinear initial hadrons. This translates into theoretical problems

when attempting to perform large infrared logarithm resummations where these correlations spoil the property of exponentiation in the two-jet limit [53][1].

The Durham (or $k_\perp$) Algorithm

A subsequent attempt to suppress artificial recombinations within the jet clustering and hence improve its theoretical properties was suggested by Dokshitzer et al. [54], termed the **Durham** or $k_\perp$-algorithm. It uses the minimum relative transverse momenta of two hadrons in the small angle limit,

$$y_{ij}^D = \frac{2 \, \min(E_i^2, E_j^2)(1 - \cos\theta_{ij})}{E_{\text{vis}}^2}. \tag{3.8}$$

This form of clustering reduces the number of spurious recombinations and permits a straightforward theoretical implementation (see Chapter 4). As such it has now become the standard algorithm in use. We use the E scheme recombination.

The Geneva Algorithm

Lastly we consider a variant termed the **Geneva** algorithm proposed by Bethke et al. [55] that also attempts to reduce the spurious mis-clusterings of the Jade algorithm using the measure,

$$y_{ij}^G = \frac{8}{9} \frac{E_i E_j (1 - \cos\theta_{ij})}{(E_i + E_j)^2}. \tag{3.9}$$

In contrast to the previous two proposals, the Geneva algorithm does not depend on the energy of the event, and has a preference to combine soft particles with hard ones. This in turn reduces the correlations between soft gluons when performing infrared logarithm resummations. We also use the E scheme for recombination.

With the jet finding algorithms in place we may now determine the n-jet rates $(R_n(y_{cut}))$ by the fraction of events with n resultant jets after clustering. We may then define the jet transition parameters, $y_{n\,n+1}$ that corresponds to the value of y_{cut} where an event changes from $n + 1$-jet-like to n-jet-like.

---

[1]Infrared logarithm resummations and the property of exponentiation will be discussed in Chapter 4

3.2.2 Event Shape Variables

Many of these variables are related and can be broadly categorised as follows. Note that they will in general contain both three and four-jet-like quantities.

Thrust and Related Variables

Thrust (T) is defined by maximising the net longitudinal momentum of final state particles along the direction of a thrust axis [56],

$$T = \max \frac{\sum_i |\mathbf{p}_i \cdot \mathbf{n}_T|}{\sum_i |\mathbf{p}_i|} \,, \tag{3.10}$$

where $\mathbf{p}_i$ denotes the final state particle momenta, and $\mathbf{n}_T$ denotes the unit vector in the direction of the thrust axis, to be determined by maximising the above quotient. Defining for convenience $\tau \equiv 1 - T$, we find that τ varies between zero, for two back-to-back final state partons, up to a maximum of $\tau = \frac{1}{2}$ for spherical (isotropic) events. For planar events with three final-state partons, one finds a maximum value of $\tau = \frac{1}{3}$ corresponding to a "Mercedes Benz" configuration. Two further variants, **thrust-major** (T_{maj}) and **thrust-minor** (T_{min}) can be defined. In T_{maj} the thrust axis $\mathbf{n}_T$ is replaced in Equation (3.10) by $\mathbf{n}_{\mathrm{maj}}$, which maximises the sum of momenta transverse to the thrust axis. In T_{min} it is replaced by an axis $\mathbf{n}_{\mathrm{min}}$ which is the vector cross product of $\mathbf{n}_T$ and $\mathbf{n}_{\mathrm{maj}}$. One can then define the **oblateness** O by [57]

$$O \equiv T_{\mathrm{maj}} - T_{\mathrm{min}} \,. \tag{3.11}$$

Invariant Mass Measures

Events can also be divided into two hemispheres ($\mathbf{H}_a, \mathbf{H}_b$) by a plane perpendicular to $\mathbf{n}_T$. We may then calculate the normalised invariant mass of each hemisphere ($x = a, b$) [58],

$$\rho_x = \frac{M_x^2}{E_{\mathrm{vis}}^2} = \frac{1}{E_{\mathrm{vis}}^2} \left(\sum_{\mathbf{p}_k \in \mathbf{H}_x} p_k \right)^2 \,. \tag{3.12}$$

This permits the possibility of four obvious combinations giving rise to

$$\rho_T = \rho_a + \rho_b, \tag{3.13}$$

$$\rho_D = |\rho_a - \rho_b|, \tag{3.14}$$

$$\rho_H = \max(\rho_a, \rho_b), \tag{3.15}$$

$$\rho_L = \min(\rho_a, \rho_b), \tag{3.16}$$

which correspond to the **sum of jet masses**, the **difference of jet masses**, the **heavy jet mass** and the **light jet mass** respectively. To lowest order in perturbative QCD, and assuming massless quarks, thrust and heavy jet mass are related by $\tau = \rho_H$ [42].

Jet Broadening Measures

Other variants on thrust and jet masses are the **jet broadening** measures proposed in [59]. In each of the above hemispheres a and b one forms a jet broadening, B, by summing over the particles in that hemisphere,

$$B_x = \frac{\sum_{\mathbf{p}_k \in \mathbf{H}_x} |\mathbf{p}_i \times \mathbf{n}_T|}{2\sum_{\mathbf{p}_k \in \mathbf{H}_x} |\mathbf{p}_i|} \ . \tag{3.17}$$

Once again we may compose a range of variables by the combinations,

$$B_T = B_a + B_b, \tag{3.18}$$

$$B_D = |B_a - B_b|, \tag{3.19}$$

$$B_W = \max(B_a, B_b), \tag{3.20}$$

$$B_N = \min(B_a, B_b), \tag{3.21}$$

to make the **sum of hemisphere broadening**, the **difference of hemisphere broadenings**, the **wide hemisphere broadening** and the **narrow hemisphere broadening** respectively. For two-parton final states $B_T = B_W = B_D = 0$, and to lowest order in perturbation theory $B_T = B_W = B_D = \frac{1}{2}O = \frac{1}{2}T_{\max}$.

The C and D Parameters

We can also define the so-called C and D-parameters from the eigenvalues of the infra-red safe linear momentum tensor [60],

$$\theta_{mn} = \frac{\sum_i p_i^m p_i^n / |\mathbf{p}_i|}{\sum_i |\mathbf{p}_i|} \ , \tag{3.22}$$

where p_i^m is the m-th component of the three-momentum $\mathbf{p}_i$, with i summed over all final state particles. As defined the tensor has unit trace. The C-parameter is then defined in terms of the eigenvalues of the tensor $\theta_{\mu\nu}$, $\lambda_1, \lambda_2, \lambda_3$ by,

$$C = 3(\lambda_1\lambda_2 + \lambda_2\lambda_3 + \lambda_3\lambda_1) \ . \tag{3.23}$$

$C = 0$ for back-to-back two parton final states and $C = 1$ for spherical (isotropic) events. For planar three-parton final states $0 \leq C \leq \frac{3}{4}$ where one of the eigenvalues is zero. For values greater than $\frac{3}{4}$ requires at least four final state particles.

The D-parameter is defined by the combination

$$D = 27\lambda_1\lambda_2\lambda_3, \tag{3.24}$$

and only becomes non-zero for non-planar events (i.e. four or greater final states particles).

3.2.3   Particle Correlations

Rather than describe an event by a single variable, we may consider inclusive two-particle correlations. The **energy-energy correlation** (*EEC*) [61] is the normalised energy-weighted cross section defined in terms of the angle, χ_{ij}, between two particles i and j in an event,

$$EEC(\chi) \equiv \frac{1}{N\Delta\chi} \sum_{\text{events}} \int_{\chi-\frac{\Delta\chi}{2}}^{\chi+\frac{\Delta\chi}{2}} \sum_{i,j} \frac{E_i E_j}{E_{\text{vis}}^2} \delta(\chi' - \chi_{ij}) \mathrm{d}\chi', \tag{3.25}$$

where the argument, χ, is the opening angle to be studied for the correlations, $\Delta\chi$, is the angular bin width and N is the number of events. The angle χ can be varied in the range $0° \leq \chi \leq 180°$ where the central region ($\chi \sim 90°$) is governed by hard gluon emission and the extremities ($\chi \sim 0°$ and $180°$), corresponding to collinear and back-to-back configurations, are expected to be sensitive to hadronisation. We may further define the **asymmetric energy-energy correlation** (*AEEC*) to be

$$AEEC(\chi) = EEC(180° - \chi) - EEC(\chi), \tag{3.26}$$

where now χ is within the range $0°$–$90°$.

3.2.4   Angular Energy Flow

A recent addition to the set of $\mathrm{e}^+\mathrm{e}^-$ jet observables is the **jet cone energy fraction** (*JCEF*) [62]. Here the energy within a conical shell of opening angle χ about the thrust axis is integrated,

$$JCEF(\chi) = \frac{1}{N\Delta\chi} \sum_{\text{events}} \int_{\chi-\frac{\Delta\chi}{2}}^{\chi+\frac{\Delta\chi}{2}} \sum_{i} \frac{E_i}{E_{\text{vis}}} \delta(\chi' - \chi_i) \mathrm{d}\chi', \tag{3.27}$$

where

$$\chi_i = \arccos\left(\frac{\mathbf{p}_i \cdot \mathbf{n}_T}{|\mathbf{p}|}\right) \tag{3.28}$$

is the opening angle between a particle, i, and the thrust axis vector, n_T defined to point from the heavy jet mass hemisphere to the light jet mass hemisphere. The angle, χ, is within the range $0° \le \chi \le 180°$ and thus the hard gluon emissions will feature when $\chi \ge 90°$.

3.2.5   Categorising the Observables

All the observables previously defined are either three or four-jet like. Additionally, we shall also investigate the two-jet rate. In the subsequent analysis we utilise experimental data at the Z^0-peak from the SLD [63], ALEPH [64], DELPHI [65, 66], L3 [67] and OPAL [68] collaborations. For convenience we summarise the variables, with the collaborations that published the relevant data, into two, three and four-jet like categories.

- Two-Jet-Like Observables

  - The Two-Jet Rate, (R_2): ALEPH, OPAL

- Three-Jet-Like Observables

  - The Three-Jet Rate, (R_3): ALEPH, OPAL

  - $2 \to 3$ Jet Transition Variable (Jade- E scheme) (y_{23}^J): ALEPH, DELPHI, L3, SLD

  - $2 \to 3$ Jet Transition Variable (JADE- E0 scheme) (y_{23}^J): SLD

  - $2 \to 3$ Jet Transition Variable (JADE- P scheme) (y_{23}^J): SLD

  - $2 \to 3$ Jet Transition Variable (JADE- P0 scheme) (y_{23}^J): SLD

  - $2 \to 3$ Jet Transition Variable (Durham) (y_{23}^D): ALEPH, DELPHI, L3, OPAL, SLD

  - $2 \to 3$ Jet Transition Variable (Geneva) (y_{23}^G): SLD

  - 1-Thrust $(1 - T)$: ALEPH, DELPHI, L3, OPAL, SLD

  - Thrust Major $(T_{\max})$: DELPHI L3

- Oblateness (O): ALEPH, DELPHI, L3, OPAL, SLD

- Sum of Hemisphere Masses (B_T): DELPHI

- Difference in Hemisphere Masses (ρ_D): DELPHI, OPAL

- Heavy Hemisphere Mass (ρ_H): ALEPH, DELPHI, L3, OPAL, SLD

- Total of Jet Broadening (B_T): DELPHI, SLD

- Difference in Jet Broadening (B_D): DELPHI

- Wide Jet Broadening (B_W): DELPHI, SLD

- C-Parameter (C): ALEPH, DELPHI, L3, OPAL, SLD

- Energy-Energy Correlation (EEC): DELPHI, SLD

- Asymmetric-Energy-Energy Correlation ($AEEC$): DELPHI, SLD

- Jet Cone Energy Fraction ($JCEF$): DELPHI, SLD

- Four-Jet-Like Observables

    - 3 → 4 Jet Transition Parameter (Durham) (y_{34}^D): DELPHI

    - Thrust Minor ($T_{\min}$): DELPHI

    - Light Hemisphere Mass (ρ_L): DELPHI

    - Narrow Jet Broadening (B_N): DELPHI

    - D-Parameter (D): DELPHI

3.3 Applying RG-Improved Perturbation Theory

3.3.1 Issues at NLO

In this section we address the task of how to apply the RG-improved perturbation theory at NLO. We have already seen in the previous chapter that we may attempt to extract a value for $\Lambda_{\overline{MS}}$ at NLO, providing we believe that the centre-of-mass energy is sufficiently high to warrant an asymptotic approximation. In this case we obtain Equation (2.64) reproduced here for convenience,

$$\Lambda_{\overline{MS}} = Q \mathcal{F}(\mathcal{R}(Q)) e^{-r/b} (2c/b)^{c/b} \, . \tag{3.29}$$

We are faced with rewriting the jet observable cross-sections and distributions in the dimensionless form of Equation (2.4)

$$\mathcal{R}(Q) = a + r_1\, a^2 + r_2\, a^3 + \ldots + r_n\, a^{n+1} + \ldots . \tag{3.30}$$

For the three-jet-like observables, $\tilde{\mathcal{R}}_3$, we will in general have a perturbative expansion at NLO of the form[2]

$$\tilde{\mathcal{R}}_3(Q) = A_3 \frac{\alpha_s(\mu)}{2\pi} + B_3(\mu)\left(\frac{\alpha_s(\mu)}{2\pi}\right)^2 . \tag{3.31}$$

Correspondingly four-jet-like observables, $\tilde{\mathcal{R}}_4$ will have the expansion

$$\tilde{\mathcal{R}}_4(Q) = A_4 \left(\frac{\alpha_s(\mu)}{2\pi}\right)^2 + B_4(\mu)\left(\frac{\alpha_s(\mu)}{2\pi}\right)^3 , \tag{3.32}$$

where A_n denotes the μ independent tree-level coefficient of an n-jet-like quantity and B_n the NLO coefficient. We may then by simple algebraic manipulation rewrite these in terms of the required dimensionless quantity as

$$\mathcal{R}_3(Q) = \frac{2\tilde{\mathcal{R}}_3(Q)}{A_3} = \frac{\alpha_s(\mu)}{\pi} + \frac{B_3(\mu)}{2A_3}\left(\frac{\alpha_s(\mu)}{\pi}\right)^2 \tag{3.33}$$

and

$$\mathcal{R}_4(Q) = \sqrt{\frac{4\tilde{\mathcal{R}}_4(Q)}{A_4}} = \frac{\alpha_s(\mu)}{\pi} + \frac{B_4(\mu)}{4A_4}\left(\frac{\alpha_s(\mu)}{\pi}\right)^2 . \tag{3.34}$$

We are now in a position to calculate $\Lambda_{\overline{\rm MS}}$ from Equation (3.29) by substituting the experimental values of $\mathcal{R}(Q)$ and the fundamental quantity, $r_1(\mu = Q)$ which can be read off Equations (3.33) and (3.34). We may then apply this to every experimental bin, enabling a direct extraction of $\Lambda_{\overline{\rm MS}}$ across the kinematic range of the variable. In all cases we use the Monte Carlo programs EERAD [69] and EERAD2 [48] to calculate the fixed order coefficients for three and four jet quantities respectively.

Before we attempt to extract a value for $\Lambda_{\overline{\rm MS}}$ there are a number of important issues worth considering. Firstly we must remember that even though we have defined a set of observables that attempt to reflect the underlying behaviour of the QCD partons, the effects of hadronisation will always be present. In some

---

[2]The two-jet case is equivalent to the three-jet case with the substitution $\tilde{\mathcal{R}}_3 \to (1 - \tilde{\mathcal{R}}_2)$.

observables this will be more pronounced in certain regions of phase space resulting in the perturbative prediction failing to provide a reliable description. A number of Monte Carlo programs exist [70, 71] that attempt to model this behaviour and have proved very successful. In addition non-perturbative power corrections have been studied phenomenologically and have displayed very positive results too.

Secondly, from a purely perturbative QCD perspective, semi-inclusive quantities suffer from large kinematic logarithms at the exclusive boundaries of phase space. This manifests itself in the r_1 parameter, growing in magnitude typically like $-\ln^2 \lambda$ for a variable λ that goes to zero in the two-jet configuration. This drags the value for $\Lambda_{\overline{MS}}$ to zero regardless of the true value. This indicates a breakdown in the NLO approximation since higher order terms will be enhanced by powers of logarithms requiring an all-orders resummation. This will be considered in the next chapter. Furthermore, at the opposite end of the kinematic range we typically encounter a similar problem due to an end point in phase space. These occur when a variable goes from being n-jet-like to $(n+1)$-jet-like. Examples of this are the 1-thrust at $\frac{1}{3}$ and the C-parameter at $\frac{3}{4}$. Above these values, the three-jet configurations do not contribute, resulting in the tree level term vanishing. Clearly this now upsets our definition of r_1 since it diverges in a direction governed by the relative sign difference between LO and NLO in this limit. These characteristics can be seen in Figure 3.1 for the 1-thrust variable and Figure 3.2 for the thrust minor variable. A more sophisticated way of handling the end point problem would be to define a new r_1 value according to the ratio of the order α_s^3 coefficient to order α_s^2 in the region corresponding to non-zero four-jet configuration contributions and then smoothly interpolate a value across the threshold.

These two difficulties must be taken into consideration when attempting to extract a value for $\Lambda_{\overline{MS}}$. For a number of the three-jet quantities, hadronisation corrected data is analysed [72], providing a means to reducing that uncertainty. In these cases the Jetset 7.4 hadronisation model was implemented (unless otherwise stated) using bin-by-bin correction factors with errors estimated via statistical uncertainty. These factors were calculated as specified in [63] and [66].

Finally it should always be remembered that it is by no means certain that a centre-of-mass energy of M_Z provides a reasonable approximation to asymptotia. It may therefore prove important to include higher order corrections to enable a
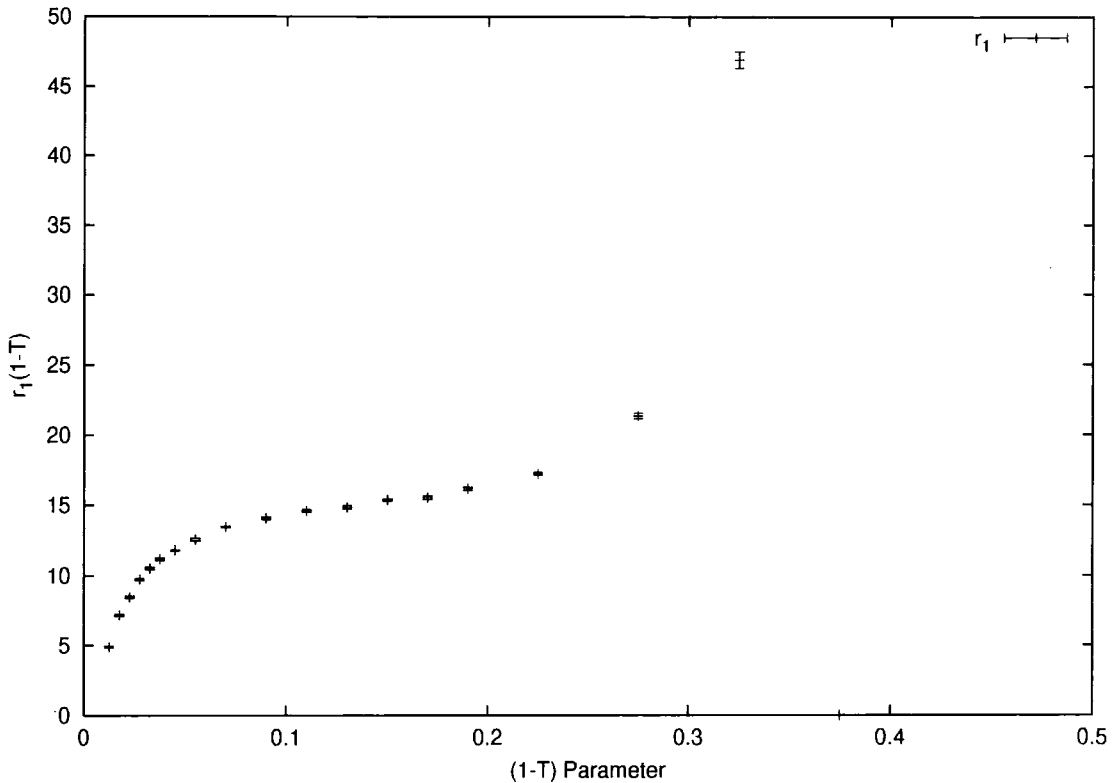
Figure 3.1: The r_1 parameter as a function of 1-thrust. It is calculated according to the ALEPH experimental bin sizes with errors attributed to the Monte Carlo integration of the LO and NLO coefficients only.

justifiable termination of the perturbation series. In the following section we consider the data analysis of the fitting procedure.

3.3.2 Data Analysis

Having identified the possible difficulties arising we must specify a set of criteria to perform a direct extraction of $\Lambda_{\overline{MS}}$. This should concentrate on a plateau region of $\Lambda_{\overline{MS}}$ in the central region of the kinematic range of the variable. We have adopted the following procedure for specifying the fit range,

1. Decrease the fit range from its maximum value such that all r_1 values lie within a variation of 20% from the flattest region.

2. Decrease the range further (if necessary) to the region where hadronisation corrections are less than 40%.
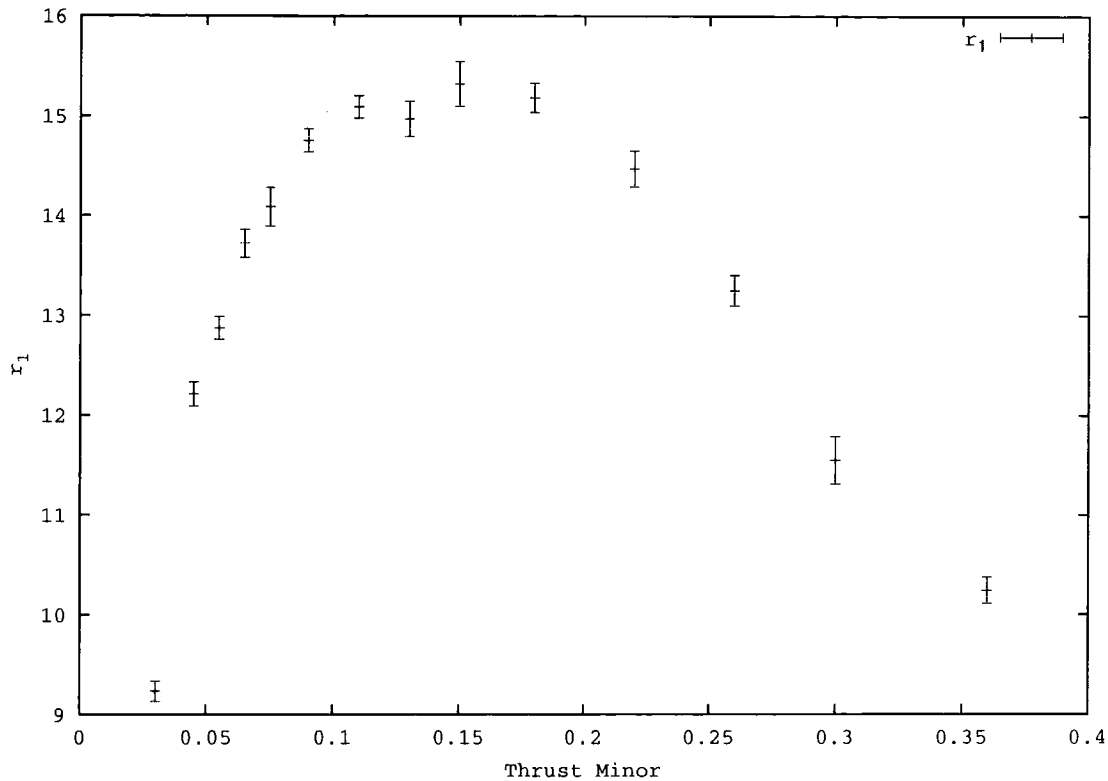
Figure 3.2: The r_1 parameter as a function of thrust minor. It is calculated according to the DELPHI experimental bin sizes with errors attributed to Monte Carlo integration of the LO and NLO coefficients only.

3. If more than three points are present, perform a single parameter χ^2 fit to a flat line to calculate a value for $\Lambda_{\overline{MS}}$ with error.

4. Rescale the error according to $\sqrt{\chi^2/N_{df}}$ to obtain a $\Lambda_{\overline{MS}}$ prediction for the given variable and collaboration.

If at any stage there are fewer than four consecutive bins surviving, the jet variable is considered unsuitable for the analysis. There is, of course, no guarantee that a variable will have a flat plateau over which to perform the fit. It may be such that the kinematic boundary effects dominate over the complete range. In these cases we are forced to disregard the variable.

We have chosen to use an r_1 criterion to avoid the problem of large kinematic logarithms spoiling the fixed order perturbation theory. The parameter, r_1, clearly indicates the region where these logarithms are dominating the series and hence the

breakdown of the NLO approximation. The value of r_1 does not indicate where hadronisation effects may be considerable though. Therefore in order to give a proper treatment of the variables, we should use experimental data that has been corrected for hadronisation effects. We attempt to include a reasonably flat region across r_1 by allowing a 20% deviation from flatness (with errors taken into account). Since the r_1 parameter varies smoothly across the kinematic range, this criterion permits a good measure of flatness. The value of 20% is chosen to tolerate minor deviations in r_1 in the vicinity of the end points and any statistical fluctuations from evaluation of the NLO coefficients which are typically small. The resulting fit range should be relatively insensitive to small variations in the permitted percentage deviation.

If hadronisation corrected data is available, we have adopted the procedure presented in a [63] for excluding any bins that suffer from greater than a 40% correction.

Finally, we adopt a minimum χ^2 test for fitting a flat line to the data points. The initial error (induced by $\Delta\chi^2 = 1$ from minimum) associated with the fit is then scaled by $\sqrt{\chi^2/N_{df}}$ for N_{df} degrees of freedom as promoted in the review of particle physics [6]. This provides a value of $\Lambda_{\overline{MS}}$ for each observable measured by each collaboration. We must then consider how to combine the values.

3.3.3 Procedure for handling the errors

In considering the forthcoming fits, we must be careful not to underestimate the errors. Dealing with different experiments' measurements of the same observable will obviously have strong correlations. Typically the greatest difference between data sets will be due to statistical errors especially in the cases without any hadronisation corrections being applied. A procedure has been put forward by Schmelling [73], termed the *method of correlated averages*, to combine correlated data when the exact correlation matrix is unknown. In this case, it is suggested that the degree of correlation is set by the χ^2/N_{df} value of the data set. In this way we are able to combine any number of correlated data without an unnatural reduction in the error. Similarly when combining errors with a χ^2/N_{df} greater than one we adopt the standard technique of rescaling the error by $\sqrt{\chi^2/N_{df}}$ to improve the error estimation according to the quality of the fit.

3.4 Results of Extracting $\Lambda_{\overline{\text{MS}}}$ from Three-Jet Observables

In this section we present the results of fitting a constant value of $\Lambda_{\overline{\text{MS}}}$ to the three-jet observables' data sets. All observables are considered separately in turn. Since hadronisation corrections must be applied bin-by-bin, we may only consider a complete discussion of those variable for which such corrections are available. Therefore in the case where hadronisation corrected data is present, it is plotted together with the uncorrected data for that experimental collaboration in a separate figure. In this way, we may contrast between them to the see the effect on $\Lambda_{\overline{\text{MS}}}$. All remaining uncorrected data is then displayed in a single plot.

The experimental data for the three-jet observables (uncorrected for hadronisation effects) is taken from [63] for SLD data, [64] for ALEPH data, [65] for DELPHI data, [67] for L3 data and [68] for OPAL data. Additionally, hadronisation corrected data [72] is applied where available.

The fit ranges are marked as dashed vertical lines and the resultant fitted $\Lambda_{\overline{\text{MS}}}$ value is plotted as a dashed line in the colour of the data points of the collaboration.
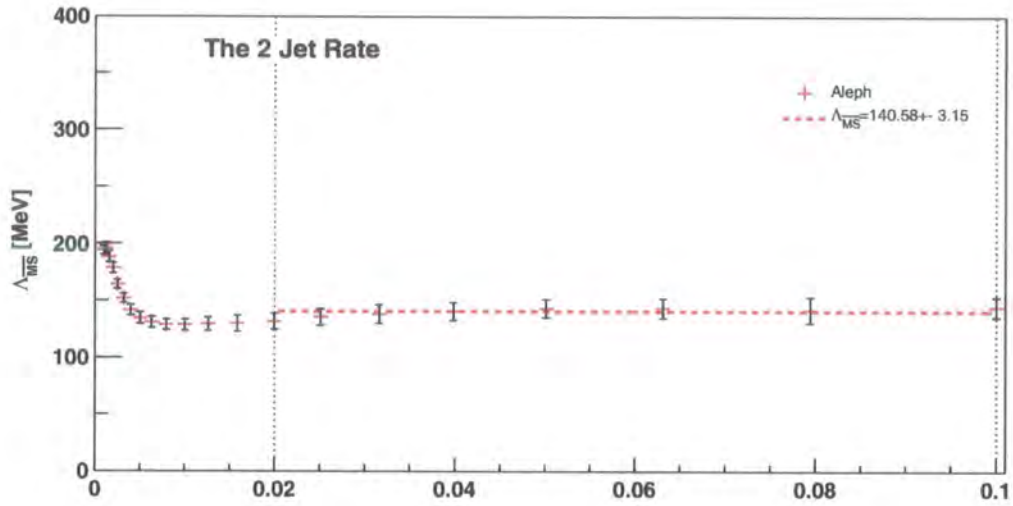
Figure 3.3: The 2 Jet Rate using ALEPH data
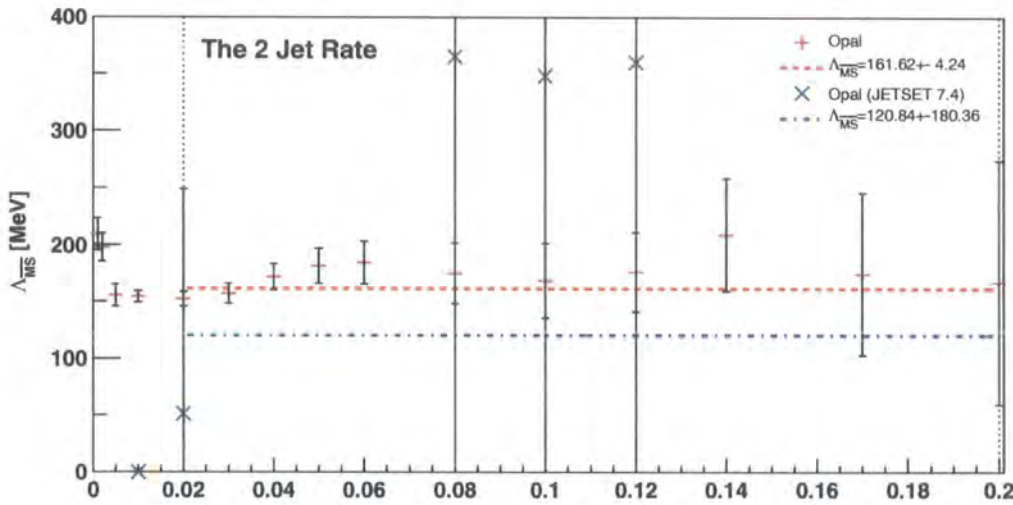
Figure 3.4: The 2 Jet Rate using OPAL data both hadronisation uncorrected and corrected
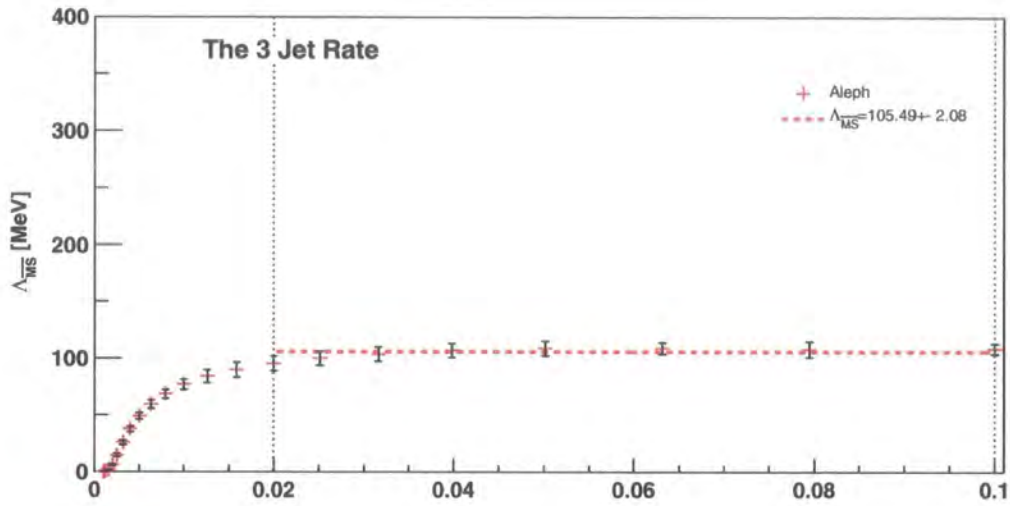
Figure 3.5: The 3 Jet Rate using ALEPH data
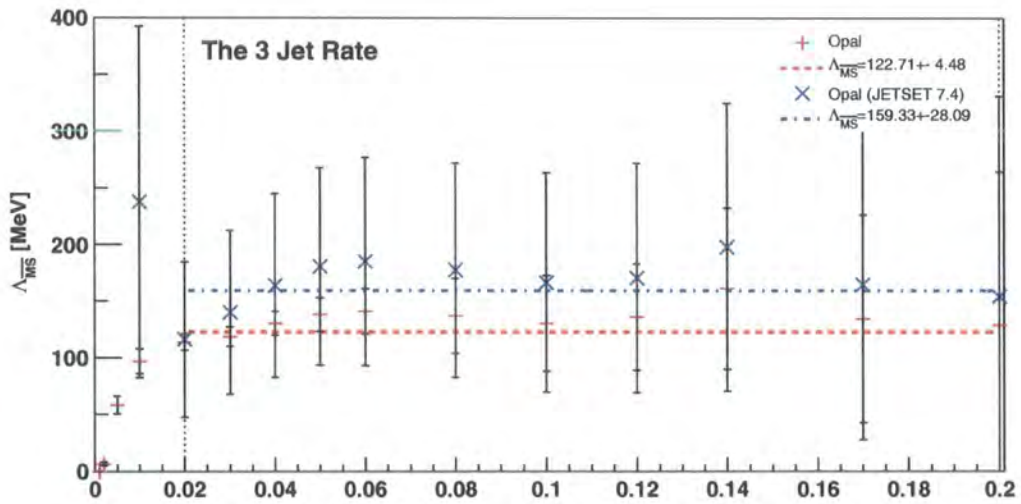
Figure 3.6: The 3 Jet Rate using OPAL data both hadronisation uncorrected and corrected
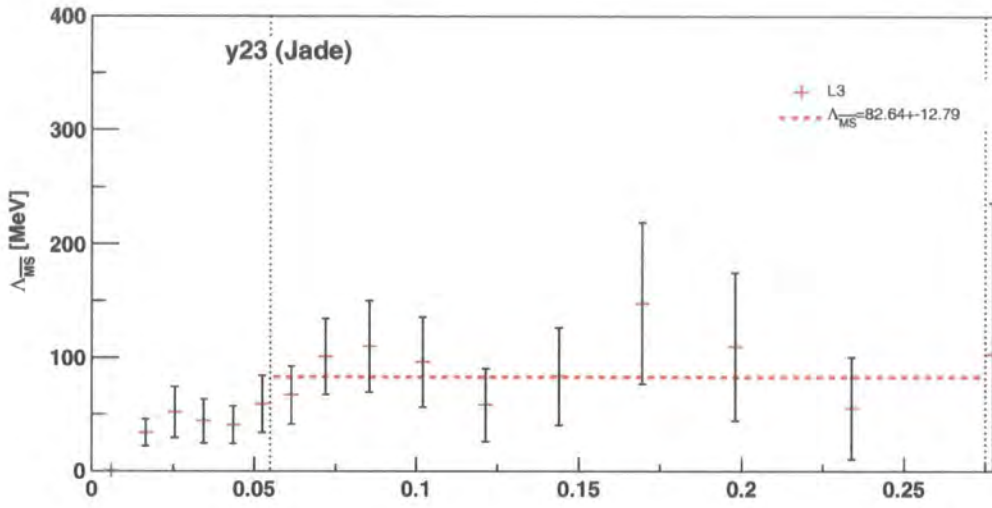
Figure 3.7: The $2 \rightarrow 3$ Jet Transition Parameter using L3 data
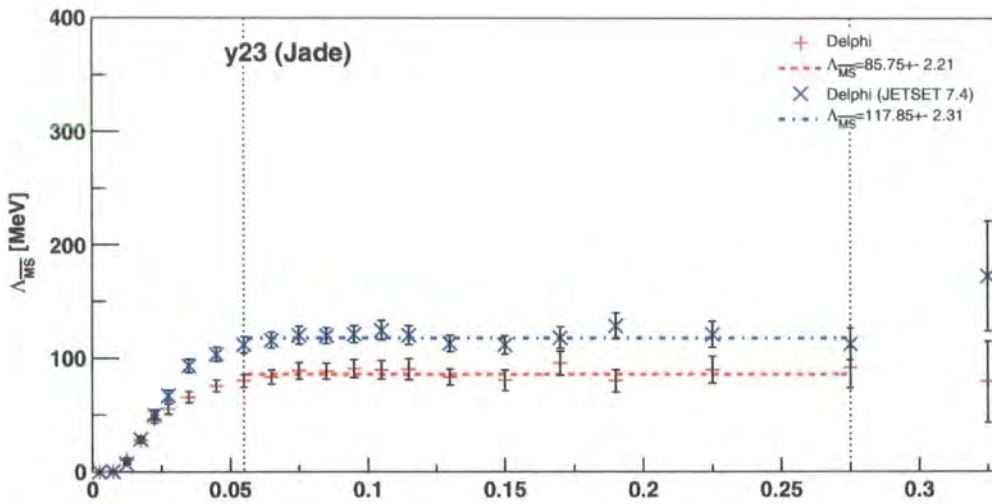
Figure 3.8: The $2 \rightarrow 3$ Jet Transition Parameter using DELPHI data both hadronisation uncorrected and corrected
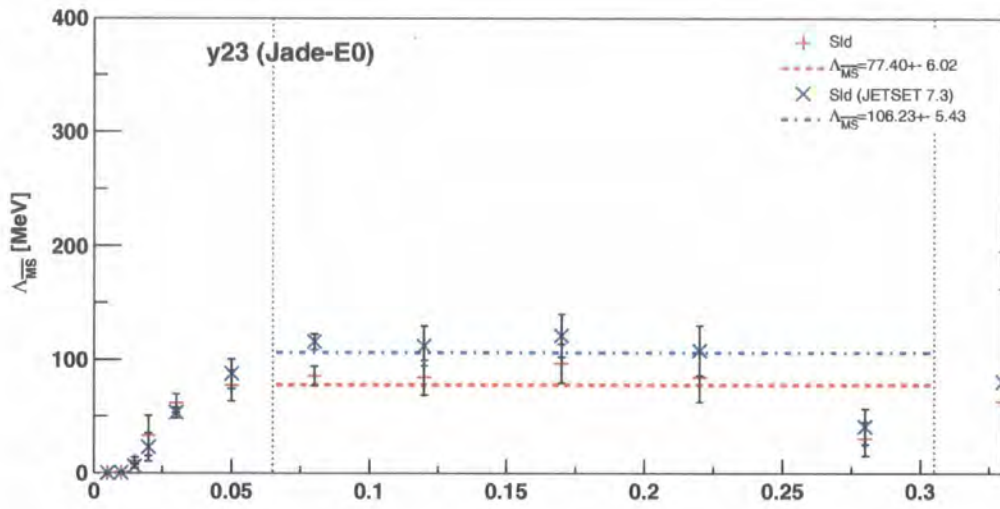
Figure 3.9: The $2 \rightarrow 3$ Jet Transition Parameter using SLD data both hadronisation uncorrected and corrected
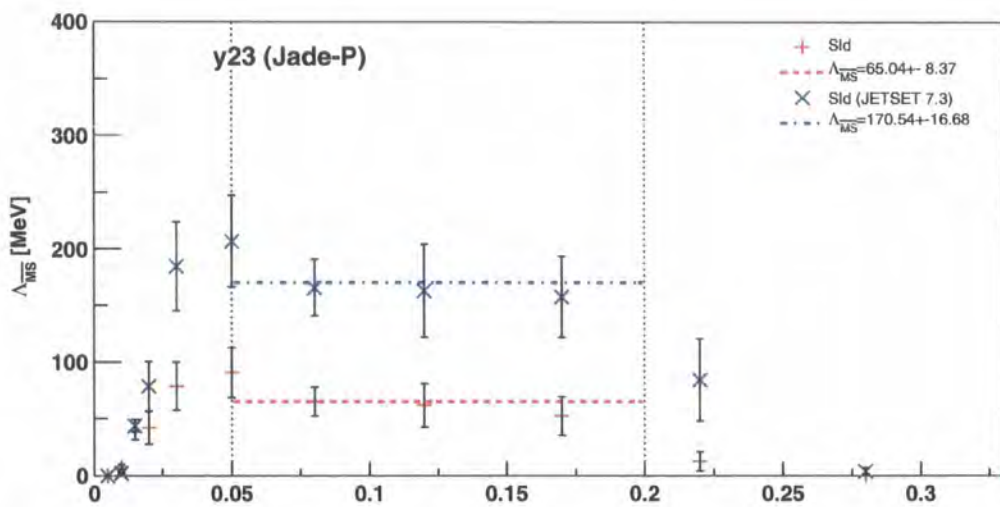
Figure 3.10: The $2 \rightarrow 3$ Jet Transition Parameter using SLD data both hadronisation uncorrected and corrected
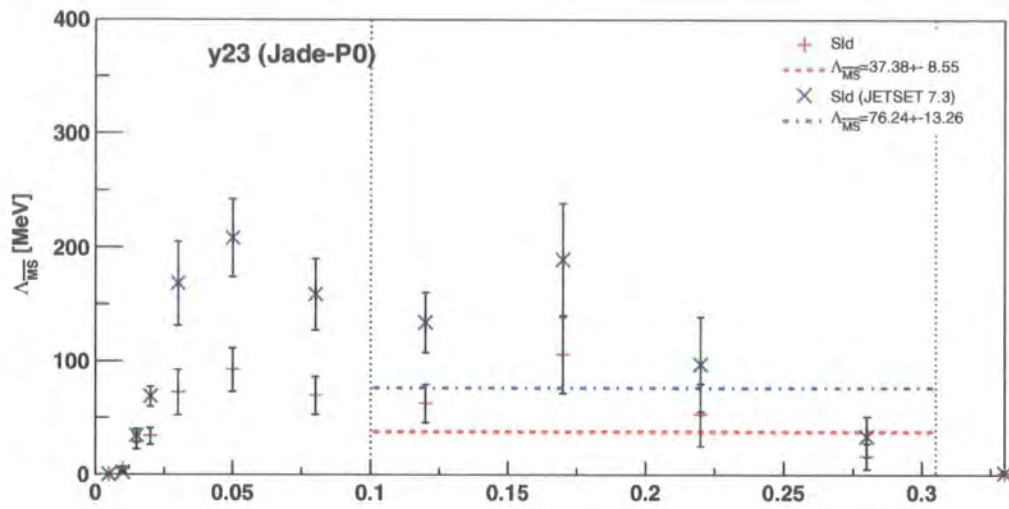
Figure 3.11: The $2 \to 3$ Jet Transition Parameter using SLD data both hadronisation uncorrected and corrected
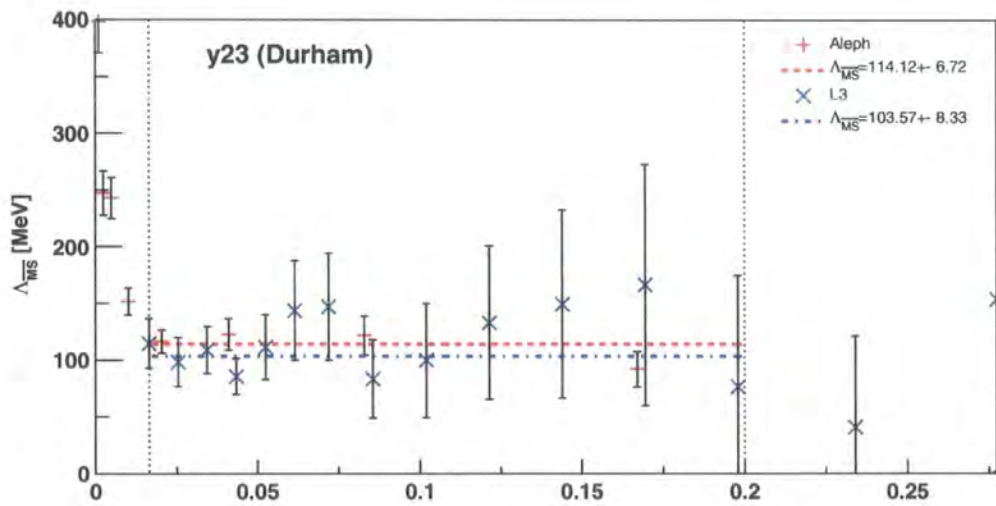
Figure 3.12: The $2 \to 3$ Jet Transition Parameter using ALEPH and L3 data
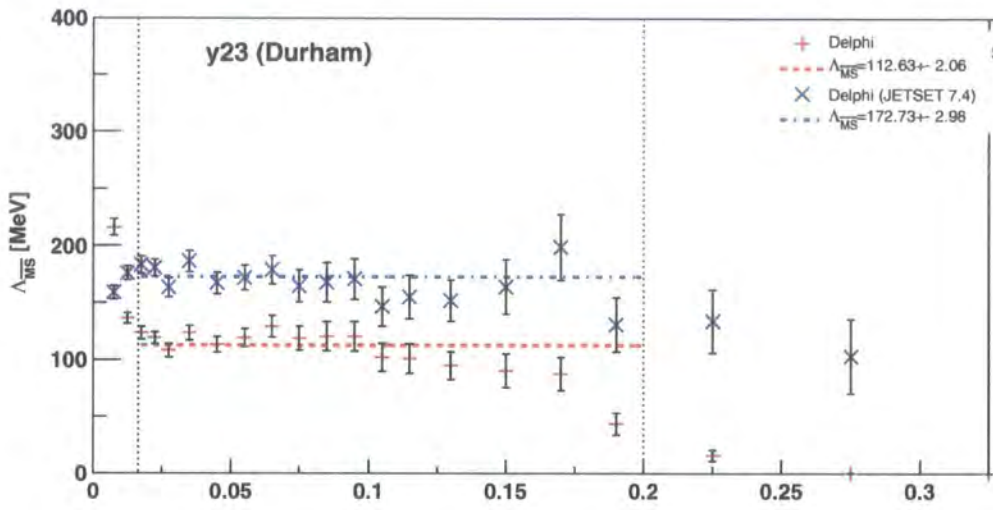
Figure 3.13: The $2 \rightarrow 3$ Jet Transition Parameter using DELPHI data both hadronisation uncorrected and corrected
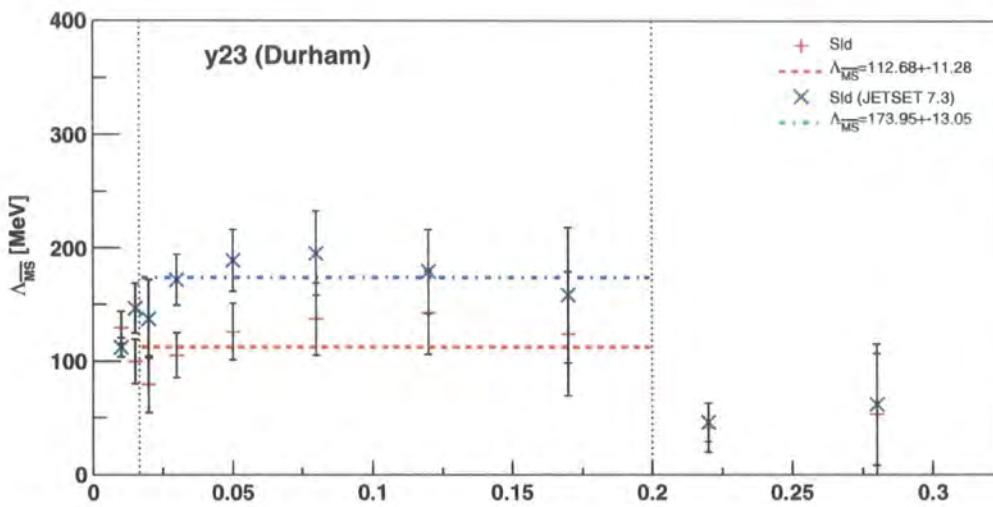
Figure 3.14: The $2 \rightarrow 3$ Jet Transition Parameter using SLD data both hadronisation uncorrected and corrected
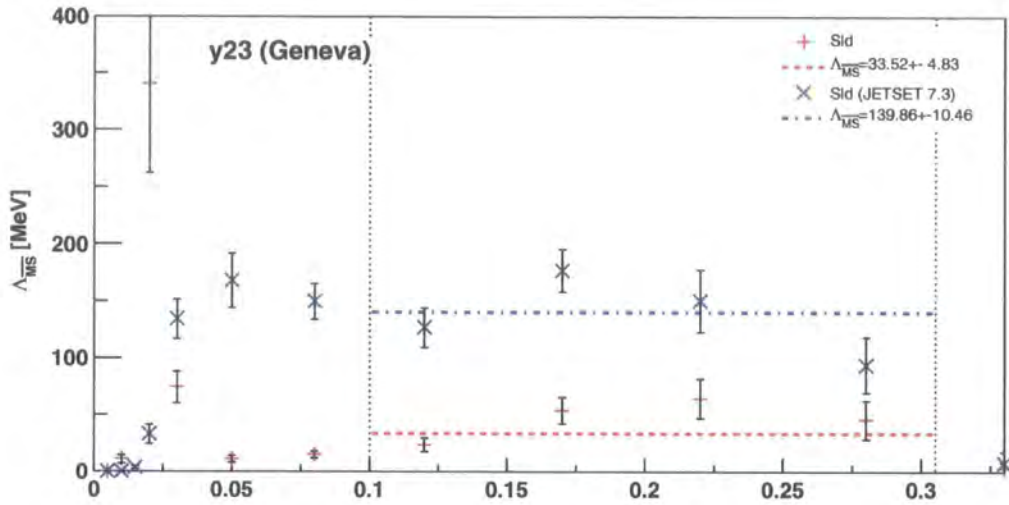
Figure 3.15: The $2 \rightarrow 3$ Jet Transition Parameter using SLD data both hadronisation uncorrected and corrected
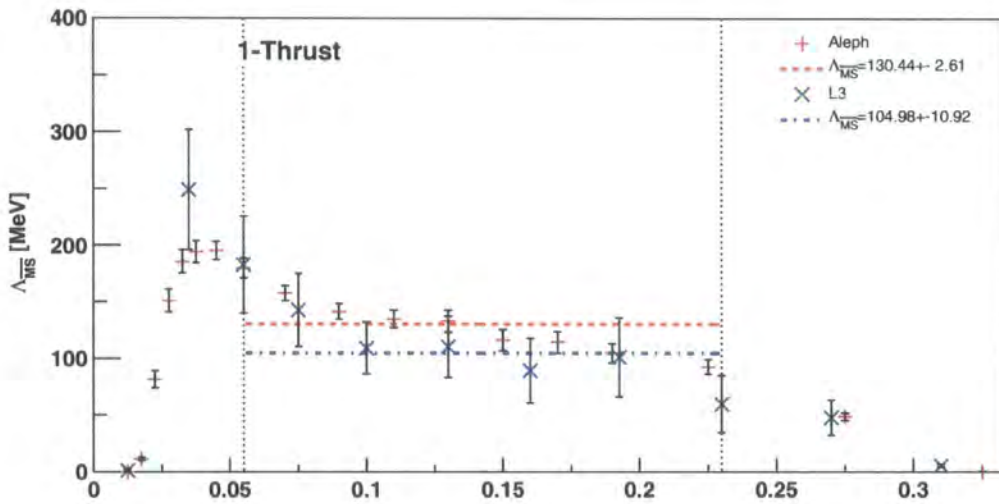
Figure 3.16: The 1-Thrust Parameter using ALEPH and L3 data
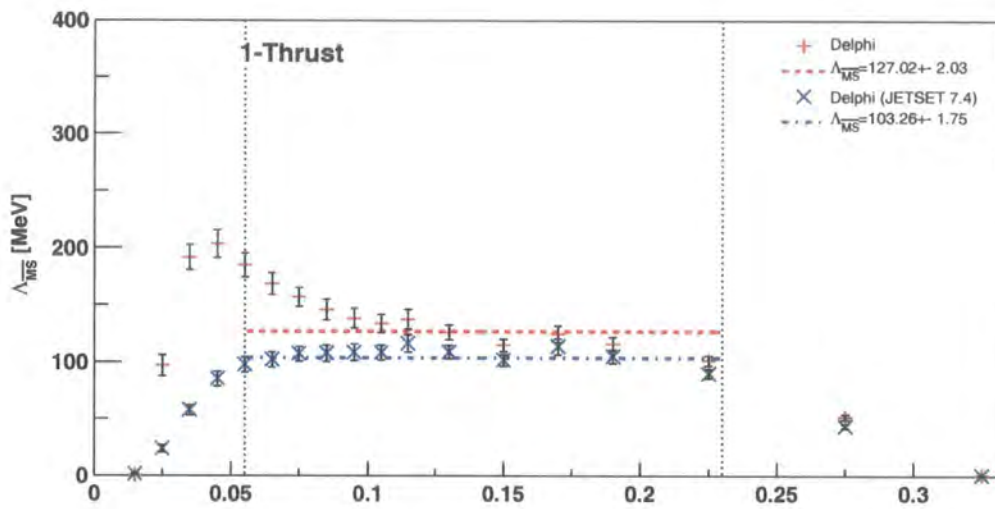
Figure 3.17: The 1-Thrust Parameter using DELPHI data both hadronisation uncorrected and corrected
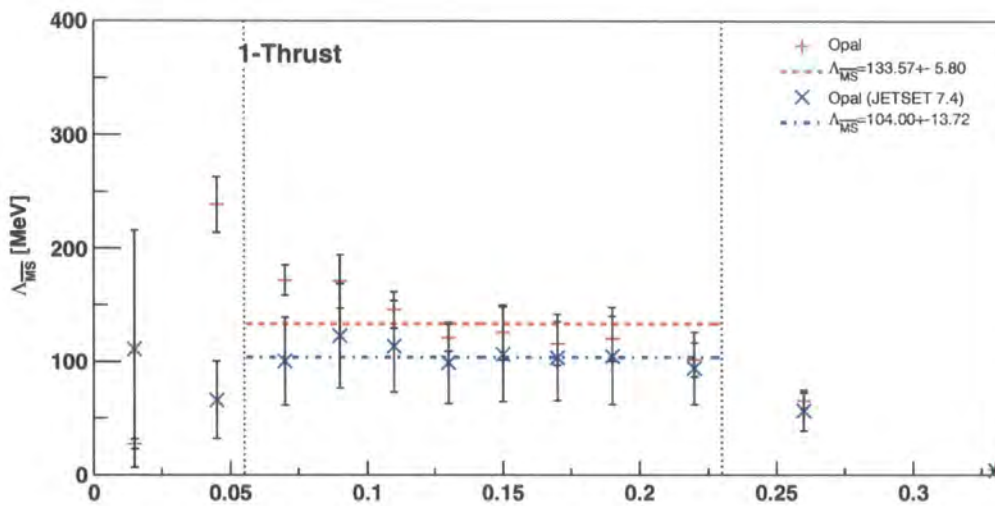
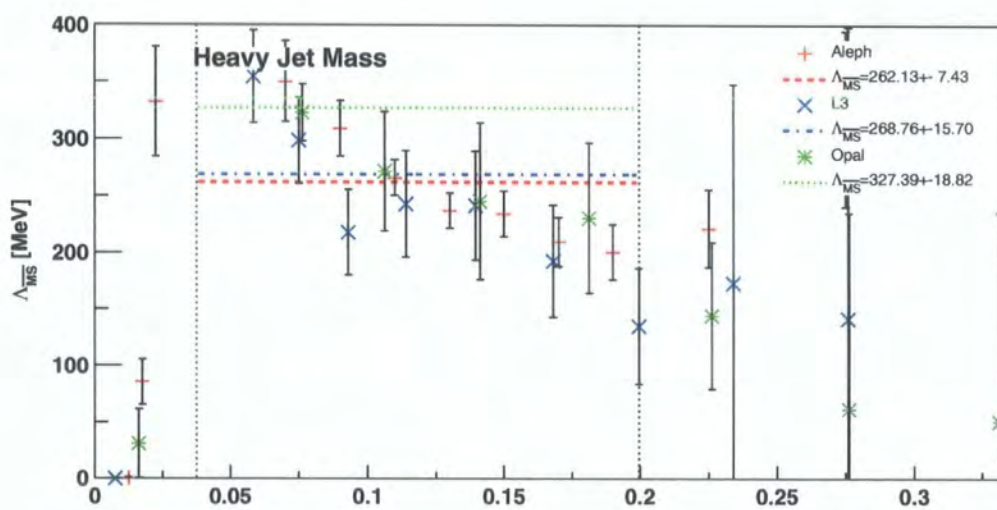Figure 3.18: The 1-Thrust Parameter using OPAL data both hadronisation uncorrected and corrected
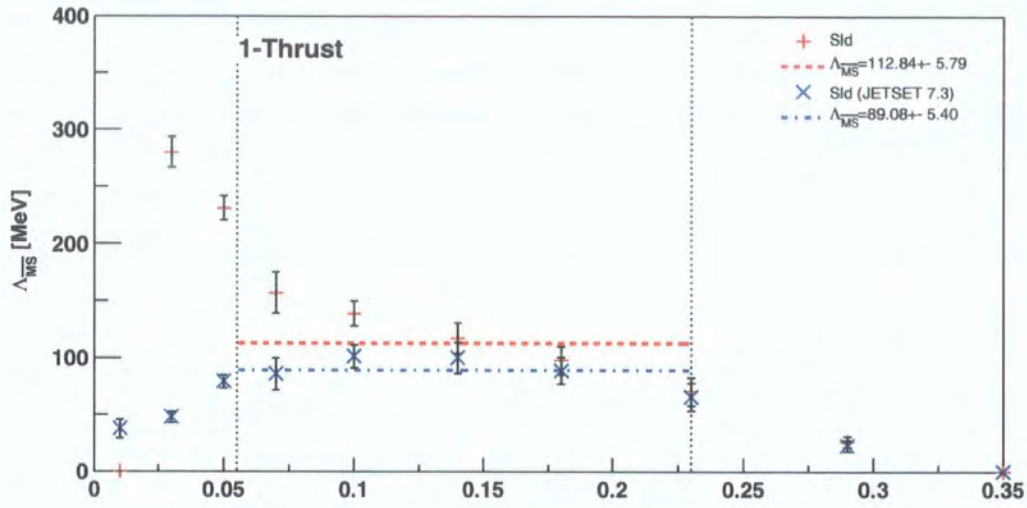
Figure 3.19: The 1-Thrust Parameter using SLD data both hadronisation uncorrected and corrected
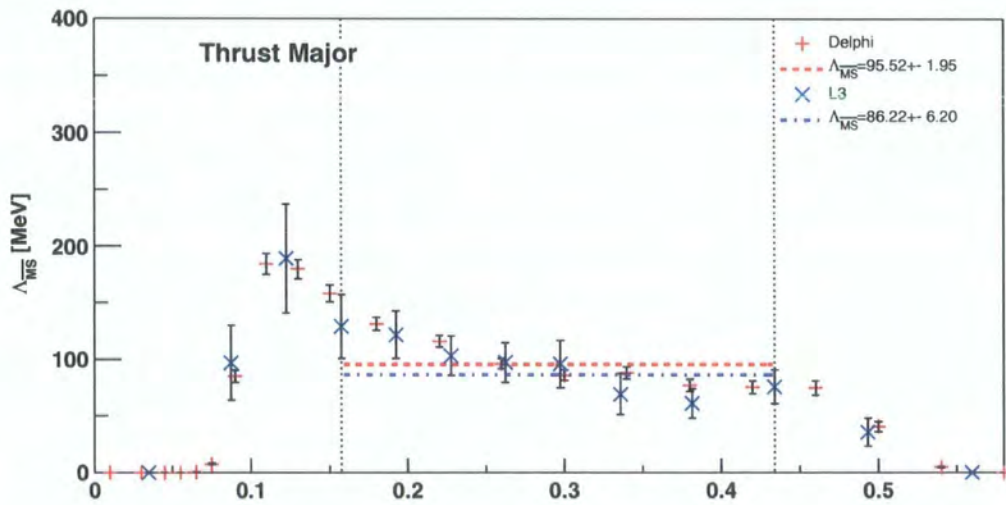
Figure 3.20: Thrust Major using DELPHI and L3 data
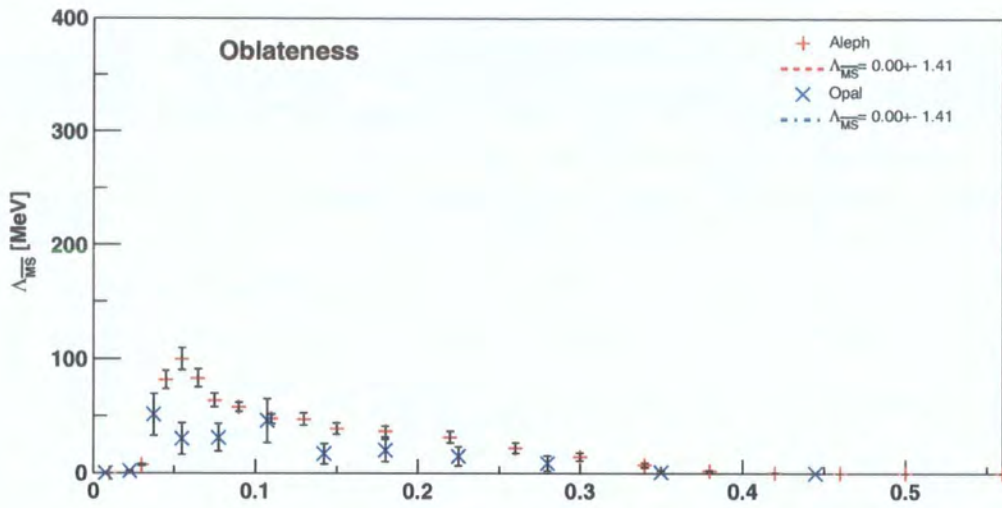
Figure 3.21: The Oblateness using ALEPH and L3 data
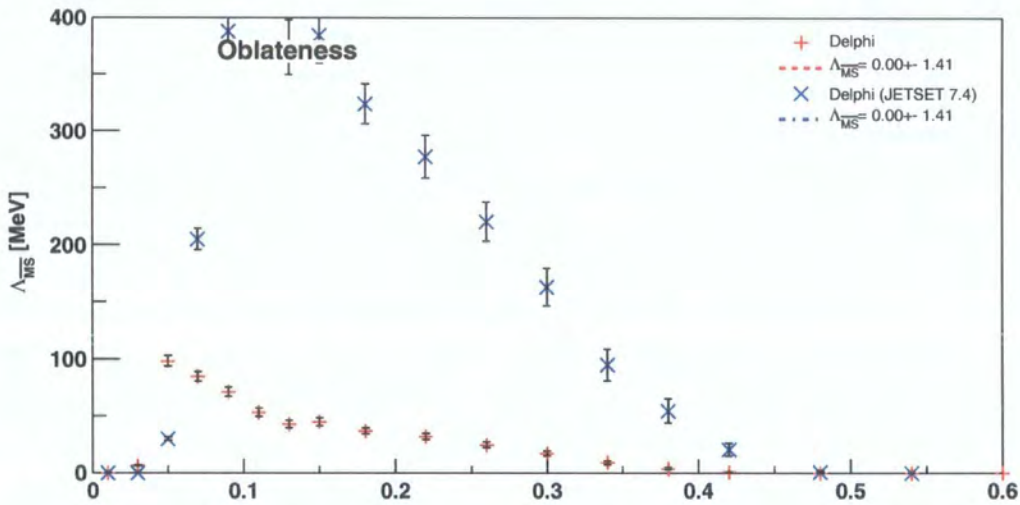
Figure 3.22: The Oblateness using DELPHI data both hadronisation uncorrected and corrected
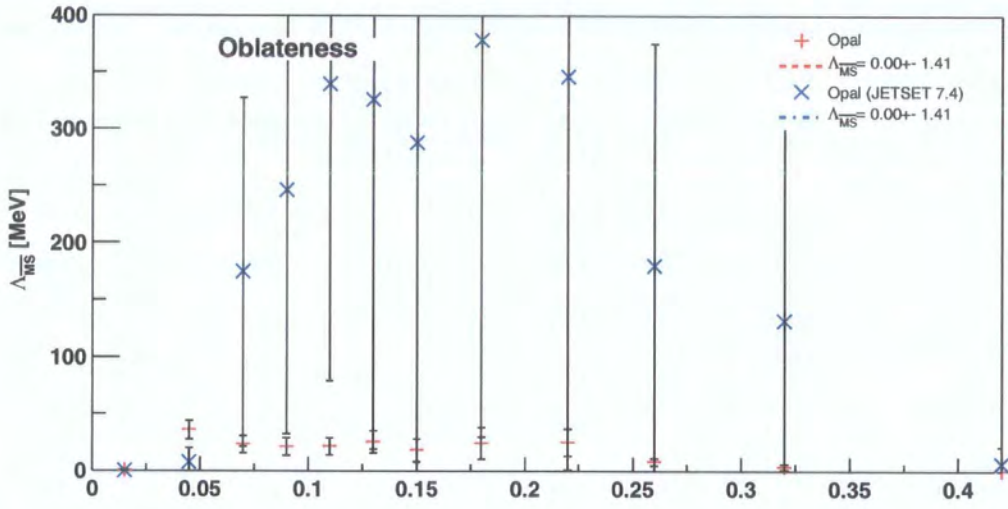
Figure 3.23: The Oblateness using OPAL data both hadronisation uncorrected and corrected
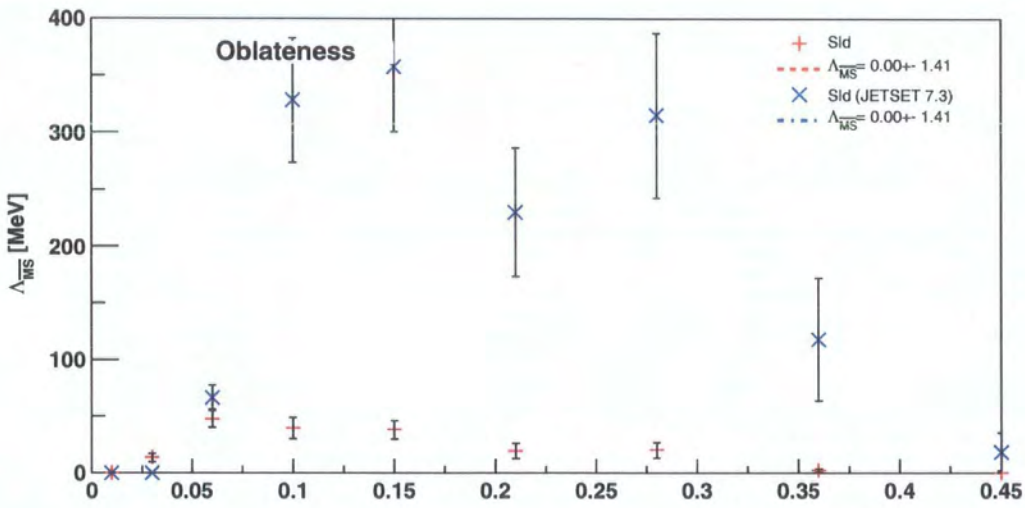
Figure 3.24: The Oblateness using SLD data both hadronisation uncorrected and corrected
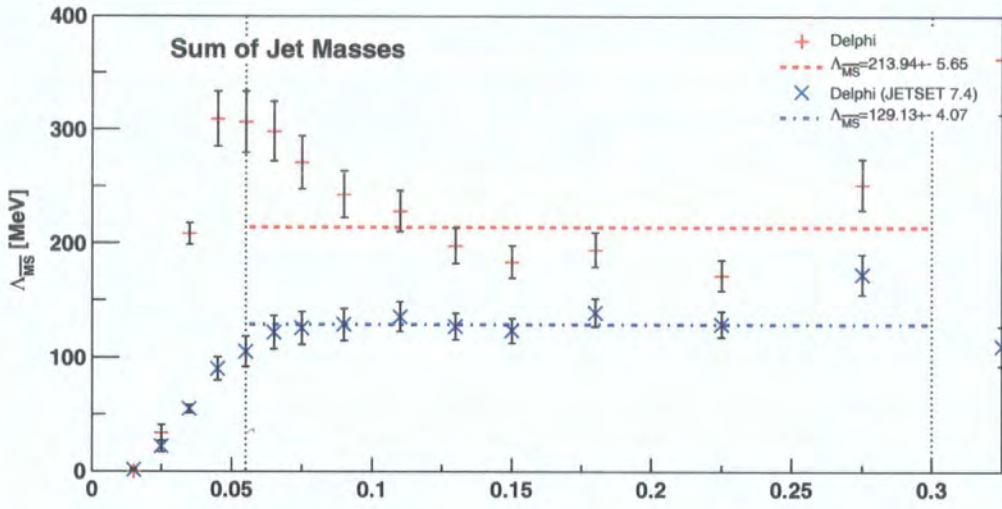
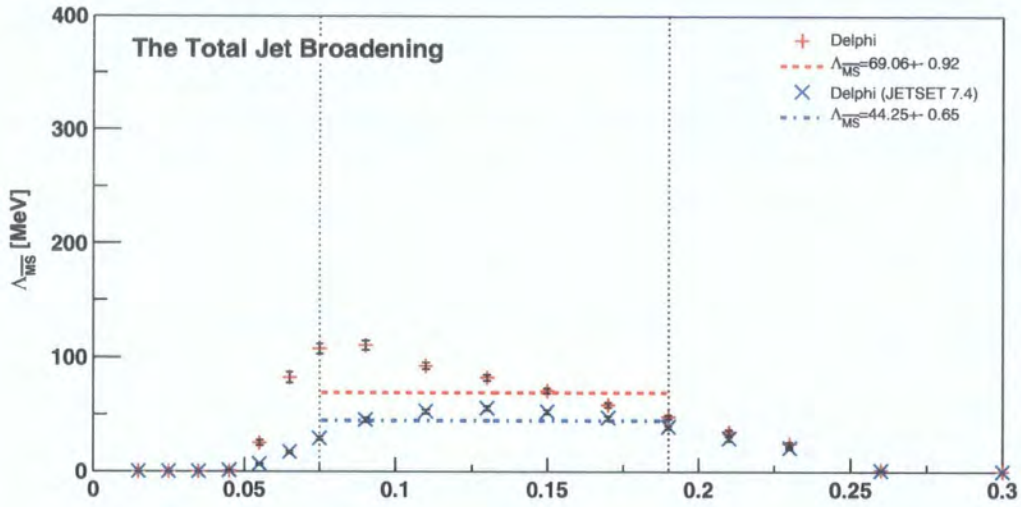Figure 3.25: The Sum of Hemisphere Masses using DELPHI data both hadronisation uncorrected and corrected
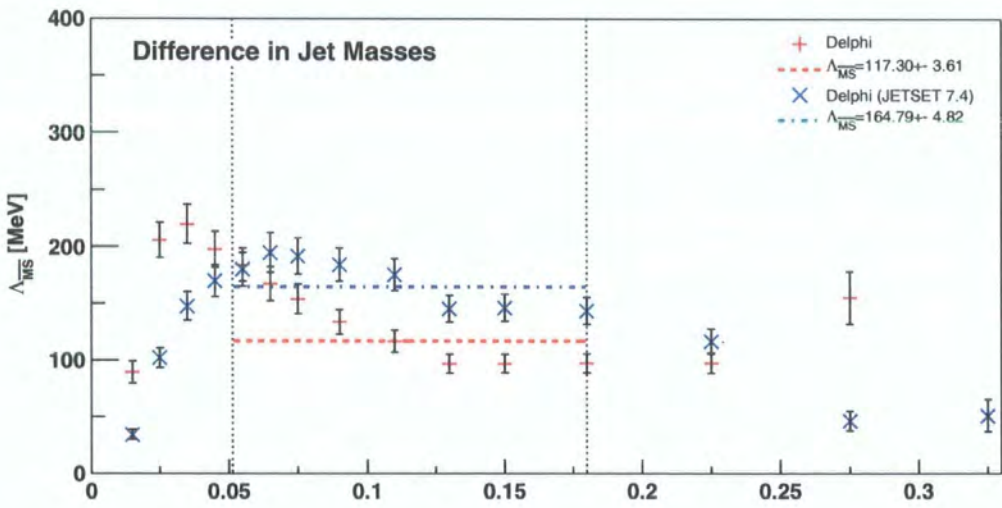
Figure 3.26: The Difference in Hemisphere Masses using DELPHI data both hadronisation uncorrected and corrected
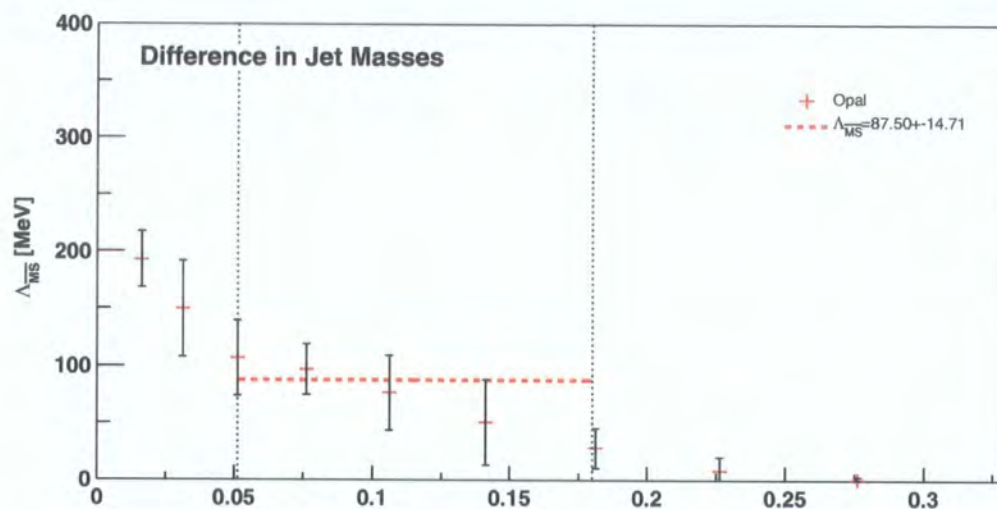
Figure 3.27: The Difference in Hemisphere Masses using OPAL data both hadroni-sation uncorrected and corrected

Figure 3.28: The Heavy Hemisphere Mass using ALEPH, L3 and OPAL data
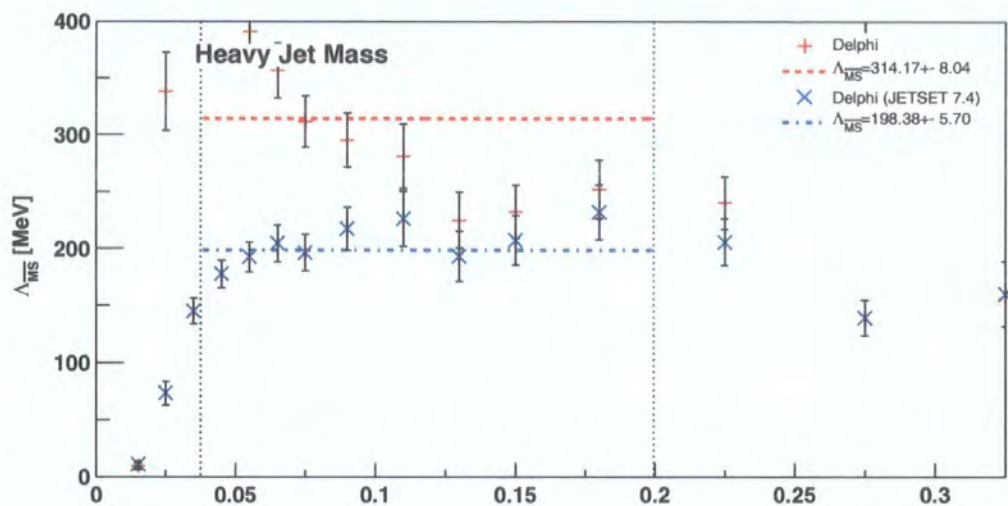
Figure 3.29: The Heavy Hemisphere Mass using DELPHI data both hadronisation uncorrected and corrected
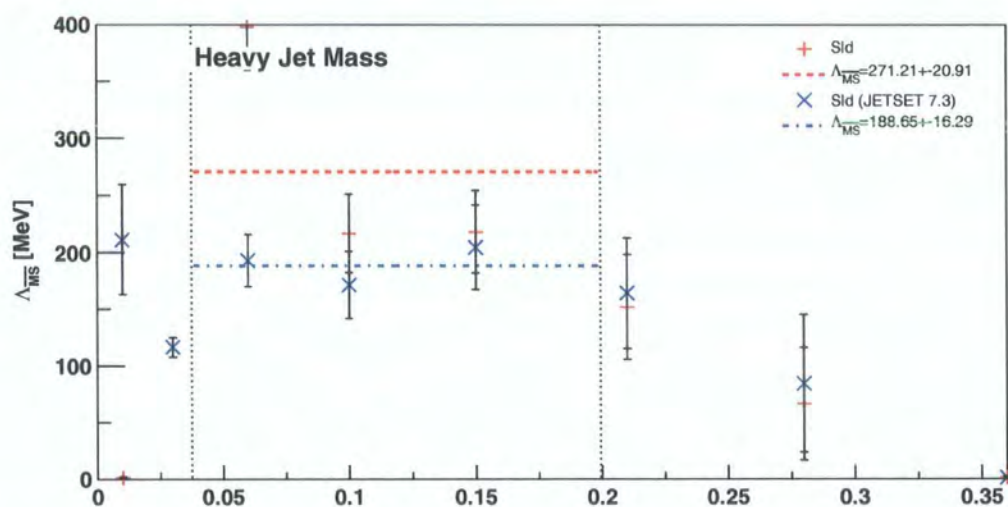
Figure 3.30: The Heavy Hemisphere Mass using SLD data both hadronisation uncorrected and corrected

Figure 3.31: The Total Jet Broadening using DELPHI both hadronisation uncorrected and correctedboth hadronisation uncorrected and corrected
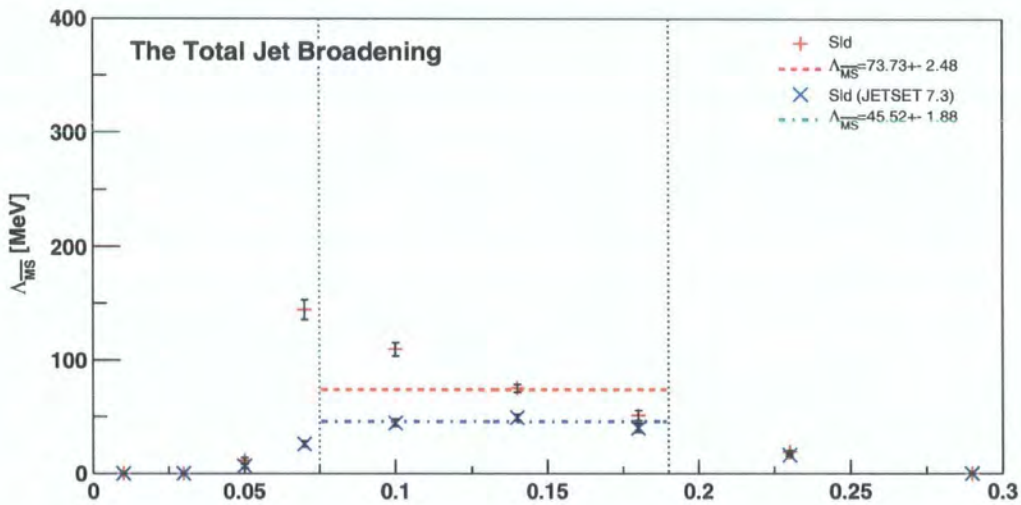

Figure 3.32: The Total Jet Broadening using SLD data both hadronisation uncorrected and corrected
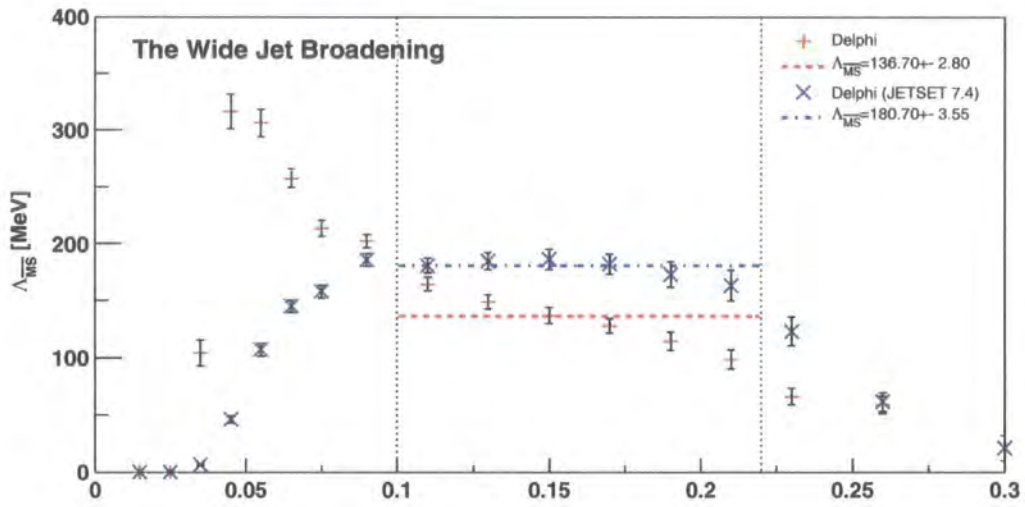
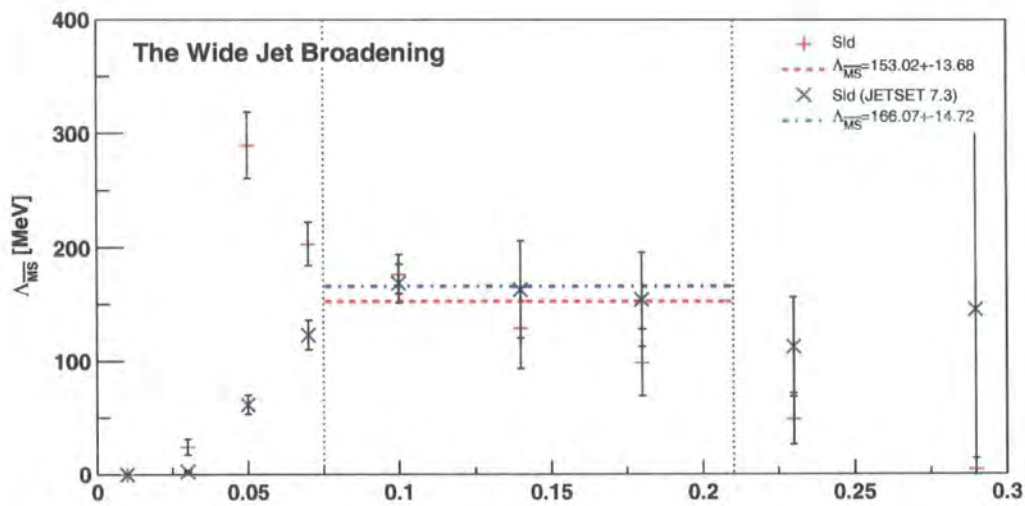Figure 3.33: The Wide Jet Broadening using DELPHI data both hadronisation uncorrected and corrected

Figure 3.34: The Wide Jet Broadening using SLD data both hadronisation uncorrected and corrected
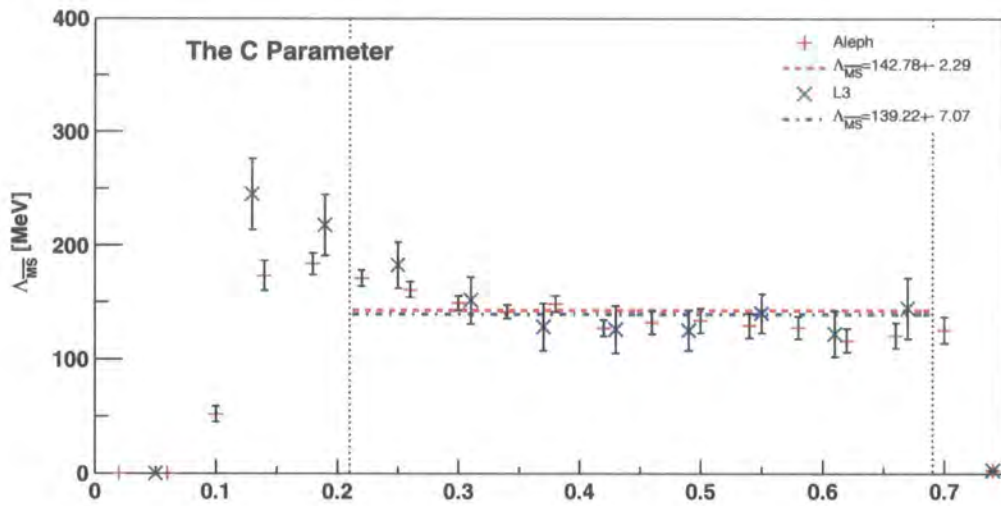
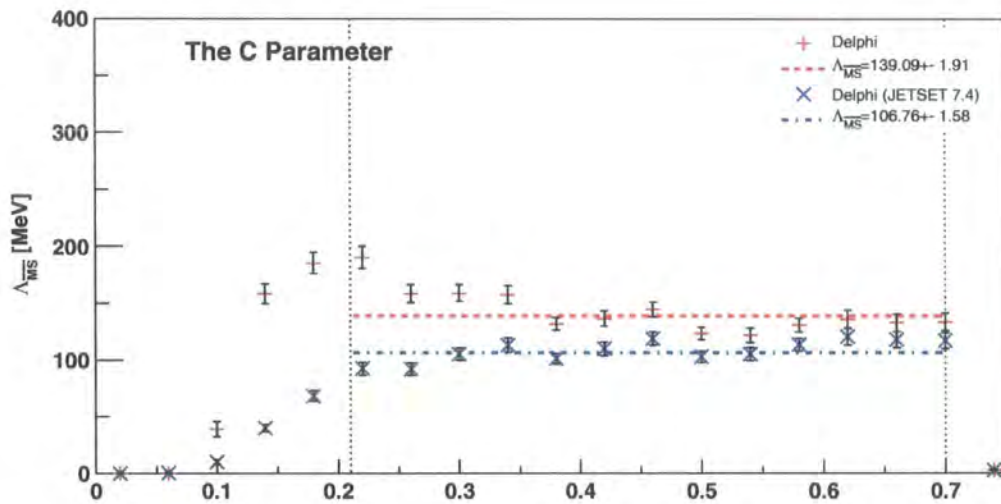Figure 3.35: The C Parameter using ALEPH and L3 data

Figure 3.36: The C Parameter using DELPHI data both hadronisation uncorrected and corrected
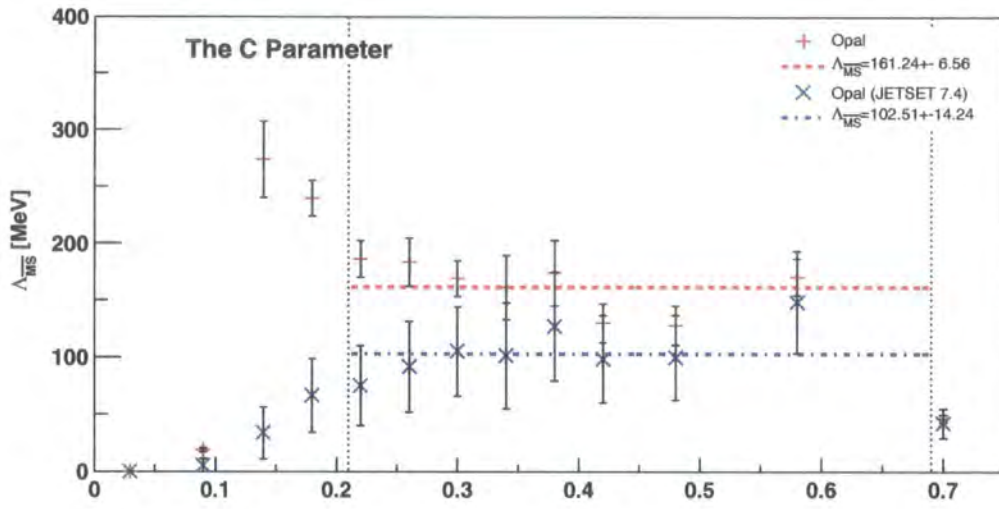
Figure 3.37: The C Parameter using OPAL data both hadronisation uncorrected and corrected
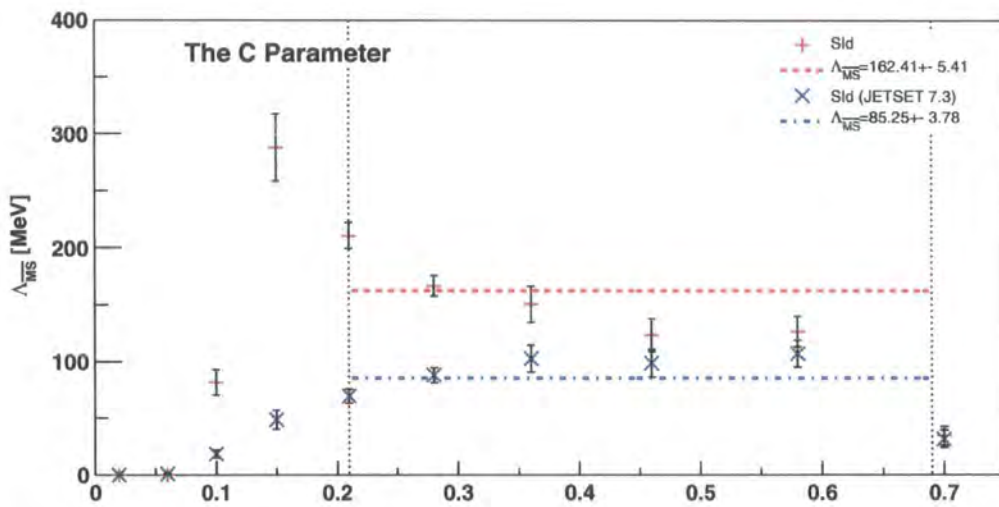

Figure 3.38: The C Parameter using SLD data both hadronisation uncorrected and corrected

Figure 3.39: The Energy-Energy Correlation using DELPHI data both hadronisation uncorrected and corrected

Figure 3.40: The Energy-Energy Correlation using SLD data both hadronisation uncorrected and corrected

Figure 3.41: The Asymmetric Energy-Energy Correlation using DELPHI data both hadronisation uncorrected and corrected

Figure 3.42: The Asymmetric Energy-Energy Correlation using SLD data both hadronisation uncorrected and corrected
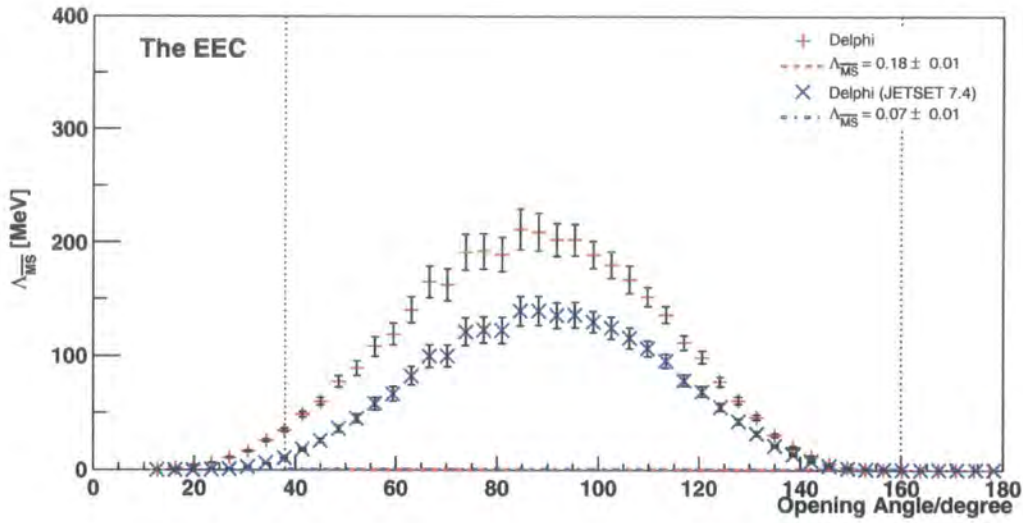
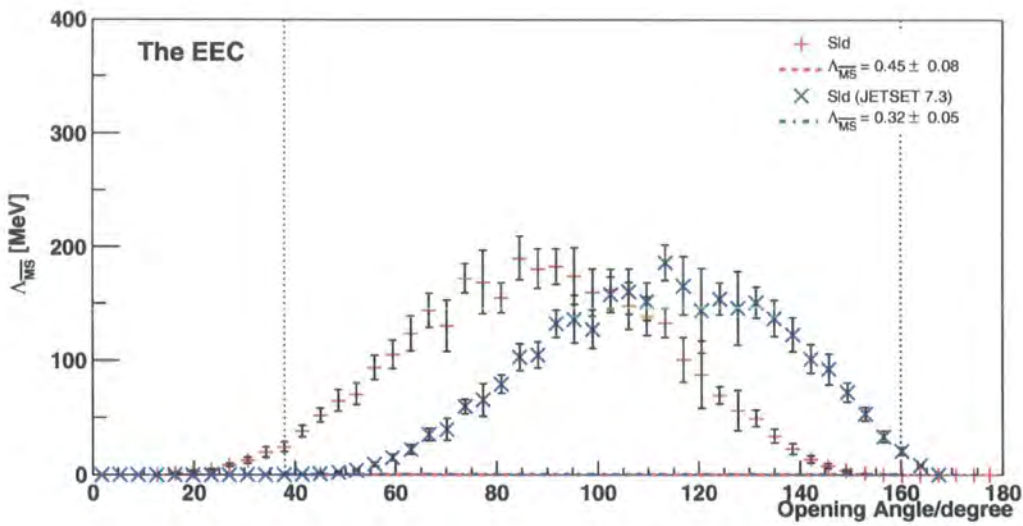Figure 3.43: The Jet Cone Energy Fraction using DELPHI data both hadronisation uncorrected and corrected

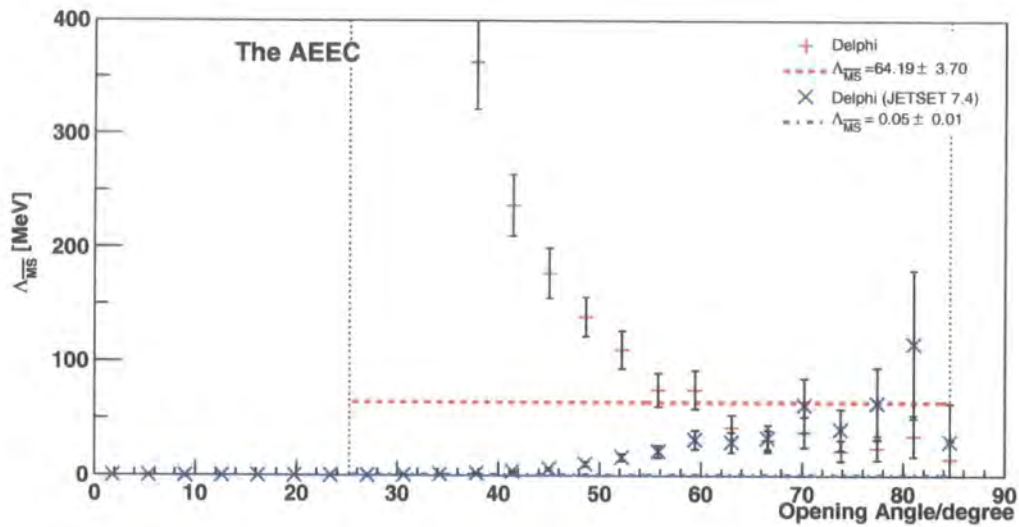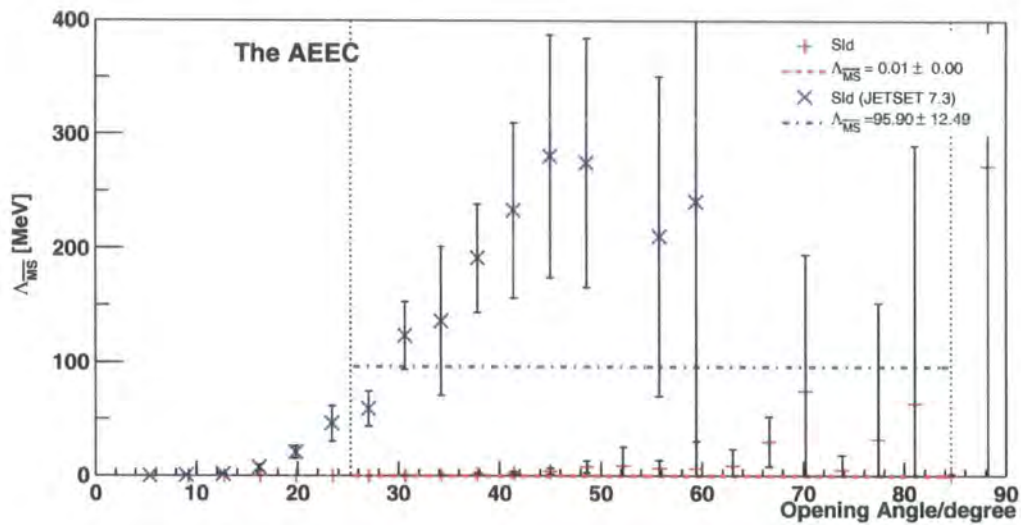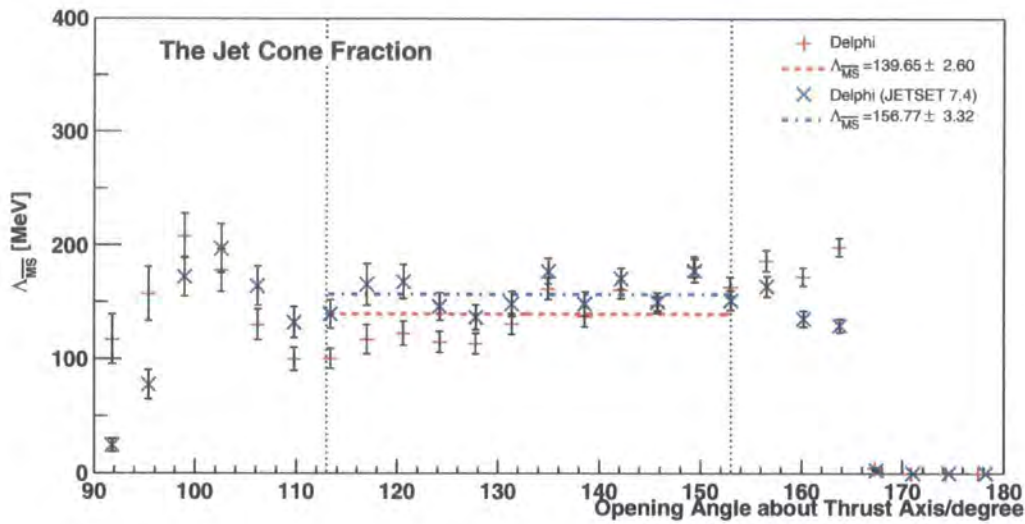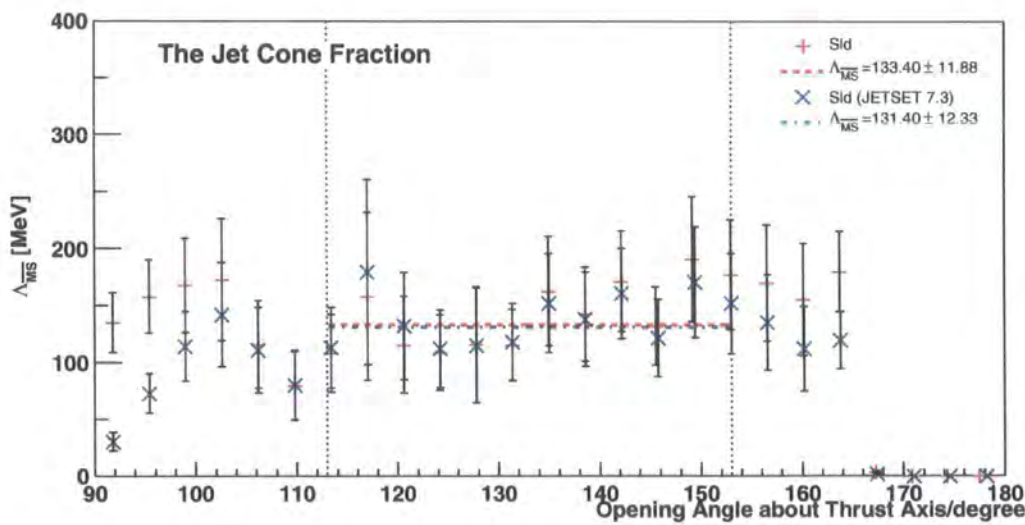Figure 3.44: The Jet Cone Energy Fraction using SLD data both hadronisation uncorrected and corrected

3.5   Discussion of the plots

On examining the plots it quickly becomes apparent that there is a large variation in quality between variables. Some variables give very flat curves while others never reach even a moderate plateau. We see that many of the variables display the anticipated kinematic end points. As mentioned earlier there is no straightforward solution to this problem and is in fact related to the difficulties between reconciling renormalisation group improvement techniques with semi-inclusive observables. For the sake of simplicity we just consider fits away from these points.

This tacitly assumes that the binning of the original experiment has a sufficiently large number of bins away from both the large log region and kinematic end point. This was confirmed by most variables reproducing consistent initial fit ranges except for three cases namely the SLD wide jet broadening, total jet broadening and heavy jet mass where there were too few bins. Therefore in these cases the corresponding DELPHI ranges were applied.

We will examine each class of variable in turn and consider its *quality* and any apparent failings.

The Two and Three-Jet Rates

For the ALEPH data, the distribution here gives an extremely flat line across most of the range in y_{cut}. At small y_{cut} the distribution requires kinematic logarithm resummation. The OPAL data confirms these within the larger error bars. A problem arises after hadronisation corrections have been applied with the errors introduced completely swamping the determination of $\Lambda_{\overline{MS}}$. Smaller errors in the original OPAL data would presumably give a far more stable result. The hadronisation correction factors themselves are not large. The three-jet case repeats the features of the two-jet case with the ALEPH data displaying an extremely good fit even with its absence of hadronisation corrections.

The $2 \to 3$ Jet Transition Parameter

On the whole, these quantities have very flat r_1 values away from the $y_{23} \to 0$ limit. Apparent fluctuations occur within the error bands and typically disappear for the data sets with reduced uncertainties (such as from DELPHI). Hadronisation has

the effect of raising the value of $\Lambda_{\overline{MS}}$ in all cases. An example is for the Durham algorithm where it goes from about 115MeV to about 170MeV.

The Thrust Related Variables

The thrust and thrust major variables have distributions with a reasonable region of flatness in r_1, permitting a well defined fit range. For thrust the effect of hadronisation is considerable. Even away from the infrared region, we see that on correcting for such effects, the value for $\Lambda_{\overline{MS}}$ becomes far more stable, enabling a better fit. The actual value for $\Lambda_{\overline{MS}}$ is only slightly decreased in these circumstances due to a better fit.

The distribution for oblateness on the other hand, fails the first fit range criterion and is excluded immediately. It is interesting to note that not only does it lack a sufficiently flat region in r_1, but it is also the only three-jet like observable to have an overall sign difference between the NLO and LO coefficient across the complete range of oblateness (i.e. r_1 remains negative across the complete kinematic range). The resultant plots verify the poor quality of this variable for extracting a value of $\Lambda_{\overline{MS}}$.

The Jet Hemisphere Masses

The hemisphere mass related variables display widely varying properties. The sum demonstrates the optimal fit with r_1 values leveling off away from the two-jet region. There is also a strong presence of hadronisation effects that once incorporated, enable a large fit range.. In contrast, the r_1 value of the distribution in "difference of hemisphere masses", behaves analogously to that of the thrust minor variable displayed in Figure 3.2. Therefore the fit range is severely limited. Within this range, the hadronisation effects can once more be seen to be crucial in generating a flat plateau for extraction of $\Lambda_{\overline{MS}}$. Lastly the heavy hemisphere mass displays much the same characteristics as the "difference". Hadronisation effects are imperative for a reasonable fit.

The Jet Broadenings

The total jet broadening has r_1 values of the same form as that of thrust, the upper kinematic bound being $\frac{1}{2\sqrt{3}} \approx 0.289\ldots$. Unfortunately it seems, from the comparatively low value of $\Lambda_{\overline{MS}}$, that the large infrared logarithm and kinematic end-point effects hinder an accurate measurement being made. It is also possible that large higher order corrections are required at this centre-of-mass energy. The difference in jet broadenings is missing as it suffers from the same problem as the oblateness. The wide jet broadening has many similarities with the heavy hemisphere mass, displaying all the same characteristics.

The C-Parameter

The C-parameter provides a very good fit away from the infrared region, with a large fit range extending nearly all the way to its extreme value of $\frac{3}{4}$. Hadronisation corrections decrease the extracted value of $\Lambda_{\overline{MS}}$ to about 100MeV from about 150MeV. The effect is most pronounced in moving towards the two-jet configuration. Here different collaborations seem to give varying results before corrections have been applied. This is most probably due to the large uncertainties of the older data sets (L3, OPAL and SLD).

The Two-Particle Energy Correlations

The correlations provide a completely different picture of events. They are built upon two-particle correlations in energy, and therefore each event can contribute to more than one bin. For the EEC, the extreme angular regions correspond to the two-jet configuration and are thus sensitive to the same form of kinematic logarithms. Strikingly though, the plots of the DELPHI and SLD hadronisation corrected data differ significantly. This can only be attributed to the difference in hadronisation models, Jetset 7.4 for DELPHI and Jetset 7.3 for SLD. Regardless of this effect, we see that in both cases, the large infrared logarithms have a strong influence over much of the distribution. The AEEC distribution suffers from a number of problems. It has very large hadronisation corrections. Additionally we find a minor deviation between the SLD and DELPHI results, although the hadronisation correction factors agree between both experiments with only very slight differences from $0°$–$15°$. The

seemingly incompatible data is due to the large errors involved. The SLD data contains large uncertainties which are amplified through hadronisation corrections. The resulting values should therefore not be trusted and are therefore disregarded.

The Jet Cone Energy Fraction

Special consideration had to be taken with this variable since unlike most of the others, this one had minor fluctuations in the distribution in r_1 due to the Monte Carlo integration of the NLO and LO coefficients. To compensate for this effect, the tolerance in extracting the fit range was increased to 25%. This increase was sufficient to hide the small perturbations from flatness in the distribution. Otherwise, we see that the hadronisation effects are small and a flat region is consistent within the errors.

Summary of Three-Jet Observables

Having obtained values for $\Lambda_{\overline{MS}}$ with errors as indicated previously we combine them as specified in Section 3.3.3. Treating the hadronisation corrected quantities separately, we combine each data set for different collaborations to get a prediction for each observable. A summary of these values are in Figures 3.45 and 3.46. In the case of the hadronisation corrected data, we convert the value of $\Lambda_{\overline{MS}}$ to $\alpha_s(M_Z)$ via the β-function equation as specified in Equation (2.80) solved exactly at two-loops. A summary of these values can be found in Figure 3.47. At this point, we have taken the information available from a next-to-leading order calculation to its limit. After hadronisation corrections have been applied, we should only be left with higher order contributions affecting the final result. Therefore, we may attribute the *scatter* in values of $\Lambda_{\overline{MS}}$ to these higher order terms. There is of course no assurance that higher order corrections will move all values closer together. We naïvely anticipate that the extreme values would move towards the more common ones. Without a guide to which variable will have small higher order corrections, we are left merely guessing to what these effects would be. Only an NNLO calculation can shed light on this matter. Strictly speaking, there is no preference for one value over another and hence no reasonable procedure for extracting an overall value for $\Lambda_{\overline{MS}}$ (or equivalently α_s).
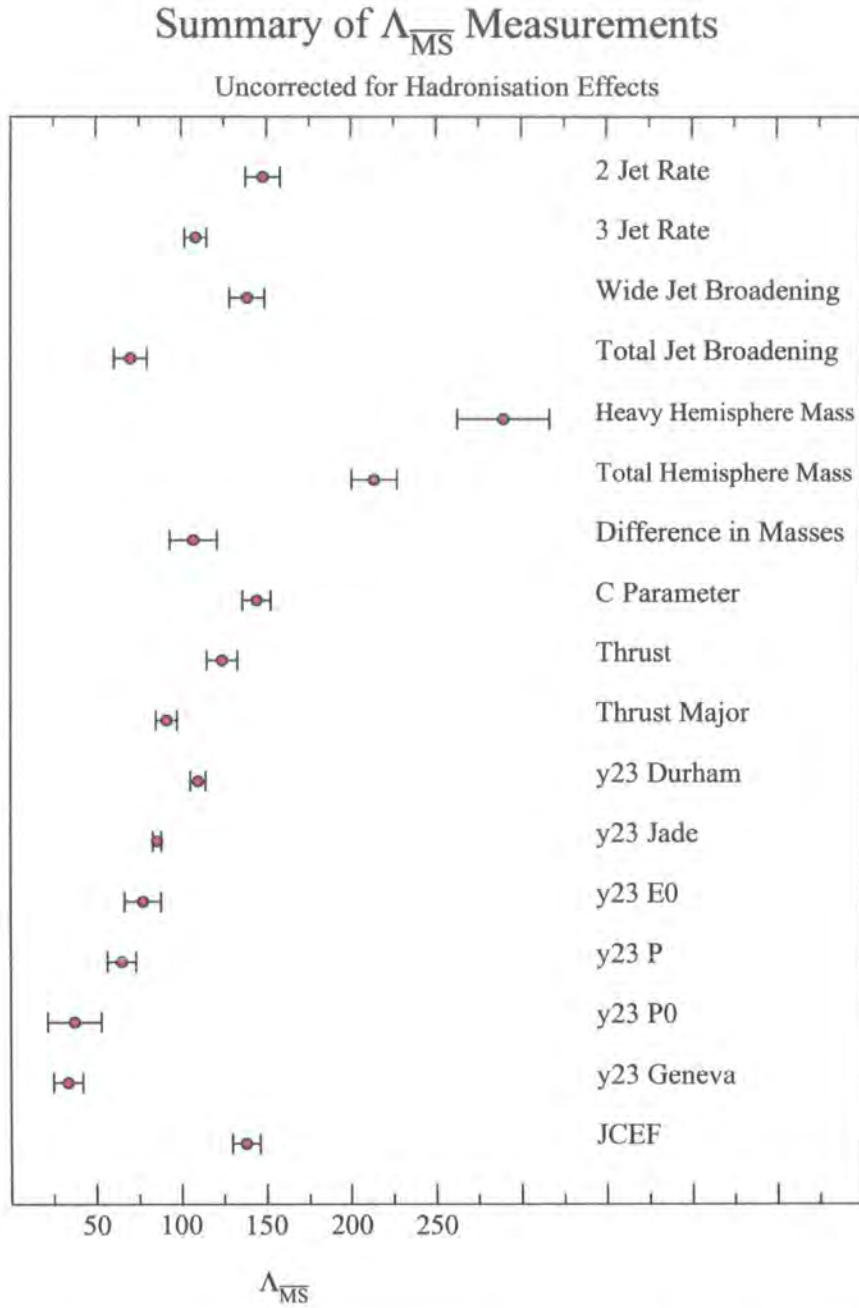
Figure 3.45: Summary of $\Lambda_{\overline{MS}}$ measurements uncorrected for hadronisation effects.
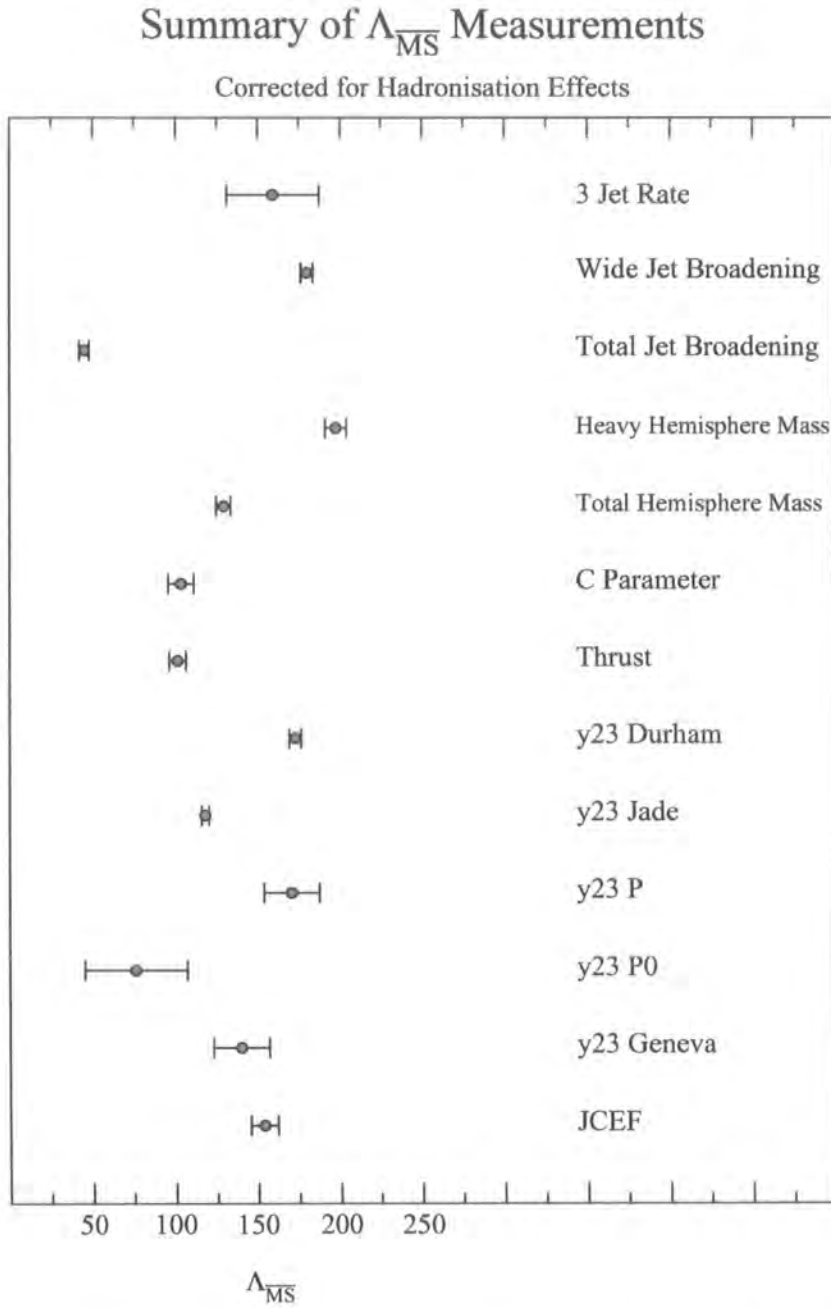
Figure 3.46: Summary of $\Lambda_{\overline{MS}}$ measurements corrected for hadronisation effects.
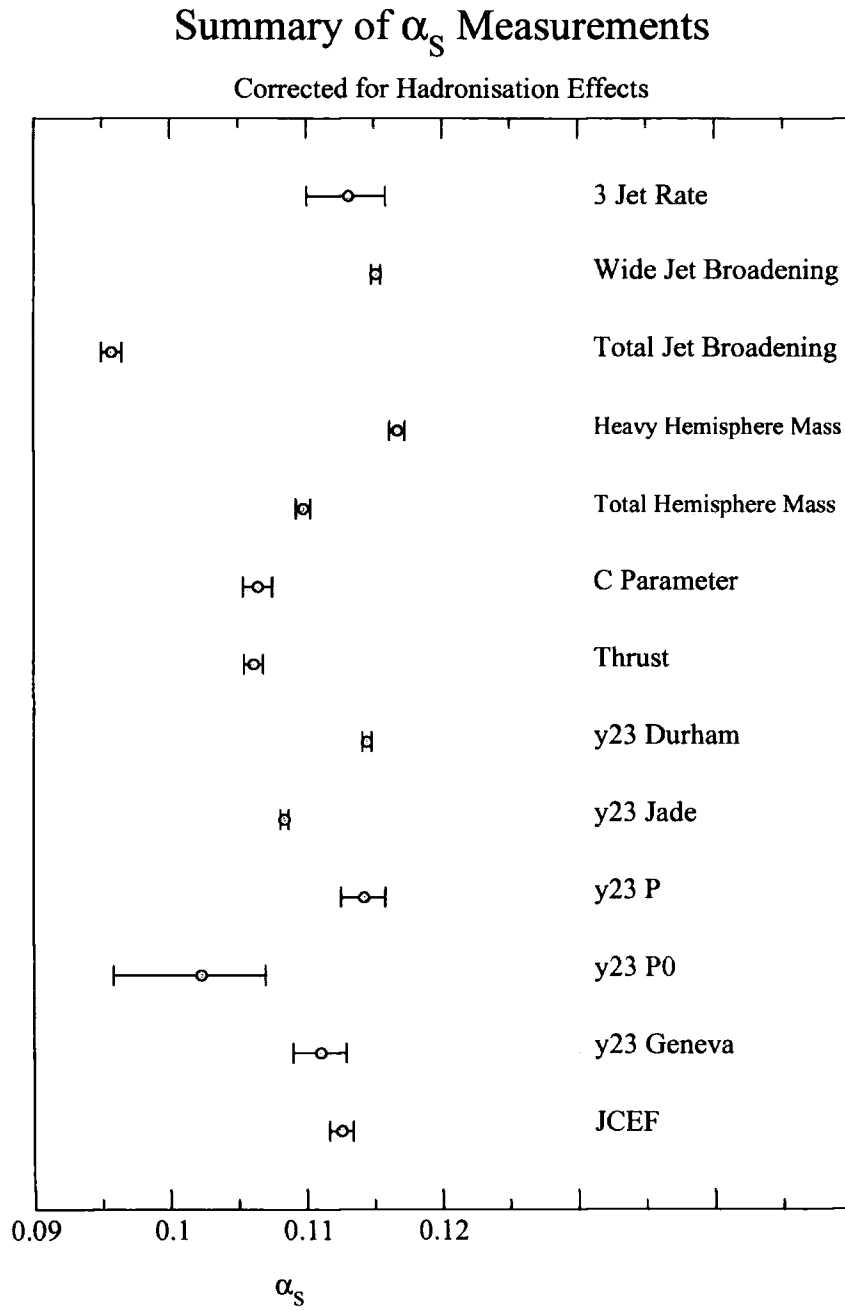
Figure 3.47: Summary of α_s measurements corrected for hadronisation effects.

3.6 Results of Extracting $\Lambda_{\overline{MS}}$ from Four-Jet Observables

In this section we present the results of fitting a constant value of $\Lambda_{\overline{MS}}$ to the four-jet observables' data sets. In each case only data uncorrected for hadronisation effects is analysed. We use the DELPHI data of [66] in all cases.
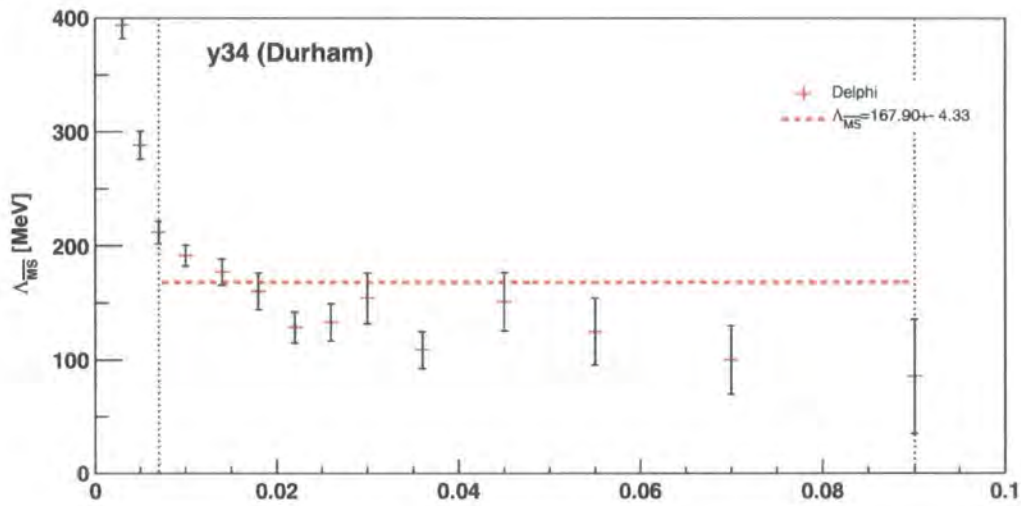
Figure 3.48: The $3 \rightarrow 4$ Jet Transition Parameter
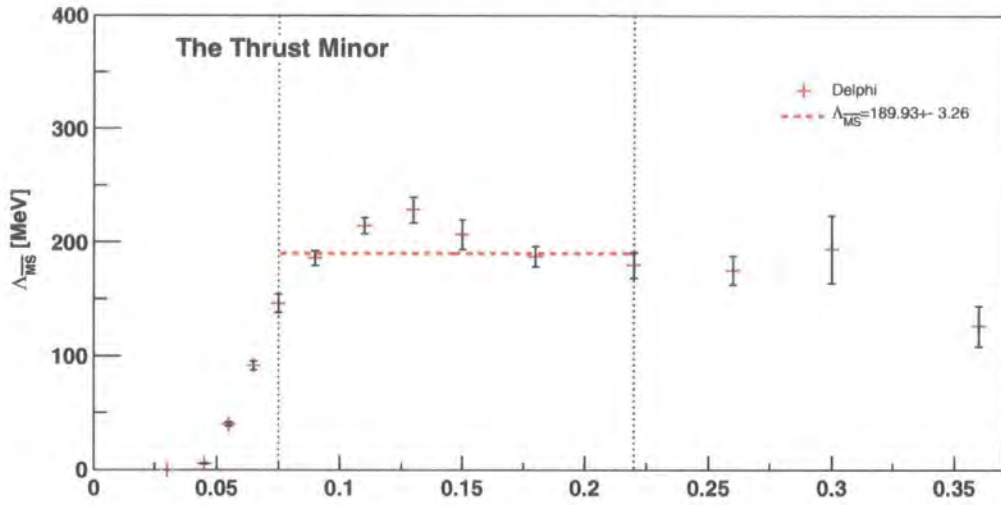
Figure 3.49: The Thrust Minor
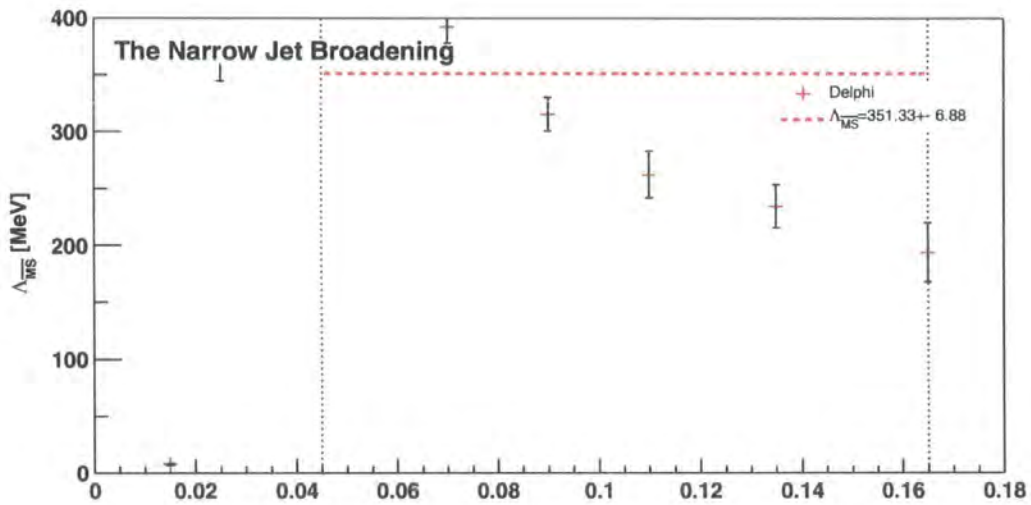
Figure 3.50: The Narrow Jet Broadening
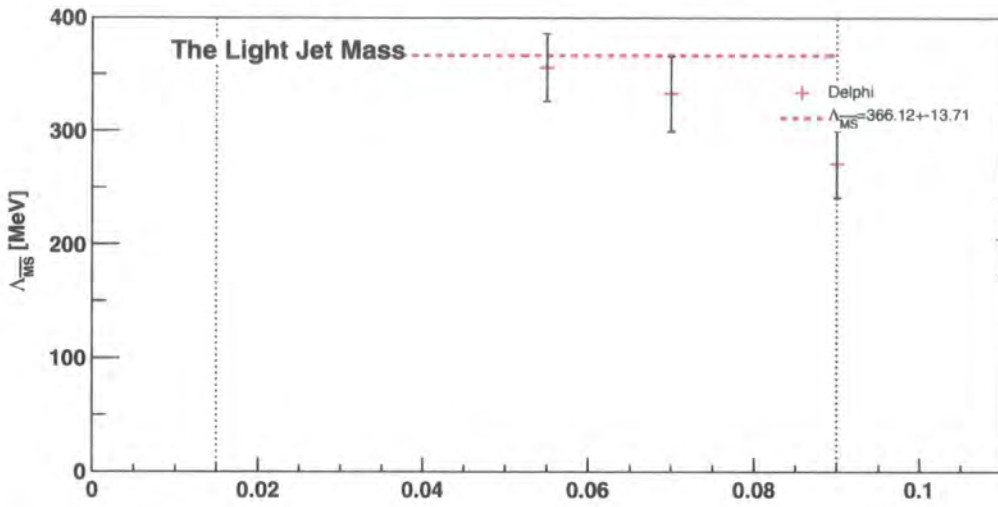
Figure 3.51: The Light Hemisphere Mass
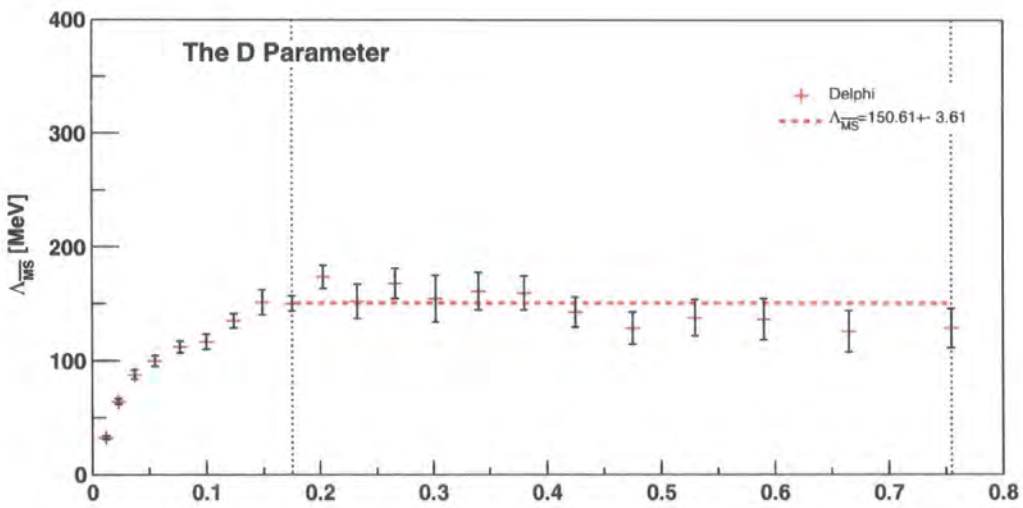
Figure 3.52: The D Parameter

3.7   Discussion of the plots

As with their three-jet counterparts, the results vary considerably due to the nature of each individual four-jet observable.

The 3 → 4 Jet Transition Parameter

The extraction of $\Lambda_{\overline{MS}}$ from the $3 \to 4$ jet transition parameter distribution is hampered by large uncertainties. This can be traced back to the relatively large errors in the r_1 parameter from the NLO coefficient.

The Thrust Minor Variable

The thrust minor variable suffers from a small fit range. As can be seen in Figure 3.2, the parameter r_1 does not have an extended flat region due to the domination of the kinematic end points. We are then forced into the small region at the turn-over of the r_1 distribution where it is momentarily horizontal.

The Narrow Jet Broadening

The narrow jet broadening seems to have a very stable and flat r_1 ratio suggesting that a decent value of $\Lambda_{\overline{MS}}$ should be obtained. This however is clearly not the case on inspection of the plot (Figure 3.50). We can attribute this deviation from flatness to dominating hadronisation corrections. We shall see in the next chapter the importance of phenomenological power corrections to this distribution.

The Light Hemisphere Mass

The light hemisphere mass in many ways reflects the problems of the narrow jet broadening. In the small "light mass" limit, the r_1 ratio goes to negative infinity and approaching the first kinematic end point, the ratio goes to positive infinity. Unfortunately within the intermediate range there is no definitive flat plateau in which to fit a stable value for $\Lambda_{\overline{MS}}$. In addition there are large hadronisation corrections analogous to those of the narrow jet broadening. Together these have the effect of raising the fitted value of $\Lambda_{\overline{MS}}$ which is reflected in the large error band.

The D-Parameter

The D-parameter provides a very good fit away from the large logarithm limit of $D \to 0$. We would therefore expect this variable to have relatively small hadronisation corrections.

Summary of Four-Jet Observables

We summarise all extracted values of $\Lambda_{\overline{MS}}$ from four-jet observables in Figure 3.53. Comparing these value with that of the three-jet variables, there is a seemingly large disparity. Closer inspection reveals that the "light hemisphere mass" and "narrow jet broadening" are both pulling the average value of $\Lambda_{\overline{MS}}$ much higher than the remaining four-jet variables would otherwise suggest. This is an indication of why we should not trust an overall average too much. Hadronisation corrections have not been applied in this case and as we shall see in the next chapter, these effects with infrared logarithm resummations are needed to describe the data.
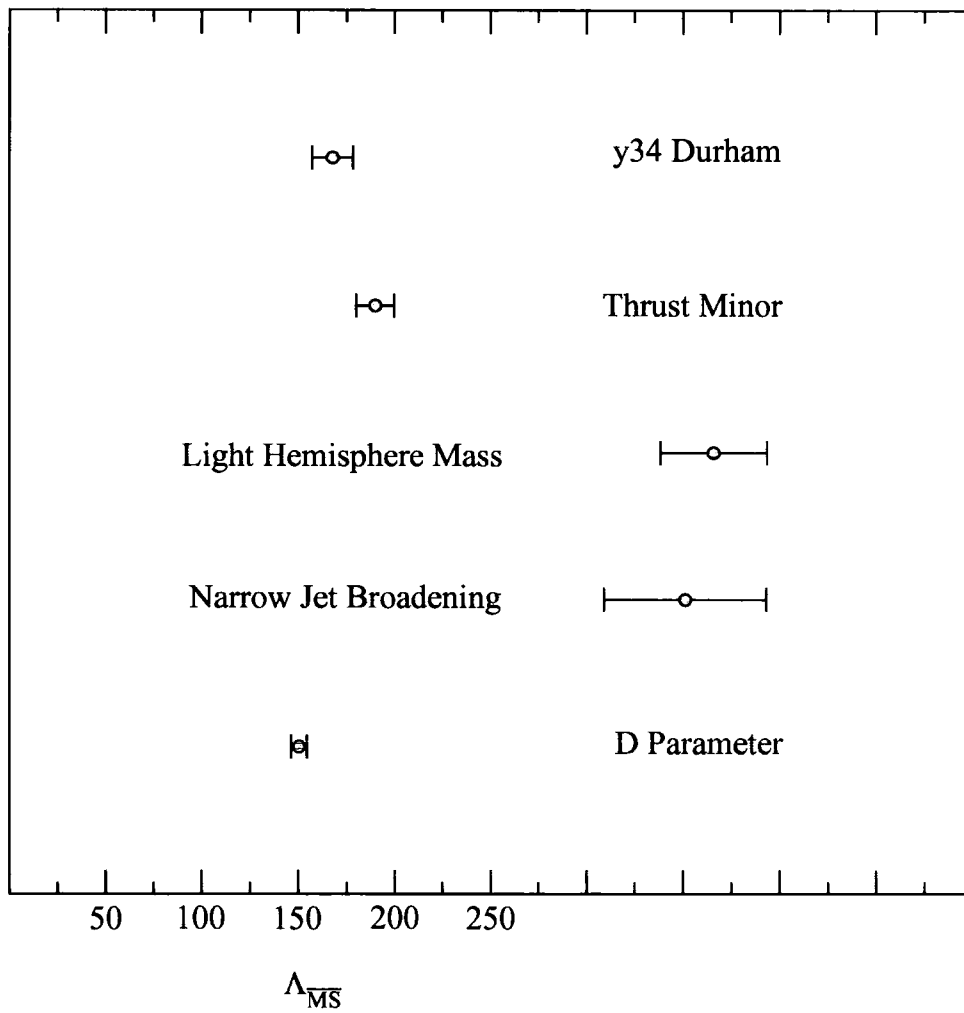
Figure 3.53: Summary of $\Lambda_{\overline{MS}}$ measurements uncorrected for hadronisation effects.

3.8   Energy Dependence of Observables

In this section we will explore the scaling behaviour of physical observables. This provides a strong motivation in favour of the RG-improved formalism. It was argued previously that it is possible to test QCD by simply examining the running of an observable quantity with energy. Away from quark mass thresholds the RGE should completely dictate the energy dependence and it is this feature we hope to explore in this section with emphasis on the thrust distribution.

3.8.1   The Thrust Distribution

We are fortunate enough to have experimental measurements of the thrust distribution at a wide variety of energy scales from PETRA to LEP2. We shall be considering the following data

- PETRA (Detector- Tasso, Facility-DESY) [74]

    – Centre of Mass Energies - 14, 22, 35 GeV

- PEP (Detector- Mark-II, Facility-SLAC) [75]

    – Centre of Mass Energy - 29GeV

- TRISTAN (Detector- Amy, Facility-KEK) [76]

    – Centre of Mass Energy - 52GeV

- SLC (Detector- SLD, Facility-SLAC)

    – Centre of Mass Energy - 91GeV

- LEP (Detectors- Aleph, Delphi, L3, Opal, Facility-CERN)

    – Centre of Mass Energy - 91GeV

Unfortunately as the LEP2 data suffers from large errors due to poor statistics, we are forced to exclude it from the analysis. Considering the energy dependence dictated by the RGE, we would expect to see that at higher energies, we are closer to asymptotia and hence our terminated series should give a more reliable estimate of $\Lambda_{\overline{MS}}$. This is clearly apparent in Figures 3.54 and 3.55 (where we have removed
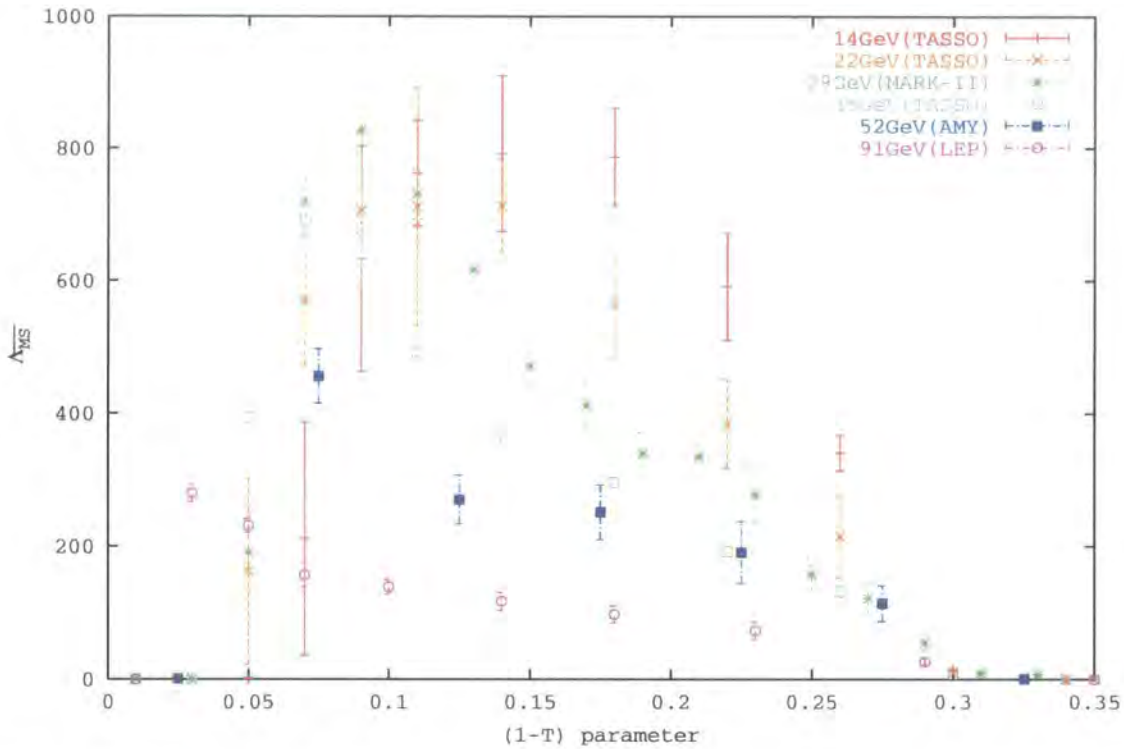
Figure 3.54: The Energy Dependence of $\Lambda_{\overline{\text{MS}}}$ Measurements from the Thrust Distribution

the error bars for clarity). In the limit $1 - T \to \frac{1}{3}$ we are faced once again with the problem of the kinematic end point dragging the value to zero. In the $1 - T \to 0$ limit, large kinematic logarithms dominate from the emission of soft and collinear gluons. Clearly in between we see a "flattening" of the $\Lambda_{\overline{\text{MS}}}$ value with $1 - T$. This can be interpreted as higher order and power-like corrections having less influence, and hence the NLO approximation is more reliable.

3.8.2 Investigating Higher Order Effects and Power Correction

As suggested in Section 2.7, it is possible to consider the formalism from a different perspective whereby we accept that $\Lambda_{\overline{\text{MS}}}$ is a constant and that any deviations from its true value are due to higher order effects and power corrections. In this case we may then try to approximate these contributions by the leading terms as given by Equation (2.97). In this section we highlight a simple mechanism for investigating
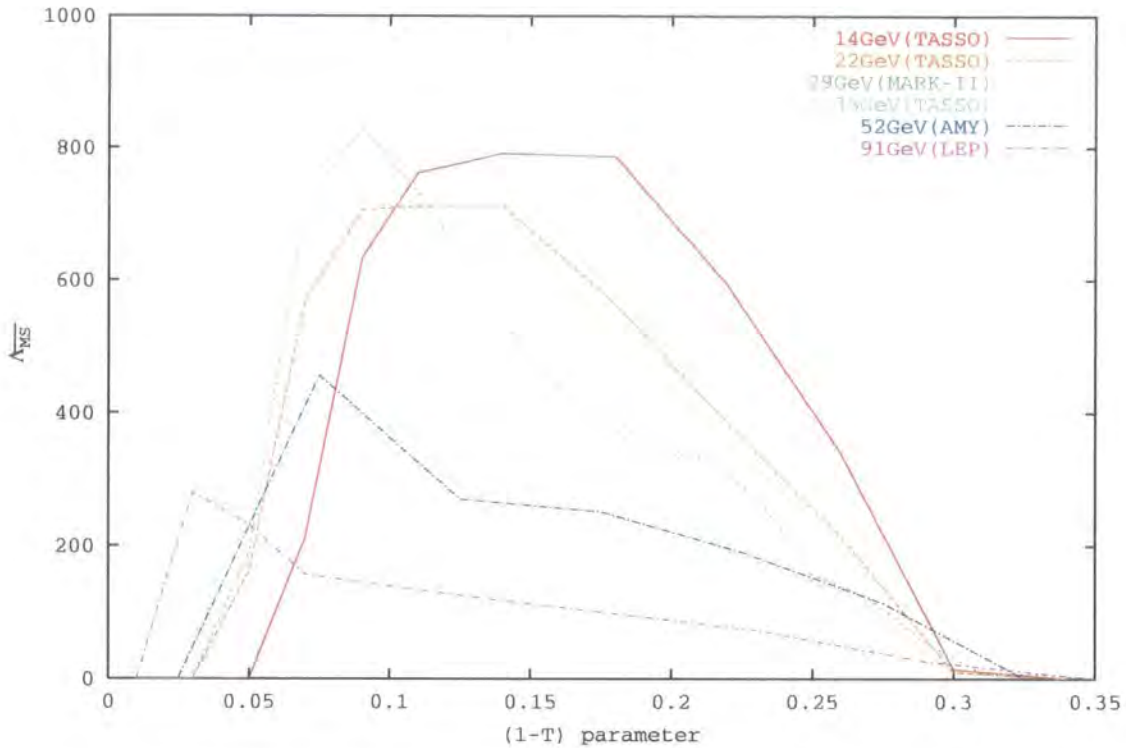
Figure 3.55: The Energy Dependence of $\Lambda_{\overline{MS}}$ Measurements from the Thrust Distribution

these effects. We stress that this by no means provides a highly accurate estimate of these terms, but merely an indication of how important they are. We begin by rewriting Equation (2.97) as

$$\kappa_0 = M(\mathcal{R}, r)\rho_2 + C(\mathcal{R}, r), \qquad (3.35)$$

where $M(\mathcal{R}, r)$ and $C(\mathcal{R}, r)$ are known terms at NLO, having specified a value for $\Lambda_{\overline{MS}}$. This is simply the equation of a straight line in (κ_0, ρ_2) space. Since these two quantities are Q-independent (see Section 2.7), we may plot the lines corresponding to different centre-of-mass energies and expect them to cross over at the solution. This is illustrated in Figure 3.56 where we have taken a value of $\Lambda_{\overline{MS}} = 200\text{MeV}$. We have made no attempt to incorporate the errors, which for the LEP-II data will be considerable. In all cases, the central value is taken. This naïve procedure does give a promising result, though. There appears to be two predominant localised cross-over regions where the lines appear to converge.
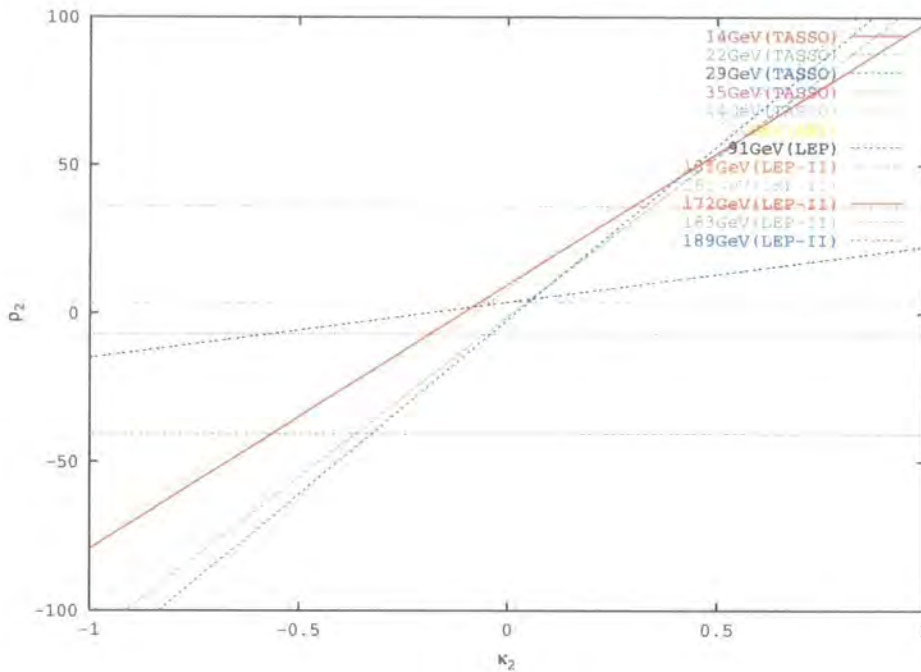
Figure 3.56: Fitting for the leading power correction (κ_0) and NNLO (ρ_2) using the thrust distribution at different energies. We use a value of $\Lambda_{\overline{MS}} = 200$MeV

3.9 Summary

In this chapter we saw the results of directly extracting $\Lambda_{\overline{MS}}$ from three and four-jet rates, event shape variable distributions and energy-weighted cross sections. On the whole this gave very reasonable results. We saw the necessity to account for hadronisation effects in order to connect perturbation theory with experiment. This reduces the scatter in the extracted values that would arise from non-perturbative power corrections. Furthermore, the formalism provides a clear indication for the regions where infrared logarithms become important. In these regions we have been forced to limit our fit range so as to avoid their undesirable effect upon $\Lambda_{\overline{MS}}$, extracted at NLO.

Otherwise, the RG-improved perturbation theory has demonstrated a consistent measurement of $\Lambda_{\overline{MS}}$ with the scatter in Figure 3.46 due to the relative size of unaccounted higher order corrections. In a sense these values are the final result of this analysis. Combining them requires making unfounded assumptions upon how they are all related, whether correlated or otherwise. Only an NNLO perturbative

calculation can truly be seen to provide a means of extracting a less scattered result.

The summary values indicate a value of $\Lambda_{\overline{MS}}$ in the region of 130 MeV that corresponds to $\alpha_s(M_Z) \approx 0.11$. Care should be taken in comparing these values with that of the "world average" quoted as $\alpha_s(M_z) = 0.1184 \pm 0.0031$ by Bethke [77]. The world average is composed using the physical scale method with theoretical errors given by varying the value for μ. This will clearly give a different resultant value of α_s.

We have seen in Chapter 2, that by demanding a complete renormalisation group improvement of QCD perturbation theory, we build the correct Q-dependence of a perturbative approximant. This was remarkably verified in Figures 3.54 and 3.55 where the property of asymptotic scaling is witnessed. This provides strong confirmation that the energy dependence is being treated in a correct manner. By plotting the value of $\Lambda_{\overline{MS}}$ in this way we may clearly see how close the centre-of-mass energy is to approximating an asymptotic limit.

Lastly, we considered a simple investigation into the effects of uncalculated terms. Clearly there is no substitute for proceeding with the explicit calculation, but by parameterising the deviation from an asymptotic limit we are able to motivate a *quality* assessment of the NLO approximation. This would be equivalent to the "theoretical error" of physical scale analyses. By variation of the unphysical scale μ, higher order terms are supposedly probed. We have seen that this is clearly not the case and a better estimate of the higher order terms can be made by considering measurements of $\Lambda_{\overline{MS}}$ at a variety of energy scales. Interestingly, if an NNLO calculation has been performed for a single distribution, this too may be used to estimate the size of NNLO corrections to other distributions. In the absence of any such calculations, there is no way of specifying which extracted value of $\Lambda_{\overline{MS}}$ is closest to the true value.

Chapter 4

Infrared Logarithm Resummations

4.1 Introduction

In Chapter 1 we encountered infrared (IR) divergences that arise as a result of the emission of soft and/or collinear massless partons. For fully inclusive observables, these divergences cancel exactly, but for more exclusive variables, logarithmic divergences occur order by order as we move towards the exclusive boundary of phase space. The problems this causes in fixed order perturbation theory became apparent when we attempted to fit a value for $\Lambda_{\overline{MS}}$ for distributions of event shape variables, requiring the need to impose an artificial cut in the fit range. In this chapter we shall consider the infrared kinematic logarithms that are at the root of this, and demonstrate the procedure for remedying the situation by resumming the dominant terms to all orders. The machinery to do this is already well established for three-jet event shape variables such as thrust, wide jet broadening, heavy hemisphere mass, C parameter etc., by means of the coherent branching formalism [54, 59, 78, 79, 80]. Furthermore, significant power suppressed effects are present and have been phenomenologically studied [81]. To accurately describe the data all the ingredients of fixed order, infrared resummation and power correction are found to be necessary.

Four-jet event shape observables also contain useful information about QCD. They are more sensitive to the triple gluon vertex and therefore the true gauge structure of QCD [82], and also to the presence of other light coloured particles such as the gluino [83] that can be pair produced by gluon splitting. However, these variables have received much less attention partly because they are suppressed by an additional power of α_s, requiring a second gluon to be radiated, but also because the theoretical description is much less developed. For most four-jet event shape
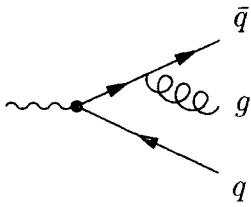
Figure 4.1: Real gluon emission contributions to LO thrust distribution
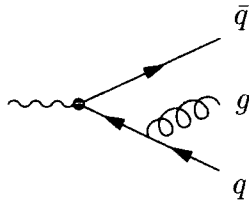
Figure 4.2: Virtual gluon contribution to LO thrust distribution

variables, the situation is the same as for the three-jet event shape variables; the NLO corrections are very large and, taking a naïve choice of renormalisation scale of the order of the centre-of-mass energy Q, still undershoot the data significantly [48]. This suggests the presence of large infrared effects as well as significant power corrections. In this chapter we will address the issue of resumming infrared logarithms for the four-jet rate in the Durham scheme and for specific four-jet event shape variable distributions, namely the light hemisphere mass, ρ_L, and narrow jet broadening, B_N.

We begin by taking a detailed look at how the infrared logarithms arise and as always we take the massless approximation. When considering semi-inclusive jet obserables such as the differential cross-sections of e^+e^- event shape variables, we are required to restrict the available phase space according to its definition. In doing so we avoid the IR divergence but are left with large logarithms of the variable as an artifact. Consider the simple case of the 1-Thrust parameter. At LO, $(\mathcal{O}(\alpha_s))$, we will have terms contributing to the total cross section due to the emission of a single gluon. This can occur either through real emission (Figure 4.1) or from the interference of a virtual gluon contribution (Figure 4.2) with the tree level. Defining the parton energy fractions

$$x_i = \frac{2E_i}{Q} \tag{4.1}$$

for each parton i $(i = q, \bar{q}, g)$ with energy E_i (and 4-momentum p_i) produced at a hard scale Q and normalised such that $x_q + x_{\bar{q}} + x_g = 2$, we can write the $q\bar{q}g$ matrix element as

$$\frac{1}{\sigma_0}\frac{\mathrm{d}\sigma_{q\bar{q}g}}{\mathrm{d}x_q\mathrm{d}x_{\bar{q}}} = C_F\frac{\alpha_s}{2\pi}\frac{x_q^2 + x_{\bar{q}}^2}{(1 - x_q)(1 - x_{\bar{q}})} \tag{4.2}$$
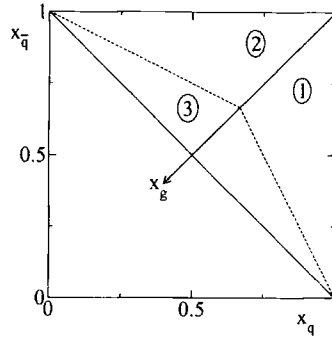
Figure 4.3: Phase space for leading order contribution to thrust distribution

where we have integrated out the angular dependence and eliminated x_g (see for example [4]). For the fully inclusive total cross section we would need to supplement this contribution with that from $d\sigma_{q\bar{q}}/\sigma_0$ for cancellation of the IR singularity. To obtain the leading α_s contribution to the thrust distribution, we must integrate the $q\bar{q}g$ matrix element over the appropriate three parton phase space by imposing the constraint $\delta(T - \max\frac{\Sigma|\mathbf{p_i}\cdot\mathbf{n_T}|}{\Sigma|\mathbf{p_i}|})$. With three final state partons the thrust variable is equal to the energy fraction of the most energetic parton and the axis, $\mathbf{n_T}$ is aligned along its direction. Performing the integration over regions ①, ② and ③ in Figure 4.3 with $(x_q > x_{\bar{q}}, x_g)$, $(x_{\bar{q}} > x_q, x_g)$ and $(x_g > x_q, x_{\bar{q}})$ respectively we find

$$\frac{1}{\sigma_0}\frac{d\sigma}{dT} = C_F\frac{\alpha_s}{2\pi}\left(2\frac{(3T^2 - 3T + 2)}{T(1-T)}\ln\left(\frac{2T-1}{1-T}\right) - \frac{3(3T-2)(2-T)}{1-T}\right). \quad (4.3)$$

The troublesome large kinematic logarithm is now apparent when we take the limit $T \to 1$,

$$\frac{1}{\sigma_0}\frac{d\sigma}{dT} \underset{T\to 1}{=} C_F\frac{\alpha_s}{2\pi}\left(\frac{4}{1-T}\ln\left(\frac{1}{1-T}\right) - \frac{3}{1-T}\right). \quad (4.4)$$

The first term arises when the gluon becomes both soft and collinear whereas the second term only collinear. Away from this limit the distribution is finite, reflecting the phase space cut imposed by the delta function. The infrared safety of the thrust variable effectively excludes the soft and collinear configurations. At this order, the virtual contribution occurs at $T = 1$ and hence proportional to $\delta(T - 1)$. When integrating over the complete region of thrust to obtain the total cross section this term exactly cancels the $T \to 1$ divergence as we would expect. Returning to the thrust distribution we find that at each order there will be terms of the form $\sim \alpha_s^n\frac{\ln^{2n-1}(1-T)}{(1-T)}$. Therefore as $T \to 1$, α_s is no longer a good expansion parameter

due to the enhancement from the logarithms at each order. In order to obtain meaningful results we must resum these terms to all orders.

4.2 The Formalism

To resum the leading powers of IR logarithm to all orders in the coupling requires knowledge of three essential details

- a description of parton splitting probabilities

- a description of dynamic constraints

- a description of phase space constraints

and we shall consider each one in turn.

4.2.1 Parton Splitting Probabilities

A description of the parton splitting probabilities is well established and has applications in many processes as a result of to its universality. The procedure to extract these terms relies on the factorisation of a single splitting, $\mathscr{F}$, from an $(n+1)$ matrix element $(\mathscr{M}_{n+1})$ in the small angle limit,

$$|\mathscr{M}_{n+1}|^2 = \mathscr{F}(t, z) |\mathscr{M}_n|^2 \tag{4.5}$$

We consider a parton a, splitting into partons b and c as in Figure 4.4. In the small angle, θ, approximation we may write

$$t = 2E_b E_c (1 - \cos\theta) = z(1 - z)E_a^2\theta^2 \tag{4.6}$$

where $\theta = \theta_b + \theta_c$ and can be decomposed using transverse momentum conservation,

$$\theta = \frac{1}{E_a}\sqrt{\frac{t}{z(1-z)}} = \frac{\theta_b}{1-z} = \frac{\theta_c}{z}. \tag{4.7}$$

Applying the Feynman rules to the splitting, we can separate the contributions from the initial parton's propagator together with the $a \rightarrow b, c$ vertex into the function $\mathscr{F}(t, z)$. The initial partons' propagator will always give rise to a $\frac{1}{\sqrt{t}}$ factor[1]

---

[1] Strictly speaking the propagator contributes a $\frac{1}{t}$ but this will always get multiplied by a $\sqrt{t}$ factor
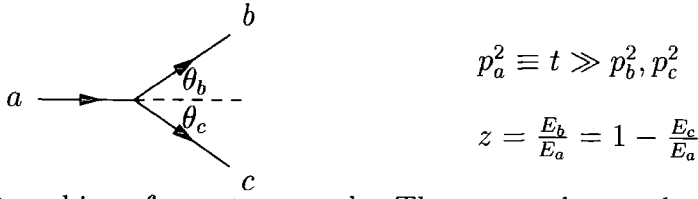
$$p_a^2 \equiv t \gg p_b^2, p_c^2$$

$$z = \frac{E_b}{E_a} = 1 - \frac{E_c}{E_a}$$

Figure 4.4: Branching of a parton $a \to bc$. The arrows denote the flow of momentum.

regardless of the specific splitting. We must then take each vertex case in turn (e.g. $q \to gq$, etc.) and consider the small angle limit. A decomposition can be performed by taking into consideration that the gluon will be nearly on mass shell and hence can be treated as purely transversely polarised. Additionally, the quark masses can be neglected enabling exact helicity conservation. Utilising these properties with Equations (4.6) and (4.7), we can evaluate the specific case of a quark emitting a gluon (parton c) at small angle. In this case we will get a colour factor of C_F from tracing the T^A matrices and obtain [4]

$$|\bar{\mathcal{M}}_{n+1}|^2 \sim \frac{4}{t} \frac{\alpha_s}{2\pi} C_F \frac{1}{4} \left(2 \frac{(1+z)^2}{1-z} + 2(1-z) \right) |\bar{\mathcal{M}}_n|^2, \tag{4.8}$$

for the spin averaged matrix element squared. The first z dependent term corresponds to the gluon with polarisation in the plane of branching. It becomes singular as $z \to 1$ corresponding to the soft gluon limit. The subsequent term linear in z is from a gluon polarisation transverse to the plane of branching.

This will occur at every $q \to qg$ splitting and gives rise to the so-called *unregularised Altarelli-Parisi splitting function*,

$$\hat{P}_{qq}[\alpha_s, z] = C_F \frac{\alpha_s}{2\pi} \left[\frac{1+z^2}{1-z} \right], \tag{4.9}$$

This can be repeated for all other splitting probabilities and are listed in Appendix A. Finally, if the phase space factorises in this limit, we obtain the probability associated with a parton, a, splitting into partons b and c of

$$d\mathcal{P}_{ab} = \frac{dt}{t} dz \hat{P}_{ba}(z), \tag{4.10}$$

for each branching. By applying these probabilities iteratively it is possible to build up a picture of parton evolution. We find that parton probability distributions are quite naturally expressed in terms of the *Sudakov form factor*,

$$\Delta_a(t, t_0) \equiv \exp \left[- \sum_b \int_{t_0}^t \frac{dt'}{t'} \int dz \frac{\alpha_s}{2\pi} \hat{P}_{ba}(z) \right]. \tag{4.11}$$

We can then write the energy fraction, x, distribution of parton a at a hard interaction scale t, as $\phi(x, t)$ in terms of a preceding distribution, $\phi(x, t_0)$,

$$\phi_a(x, t) = \Delta_a(t, t_0)\phi_a(x, t_0) + \int_{t_0}^{t} \frac{dt'}{t'} \frac{\Delta_a(t, t_0)}{\Delta_a(t_0, t')} \sum_b \int \frac{dz}{z} \frac{\alpha_s}{2\pi} \hat{P}_{ba}(z)\phi_b(\tfrac{x}{z}, t'). \quad (4.12)$$

It is clear from this equation that the Sudakov form factor, $\Delta_a(t, t_0)$ represents the probability of evolving a parton, a at a scale t_0 to scale t. The Sudakov factor also includes virtual contributions through the constraint of unitarity and is required to generate the first term on the r.h.s. of Equation (4.12) correctly. The limits of the z integration have been left undefined as these will be enforced next through the dynamic constraints.

4.2.2 Dynamic Constraints within the Matrix Elements

The parton splitting formulae given in section 4.2.1 are not complete as the z integration needs to be regulated to avoid the $z \to 0$ soft singularity. In fact the formulae given are only true for collinear enhancements. In this section we shall consider the dynamics within the matrix elements that are due to soft gluon emission and give rise to the remarkable property of *angular ordering*. In QED, it is possible to factorise soft photons completely from within the matrix elements by considering their independent emission. Providing the phase space constraints do not spoil this, it is possible to perform a resummation of infra-red logarithms to all orders. In QCD, we encounter the difficulty that the gauge bosons carry colour charge and thus may self-interact. The factorisation of soft photons hinges upon uncorrelated emission which is clearly untrue for QCD gluons. It has been shown [84] that nevertheless there is a *colour coherence* phenomenon whereby the amplitude for parton emission outside a cone of specific opening angle vanishes in the region of phase space close to the exclusive boundary. The effect is such that subsequent parton branchings have decreasing opening angle resulting in the powerful property of angular ordering. This can be enforced in the branching formalism by changing variables from [4]

$$t \to \tilde{t} = \frac{p_b \cdot p_c}{E_b E_c} E_a^2 \simeq (1 - \cos\theta) E_a^2.$$

The angular ordering constraint requires $\theta_b < \theta_a$ for subsequent branchings. This becomes

$$\tilde{t}_b < z^2\tilde{t}, \quad \tilde{t}_c < (1-z)^2\tilde{t}.$$

giving z integration limits of

$$\sqrt{\frac{t_0}{\tilde{t}}} < z < 1 - \sqrt{\frac{t_0}{\tilde{t}}},$$

Imposing these constraints we get a modified Sudakov factor

$$\tilde{\Delta}_a(\tilde{t}, t_0) = \exp\left[-\sum_b \int_{4t_0}^{\tilde{t}} \frac{dt'}{t'} \int_{\sqrt{t_0/t'}}^{1-\sqrt{t_0/t'}} dz \hat{P}_{ba}[\alpha_s(z^2(1-z)^2t'), z]\right] \qquad (4.13)$$

The factor of 4 in the lower limit of the t' integration is merely due to a change in definition of the infrared cut off, t_0, and the argument of α_s is given by $z^2(1-z)^2t'$ which is equal to the transverse momentum squared of the branching, p_T^2. It has been demonstrated that the transverse momentum should be used [85] as it generates the correct next-to-leading behaviour of the splitting functions when expanded.

The modified Sudakov factor is the foundation of the coherent branching formalism when applied to parton distributions. This enables an efficient resummation of logarithms to a next-to-leading approximation, providing the phase space constraints do not induce correlations between final state partons and spoil the factorisation.

4.2.3   Phase Space Constraints

The phase space constraints depend on the particular choice of variable to be calculated. There will always be a conservation of momentum imposed with typically a further constraint reflecting the nature of an event shape variable or number of final state jets. To perform a resummation to all orders, it is imperative that the phase space displays a similar factorisation to the matrix elements up to the required logarithmic approximation [78]. This is never guaranteed and has to be investigated variable by variable. Providing the phase space factorises, it should then be possible to resum all leading logarithms (LL) and next-to-leading logarithms (NLL) to all orders.

4.3   Exponentiation

For a given event shape variable, λ, that goes to zero when approaching the exclusive phase space boundary, there will in general be large logarithms, $L = \log(1/\lambda)$. The algorithm defined above for resumming these IR logarithms can, in certain circumstances, provide a resummation of all logarithms of the form $\alpha_s^n L^m$ where $n-1 \leq m \leq 2n{-}1$ in the perturbative expansion of an event shape variable distribution. This requires the special property of *exponentiation*. This is most clearly expressed when considering event fractions or rates. That is to say that the fraction of events where the observable λ has a value less than λ,

$$R(\lambda, \alpha_s(Q)) \;=\; \int_0^\lambda \frac{1}{\sigma}\frac{\mathrm{d}\sigma}{\mathrm{d}\lambda}\mathrm{d}\lambda. \tag{4.14}$$

Now there will be two logarithms for every order of α_s, giving a leading logarithm contribution of $\mathcal{O}(\alpha_s^n L^{2n})$ and next-to-leading of $\mathcal{O}(\alpha_s^n L^{2n-1})$ in the perturbative expansion. The property of exponentiation permits the event fraction to be factorised as

$$R(\lambda, \alpha_s(Q)) \;=\; C(\alpha_s(Q))\Sigma(\lambda, \alpha_s(Q)) + D(\lambda, \alpha_s(Q)), \tag{4.15}$$

where

$$C(\alpha_s(Q)) \;=\; 1 + \sum_{n=1}^{\infty} C_n \alpha_s^n, \tag{4.16}$$

$$\ln\!\left(\Sigma(\lambda, \alpha_s(Q))\right) \;=\; \sum_{n=1}^{\infty}\sum_{m=1}^{n+1} G_{nm}\alpha_s^n L^m,$$
$$=\; L g_1(\alpha_s L) + g_2(\alpha_s L) + \alpha_s g_3(\alpha_s L) + \ldots, \tag{4.17}$$

$$D(\lambda, \alpha_s(Q)) \;=\; \sum_{n=0}^{\infty} D_n \alpha_s^n. \tag{4.18}$$

Here C_n and G_{nm} are constants and the perturbatively calculable coefficients $D_n \to 0$ as $\lambda \to 0$. Knowledge of g_2 (or equivalently all G_{nn}) allows resummation of terms down to $\mathcal{O}(\alpha_s^n L^n)$. It has been demonstrated that a number of e^+e^- event shape variables exponentiate in the two-jet limit [59, 78, 79, 80] although this is not always the case as we shall see in the next section.

4.4 The Four Jet Rate

4.4.1 Introduction

Multi-jet rates[2] enable us to examine the perturbative nature of QCD with long distance effects kept comparatively small. Jet rates can satisfy the criterion for infrared safety, provided care is taken in the choice of the jet clustering algorithm. In this section we calculate the leading and next-to-leading logarithmic contribution to the four-jet rate for e^+e^- annihilation using the Durham algorithm. (For an explanation of various algorithms and the reasoning behind choosing the Durham one see refs. [51, 53, 54]). We then obtain an expression for the jet rate in terms of a dimensionless jet resolution parameter, y_{cut}, which can be considered as a measure of how well we are able to resolve two approximately collinear partons. According to the Durham algorithm, we define $y_{cut} = Q_0^2/Q^2$, where $Q \sim \sqrt{s}$ is the scale of the jet-production process and hence the cut-off energy scale Q_0 can be considered to be the energy threshold below which the process starts to become non-perturbative.

In the region of small $y_{cut} (\ll 1)$ the emitted gluons are predominantly soft and collinear resulting in the logarithmic enhancement of higher orders [54, 86]. It is therefore necessary to resum them to all orders in α_s to obtain a reliable prediction for the four-jet rate.

4.4.2 Leading Logarithms and Exponentiation

First it is important to stress what we are actually calculating in the resummation procedure. Using the coherent branching formalism [4, 78, 87, 88], we are able to resum *exactly* all contributions to the shape variable at leading logarithms, LL $(\alpha_s^n L^{2n})$ and next-to-leading logarithms, NLL $(\alpha_s^n L^{2n-1})$ in the perturbative expansion where $L = -\ln(y_{cut})$. This means that all terms sub-leading are not completely reproduced and therefore they are dropped in our calculation.

The idea behind exponentiation is to increase the domain of applicability of the shape variable such that it extends into the region of $\alpha_s L \leq 1$. The result of this procedure is to obtain a closed function of the form $\mathcal{F}(Lg_1(\alpha_s L) + g_2(\alpha_s L))$, where $g_1(\alpha_s L)$ resums all leading-logarithmic contributions and $g_2(\alpha_s L)$ resums the next-to-leading ones such that when expanded the whole perturbation series is reproduced

---

[2]The n-jet rate is defined as $R_n(Q) = \sigma_{n\text{-}jet}/\sigma_{hadrons}$

down to terms of the form $\alpha_s^n L^m$, where $n \le m \le 2n$. For the jet fractions being studied, a simple exponentiation does not arise. It therefore only makes sense to calculate the LL and NLL contributions of the perturbative series.

4.4.3   Calculation

To find an analytic expression for the four-jet rate, $R_4(y_{cut})$, the most simple method is to work in terms of a generating function defined by

$$\phi^p(Q, Q_0; u) = \sum_{n=0}^{\infty} u^n R_n^p(Q, Q_0), \tag{4.19}$$

where $R_n^p(Q, Q_0)$ is the probability of finding n-partons of a particular type in the final state of a process, p, and u is a jet label to distinguish each of the probabilities. In this case we are dealing with $e^+e^- \to$ hadrons, therefore $\phi^{(e^+e^-)} = [\phi_q]^2$, where ϕ_q is the generating function for a single quark to branch. This can be obtained using the coherent branching formalism of Section 4.2 [4, 54]. By changing variables from $\tilde{t} \to \tilde{q} = \sqrt{\tilde{t}}$, we arrive at the generating function for a parton a branching to b and c

$$\begin{aligned}
\phi_a(Q, Q_0; u) &= \phi_a(Q_0, Q_0; u) \\
&+ \sum_b \int_0^Q \frac{d\tilde{q}}{\tilde{q}} \int_0^1 \hat{P}_{ba}(\alpha_s(z(1-z)\tilde{q}), z)\ \theta(\min(z, 1-z)\tilde{q} - Q_0) \\
&\times [\phi_b(z\tilde{q}, Q_0; u)\, \phi_c((1-z)\tilde{q}), Q_0; u) - \phi_a(\tilde{q}, Q_0; u)], \tag{4.20}
\end{aligned}$$

where we have used the fact that after branching, $\phi_a \to \phi_b\,\phi_c$. The theta function represents the infrared cut-off which for the Durham jet clustering algorithm translates to a requirement that the transverse momentum $z^2\tilde{q}^2$ and $(1-z)^2\tilde{q}^2$ of two final state jets be larger than the resolution cut,

$$\min(z^2\tilde{q}^2, (1-z)^2\tilde{q}^2) > Q_0^2 \equiv Q^2 y_{cut}. \tag{4.21}$$

Furthermore with this cut, the generating function at Q_0 corresponds to resolving precisely one jet. Therefore squaring this will describe the limiting case of resolving two jets only,

$$\phi_q^2(Q_0, Q_0; u) = u^2 R_2(Q_0, Q_0) = u^2 \tag{4.22}$$

providing the boundary condition

$$\phi_{q,g}(Q_0, Q_0; u) = u. \tag{4.23}$$

Applying this to the quark generating function, averaging over slowly varying z dependence and approximating $z \to 1$ in the arguments (except for the singular $\frac{1}{1-z}$ term) we obtain [54]

$$\phi_q(Q, Q_0; u) = u + \int_{Q_0}^{Q} \frac{d\tilde{q}}{\tilde{q}} \int_{Q_0/\tilde{q}}^{1} dz \, \alpha_s(z\tilde{q}) \frac{C_F}{\pi} \left(\frac{2}{z} - \frac{3}{2} \right) [\phi_g(z\tilde{q}, Q_0; u) - 1]. \tag{4.24}$$

To obtain the n-jet rate, R_n, is simply a matter of differentiating the generating function n times at $u = 0$. The n-jet rate is then

$$R_n(y_{cut}) = \frac{1}{n!} \left(\frac{\partial}{\partial u} \right)^n [\phi_q(Q, Q_0; u)]^2 \Big|_{u=0}. \tag{4.25}$$

We find from the application of the coherent branching formalism, the generating function obeys the following implicit coupled equations [54]:

$$\phi_q(Q, Q_0; u) = u \exp \left(\int_{Q_0}^{Q} dq \, \Gamma_q(Q, q)[\phi_g(q, Q_0; u) - 1] \right) \tag{4.26}$$

and

$$\phi_g(Q, Q_0; u) = u \, \exp \left(\int_{Q_0}^{Q} dq \{ \Gamma_g(Q, q)[\phi_g(q, Q_0; u) - 1] - \Gamma_f(q) \} \right)$$
$$\times \left(1 + u \int_{Q_0}^{Q} dq \, \Gamma_f(q) \exp \left(\int_{Q_0}^{q} dq' \{ [2\Gamma_q(q, q') - \Gamma_g(q, q')][\phi_g(q', Q_0; u) - 1] + \Gamma_f(q') \} \right) \right). \tag{4.27}$$

Where the emission probabilities are defined as

$$\Gamma_q(Q, q) = \frac{2C_F}{\pi} \frac{\alpha_s(q)}{q} \left(\ln \frac{Q}{q} - \frac{3}{4} \right), \tag{4.28}$$

$$\Gamma_g(Q, q) = \frac{2C_A}{\pi} \frac{\alpha_s(q)}{q} \left(\ln \frac{Q}{q} - \frac{11}{12} \right), \tag{4.29}$$

$$\Gamma_f(q) = \frac{N_f}{3\pi} \frac{\alpha_s(q)}{q}. \tag{4.30}$$

The two-jet limit is important as the jet rate becomes semi-inclusive and exponentiation holds exactly. This gives

$$R_2(y_{cut}) = \exp \left(\frac{C_F a L}{2} (3 - L) - \pi \beta_0 \frac{C_F a^2 L^3}{3} \right), \tag{4.31}$$

where $L = \ln(1/y_{cut})$, $a = \alpha_s(Q)/\pi$ and we have used $\beta_0 = (11C_A - 2N_f)/12\pi$. The three-jet case was evaluated in [89] and we proceed in a similar way.

Firstly we find Equation (4.25) gives, in the n=4 case [54],

$$
\begin{aligned}
R_4(y_{cut}) &= 2R_2(y_{cut}) \left(\int_{Q_0}^Q dq\, \Gamma_q(Q,q) \Delta_g(q) \int_{Q_0}^q dq'\, \Gamma_g(q,q') \Delta_g(q') \right) \\
&+ 2R_2(y_{cut}) \left(\int_{Q_0}^Q dq\, \Gamma_q(Q,q) \Delta_g(q) \int_{Q_0}^q dq'\, \Gamma_f(q') \Delta_f(q') \right) \\
&+ R_3(y_{cut}) \left(\int_{Q_0}^Q dq \Gamma_q(Q,q) \Delta_g(q) \right),
\end{aligned}
\tag{4.32}
$$

where we have introduced the Sudakov form factors

$$
\Delta_q(Q) = \exp\left(- \int_{Q_0}^Q dq\, \Gamma_q(Q,q) \right),
\tag{4.33}
$$

$$
\Delta_g(Q) = \exp\left(- \int_{Q_0}^Q dq\, [\Gamma_g(Q,q) + \Gamma_f(q)] \right),
\tag{4.34}
$$

$$
\Delta_f(Q) = \exp\left(- \int_{Q_0}^Q dq\, [2\Gamma_q(Q,q) - \Gamma_g(Q,q) - \Gamma_f(q)] \right).
\tag{4.35}
$$

Equation (4.32) has a simple probabilistic interpretation illustrated in Figure 4.5. The first term on the r.h.s. corresponds to an initial two-jet configuration with a subsequent gluon emission which itself splits into two further gluons and ultimately all four partons showering soft and/or collinear gluons (see Figure 4.5(a) and Figure 4.5(b)). The second term corresponds to an initial two-jet configuration with a subsequent gluon emission which then splits into a quark-antiquark pair with further soft and/or collinear gluon showering (see Figure 4.5(c) and Figure 4.5(d)). The last term corresponds to a three-jet configuration with a further gluon emission and then soft and/or collinear gluon showering.

In the NLL approximation we need only work with the one-loop definition of the strong coupling constant,

$$
\alpha_s(Q) = \frac{\alpha_s(\mu)}{1 + 2\beta_0 \alpha_s(\mu) \ln\left(\frac{Q}{\mu}\right)},
\tag{4.36}
$$

as higher order corrections will be sub-leading. Even at this order we are still faced with an extremely complicated set of nested integrals. Therefore, as in [89] we proceed by expressing $R_4(y_{cut})$ as

$$
R_4(y_{cut}) = R_4 \Big|_{\beta_0 = 0} + \beta_0 \frac{\partial R_4}{\partial \beta_0} \Big|_{\beta_0 = 0}.
\tag{4.37}
$$
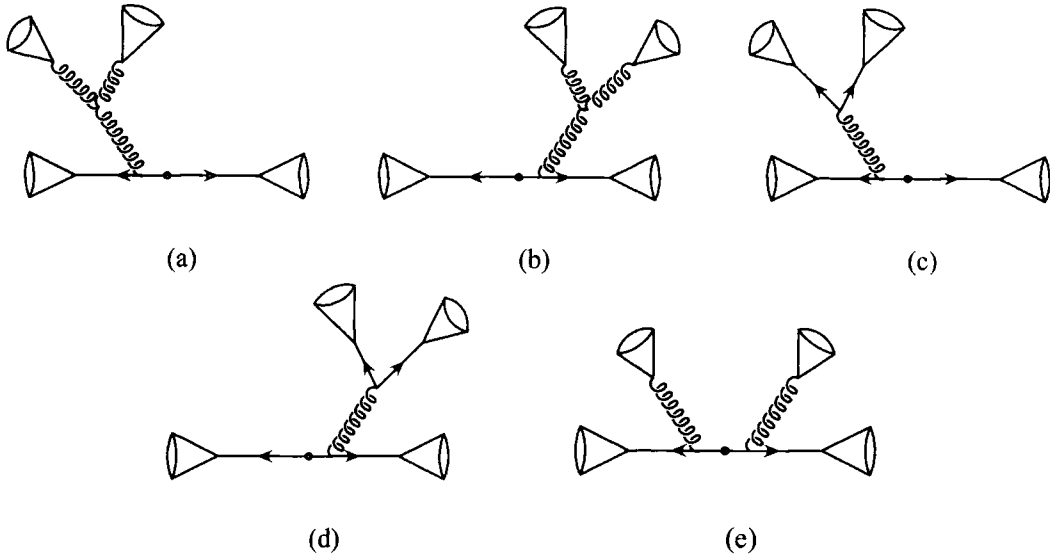
Figure 4.5: Four-parton configurations contributing to the resummed four jet rate at NLL. (a) and (b) through a two-jet configuration with $g \to gg$ emission, (c) and (d) through a two-jet configuration with $g \to q\bar{q}$ emission and (e) through a three-jet configuration with an independent gluon emission. The cones represent subsequent coherent soft and collinear gluon emission.

This is permissable for any jet multiplicity evaluated at next-to-leading logarithmic order because in general we will have

$$
\begin{aligned}
R_n \;=\;& \mathscr{C}_{12} a L^2 + \mathscr{C}_{11} a L + \cdots \\
& + \mathscr{C}_{24} a^2 L^4 + \mathscr{C}_{23} a^2 L^3 + \cdots \\
& \;\;\vdots \\
& + \mathscr{C}_{n\,2n} a^n L^{2n} + \mathscr{C}_{n\,2n-1} a^n L^{2n-1} + \cdots,
\end{aligned} \tag{4.38}
$$

where the coefficients $\mathscr{C}_{pq}$ are either β_0 independent ($\mathscr{C}_{p\,2p}$) or contain a single β_0 ($\mathscr{C}_{p\,2p-1}$). All other β_0 dependence is contained in the strong coupling constant. We note that

$$
\left. \frac{\partial [\alpha_s(Q)]^m}{\partial \beta_0} \right|_{\beta_0 = 0} = -2m[\alpha_s(Q)]^{m+1} \ln\left(\frac{Q}{Q_0}\right) \sim a^{m+1} L. \tag{4.39}
$$

It is now apparent that beyond the first derivative there will only be terms of the form $a^n L^{2n-2}$ which in the NLL approximation can be dropped. The assumption of Equation (4.37) is then valid. In fact this expansion greatly simplifies the calculation by enabling us to work with terms evaluated with β_0 equal to zero. In doing so the

coupling α_s can really be treated as a constant and hence no longer depends on the integration variable. Proceeding in this way, we then calculate the four jet rate to be [90]

$$
\begin{aligned}
R_4 \;=\; & \frac{C_F^2}{C_A^2}\Big(e^{-2(A+F)}\big((e^A-1)^2(2+3C_FaL) \\
& -\sqrt{C_Aa}\,e^A(e^A-1)(-3+12F+2L)\sqrt{\pi}\,\mathrm{erf}(\sqrt{A})\big)\Big) \\
& +\frac{C_F}{C_A}\Big(\tfrac{1}{24}e^{-2F}\big(-24e^{-2A}(e^A-1)(2+3aC_FL) \\
& \qquad -4\sqrt{C_Aa}\,e^{-A}(2+3e^A(-3+12F+2L))\sqrt{\pi}\,\mathrm{erf}(\sqrt{A}) \\
& \qquad -(12+aL(11C_A-6C_F(-9+12F+2L)))\pi\,\mathrm{erf}(\sqrt{A})^2 \\
& \qquad +2\sqrt{C_Aa}(-7+72F+12L)\sqrt{2\pi}\,\mathrm{erf}(\sqrt{2A})\big)\Big)-\tfrac{11}{3}\,\varphi \\
& +\frac{4\pi\beta_0}{C_A}\Bigg(\frac{C_F^2}{C_A^2}\tfrac{1}{12}\Big(e^{-2(A+F)}\big(-2\sqrt{C_Aa}e^A(3+2A(-3+4F))\sqrt{\pi}\,\mathrm{erf}(\sqrt{A})\big) \\
& \qquad \big(1+e^A(-1+\sqrt{A}\sqrt{\pi}\,\mathrm{erf}(\sqrt{A}))\big)\Big) \\
& \quad +\frac{C_F}{C_A}\tfrac{1}{12}\Big(e^{-2(A+F)}2C_FaL(1+2e^A+4(e^A-1)F) \\
& \qquad \big(1+e^A(-1+\sqrt{A}\sqrt{\pi}\,\mathrm{erf}(\sqrt{A}))\big)\Big) \\
& \quad +\sqrt{\frac{C_F}{C_A}}\tfrac{1}{24}\Big(\sqrt{C_Fa}\,e^{-2(A+F)}\big(2e^A(5+e^A \\
& \qquad +A(-4-2e^A(3-8F)))\sqrt{\pi}\,\mathrm{erf}(\sqrt{A}) \\
& \qquad -e^{2A}(9-4A(3-8F))\sqrt{2\pi}\,\mathrm{erf}(\sqrt{2A})\big)\Big) \\
& \quad +\tfrac{1}{12}C_FaL\,e^{-2(A+F)}(1-e^A(1-3e^A)-8F(1-e^A) \\
& \qquad +2Fe^{2A}\pi\,\mathrm{erf}^2(\sqrt{A}))+\varphi\Bigg),
\end{aligned}
\tag{4.40}
$$

where

$$
\begin{aligned}
\varphi \;=\; & \Big(\tfrac{1}{4}\sqrt{C_Fa}\,e^{-2F}\big(\sqrt{2\pi}\,\mathrm{erf}(\sqrt{2F})-2\sqrt{\tfrac{C_F}{C_A-2C_F}}\,e^{-A}\sqrt{\pi}\,\mathrm{erfi}(\sqrt{A-2F})\big)\Big) \\
& +\tfrac{1}{2}\Big(C_FaL\,e^{-2F}\sqrt{\pi}\,\mathcal{G}\big(\tfrac{C_A}{C_A-2C_F},i\sqrt{A-2F}\big)\Big),
\end{aligned}
$$

$\mathrm{erf}(x)$ is the error function defined to be $\frac{2}{\sqrt{\pi}}\int_0^x e^{-y^2}dy$ and $\mathrm{erfi}(x)=\mathrm{erf}(ix)/i$. We have also defined $A=C_AaL^2/4$, $F=C_FaL^2/4$ and $\mathcal{G}(x,z)=x\int_0^z e^{xy^2}\mathrm{erf}(y)dy$. Attempts were made to solve $\mathcal{G}$ exactly, but no closed form was found. It appears that the integral is just a generalisation of the error function and hence cannot be solved, except in certain cases. A reference containing various properties of this function is given [91].

4.4.4 Properties of the Four-Jet Rate

With the complete result calculated we are able to reproduce the exact LL and NLL coefficients of α_s at any order. The first three orders in α_s/π are given.

i.e. $R_4(y_{cut}) = a^2(B_4 L^4 + B_3 L^3 + \mathcal{O}(L^2)) + a^3(C_6 L^6 + C_5 L^5 + \mathcal{O}(L^4))$
$+ a^4(D_8 L^8 + D_7 L^7 + \mathcal{O}(L^6)) + \cdots$.

$$B_4 = \tfrac{1}{8}C_F{}^2 + \tfrac{1}{48}C_F C_A.$$

$$B_3 = \tfrac{-3}{4}C_F{}^2 - \tfrac{5}{18}C_F C_A + \tfrac{1}{36}C_F N_f.$$

$$C_6 = \tfrac{-1}{16}C_F{}^3 - \tfrac{1}{48}C_F{}^2 C_A - \tfrac{7}{2880}C_F C_A^2.$$

$$C_5 = \tfrac{9}{16}C_F{}^3 + \tfrac{71}{144}C_F{}^2 C_A + \tfrac{217}{2880}C_F C_A^2 - \tfrac{41}{720}C_F{}^2 N_f - \tfrac{1}{120}C_A C_F N_f.$$

$$D_8 = \tfrac{1}{64}C_F{}^4 + \tfrac{1}{128}C_F{}^3 C_A + \tfrac{1}{512}C_F{}^2 C_A^2 + \tfrac{1}{5120}C_F C_A^3.$$

$$D_7 = \tfrac{-3}{16}C_F{}^4 - \tfrac{17}{64}C_F{}^3 C_A - \tfrac{1439}{17280}C_F{}^2 C_A^2 - \tfrac{2371}{241920}C_F C_A^3 + \tfrac{323}{10080}C_F{}^3 N_f + \tfrac{31}{3024}C_F{}^2 C_A N_f$$
$$+ \tfrac{1}{840}C_F C_A^2 N_f.$$

This is in agreement with [54] which gives the $B_{4,3}$ coefficients. The $C_{6,5}$ coefficients were in addition calculated by expanding out the integral equation (10) as a function of α_s. Another test was to calculate R_4 in the large N_c limit (N_c is the number of colours) to the order of leading logarithms. This greatly simplifies the equations as $C_A \to N_c$, $C_F \to N_c/2$ and N_f can be disregarded. Equation (4.26) now collapses down to

$$\phi(Q, Q_0; u) = u \exp\left(\int_{Q_0}^{Q} dq\, \Gamma_q(Q, q) \left[\frac{1}{u}\phi(q, Q_0; u) - 1\right]\right). \qquad (4.41)$$

Also noting that at leading logarithmic order R_4 will be independent of β_0, we can safely set it to zero. We then get

$$R_4^{N_c} = \frac{1}{4}e^{-3A}\left(6 - 8e^A + 4\sqrt{A}\,e^A(1 - 2e^A)\sqrt{\pi}\,\mathrm{erf}\sqrt{A} - (1 - 2A)\,e^{2A}\,\mathrm{erf}^2\sqrt{A}\right.$$
$$\left. + 2e^{2A}(1 + 2\sqrt{A}\,\sqrt{2\pi}\,\mathrm{erf}\sqrt{2A})\right)(4.42)$$

This is in agreement with the full NLL result in the appropriate limit.

We also note that in the psuedo-abelian limit of simply C_A and N_f going to zero, exact exponentiation holds. We also find that this gives a reasonably good approximation to the full non-abelian case within about 15-20%.

4.5   Four Jet Event Shape Variables

4.5.1   Introduction

In this section we extend the analysis of resumming large infrared logarithms to the cases of four-jet event shape variable distributions. It is clear from the fixed order analysis that these contributions are of paramount importance to the narrow jet broadening and light hemisphere mass. We shall also explore the need for power correction and apply the most naïve model to see the effect. For clarity we repeat the definition of these variables here. We first separate the event at centre-of-mass energy $Q = \sqrt{s}$ into two hemispheres H_1, H_2 divided by the plane normal to the thrust axis $\mathbf{n}_T$. Particles that satisfy $\mathbf{p}_i.\mathbf{n}_T > 0$ are assigned to hemisphere H_1, while all other particles are in H_2. "Jet broadening" measures the summed scalar momentum transverse to the thrust axis in one of the hemispheres while the hemisphere mass is the invariant mass of the hemisphere,

$$B_N = \min_{i=1,2} \frac{\sum_{\mathbf{p}_k \in H_i} |\mathbf{p}_k \times \mathbf{n}_T|}{2 \sum_k |\mathbf{p}_k|} \tag{4.43}$$

$$\rho_L = \frac{1}{s} \cdot \min_{i=1,2} \left(\sum_{\mathbf{p}_k \in H_i} p_k \right)^2 . \tag{4.44}$$

These four-jet event shape variables are intimately connected to their three-jet event shape counterparts, the wide jet broadening and heavy hemisphere mass,

$$B_W = \max_{i=1,2} \frac{\sum_{\mathbf{p}_k \in H_i} |\mathbf{p}_k \times \mathbf{n}_T|}{2 \sum_k |\mathbf{p}_k|} \tag{4.45}$$

$$\rho_H = \frac{1}{s} \cdot \max_{i=1,2} \left(\sum_{\mathbf{p}_k \in H_i} p_k \right)^2 \tag{4.46}$$

that have the property of exponentiation (see Section 4.3 and References [59, 79]).

4.5.2   Coherent Branching

The coherent branching formalism allows the resummation of soft and collinear logarithms due to the emission of gluons from a hard parton. As a specific example, let us consider the jet mass distribution $J^a(Q, k^2)$ as the probability of producing a final state jet with invariant mass k^2 from a parent parton a produced in a hard

process at the scale Q^2. For an initial quark this is [92]

$$J^q(Q^2, k^2) = \delta(k^2) + \int\limits_0^{Q^2} \frac{d\tilde{q}^2}{\tilde{q}^2} \int\limits_0^1 dz\, \Theta(z^2(1-z)^2\tilde{q}^2 - Q_0^2) P^{qq}[\alpha_s(z(1-z))\tilde{q}^2), z] \quad (4.47)$$

$$\times \left[\int\limits_0^\infty dq^2 \int\limits_0^\infty dk'^2 \delta\left(k^2 - z(1-z)\tilde{q}^2 - \frac{k'^2}{z} - \frac{q^2}{1-z}\right) J^q(z^2\tilde{q}^2, k'^2) J^g((1-z)^2\tilde{q}^2, q^2) \right.$$

$$\left. - J^q(\tilde{q}^2, k^2) \right]$$

normalised such that

$$\int_0^\infty dk^2 J^a(Q^2, k^2) = 1 \qquad (4.48)$$

and where the next-to-leading order $q \to qg$ splitting kernel in the $\overline{\text{MS}}$ scheme with N_f flavours is

$$P_{qq}[\alpha_s, z] = \frac{\alpha_s}{2\pi} C_F \frac{1+z^2}{1-z}\left(1 + \frac{\alpha_s}{2\pi} K\right) + \dots, \qquad (4.49)$$

where

$$K = C_A\left(\frac{67}{18} - \frac{\pi^2}{6}\right) - \frac{5}{9} N_f. \qquad (4.50)$$

Eq. (4.47) has a simple physical interpretation. The first term is the possibility that the originating parton does not emit any radiation. The transverse momentum of the parton is therefore unchanged. Alternatively, the quark may branch into a quark and a gluon subject to the phase space constraints of two body decay and which subsequently undergo further emissions. This is described by the term proportional to $J^q J^g$. The last term is due to virtual corrections and ensures that soft and collinear singularities are regularised. A similar equation holds for J^g and involves the $g \to gg$ and $g \to q\bar{q}$ splitting kernels. Solving the integral equation for J^a is equivalent to resumming the infrared logarithms. In particular, the probability that an isolated parton a forms a jet with mass less than ρQ^2 is given by

$$\Sigma^a(\rho, \alpha_s(Q)) = \int_0^{\rho Q^2} dk^2 J^a(Q^2, k^2). \qquad (4.51)$$

In Ref. [92], $\ln(\Sigma_H^a)$ is solved to next-to-leading logarithmic accuracy and Σ_H^a is therefore known to $\mathcal{O}(\alpha_s^n L^n)$.
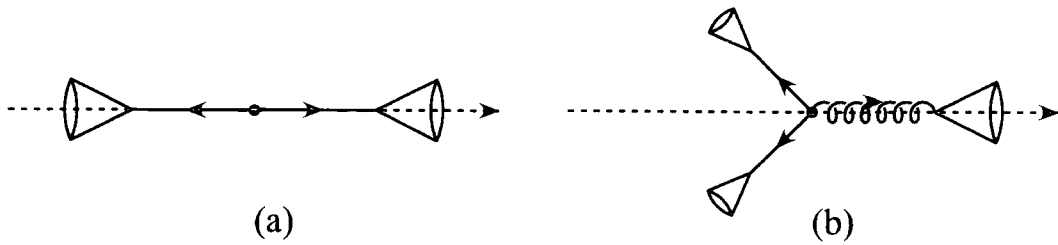
Figure 4.6: Event pictures of (a) two-jet configurations from quark-antiquark final states and (b) three-jet configurations originating from $q\bar{q}g$ events where the gluon is the hardest parton. The cones represent coherent soft and collinear gluon emission. The thrust axis is denoted by a dashed line.

Similarly we can define the function $T^a(Q, \mathbf{k}_t; p_t)$ [59] which describes the distribution of the summed scalar transverse momentum p_t in a jet of parton type a produced with vector transverse momentum $\mathbf{k}_t$, at scale Q. The structure is identical to Equation (4.47).

4.5.3   The Probabilistic Interpretation

We can apply the coherent branching formalism to event shapes in the following schematic way illustrated in Figure 4.6. The underlying configuration in e^+e^- annihilation is the production of a quark-antiquark pair aligned with the thrust axis (Figure 4.6(a)). A fraction r_2 of the events have this structure where

$$r_2 = 1 + \mathcal{O}(\alpha_s). \tag{4.52}$$

Each parton then undergoes soft and collinear gluon emission (denoted by the open cone at the head of the parton). This contribution describes small angle and soft emission accurately in *two-jet-like* events when B_W and ρ_H are small and gives rise to the exponentiated first term in Equation (4.15). However, it does not describe the possibility of wide angle gluon emission shown in Figure 4.6(b) where the gluon is the hardest parton. This correspond to region ③ of Figure 4.3. This *three-jet-like* matrix element correction is not logarithmically enhanced at $\mathcal{O}(\alpha_s)$ and produces a correction given by

$$R_L^{(3)} = C_F \frac{\alpha_s}{2\pi} \int \mathrm{d}x_g \left[\frac{4 - 4x_g + 4x_g^2}{x_g} \ln\left(\frac{2x_g - 1}{1 - x_g}\right) - 6x_g + 4 \right] \mathscr{S}(x_g Q) + \mathcal{O}(\alpha_s^2). \tag{4.53}$$

The function $\mathscr{S}(x_g Q)$ represents the subsequent showering of the hard gluon. This will have a non-trivial dependence on the energy fraction x_g, setting the initial scale for the branching. In this configuration the gluon energy fraction will be in the region $\frac{2}{3} \leq x_g \leq 1$. Taking the approximation $x_g = 1$ enables the factorisation of the fraction of events, r_3,

$$R_L^{(3)} = r_3\,\mathscr{S}(Q) + \mathcal{O}(\alpha_s^2), \qquad (4.54)$$

where at $\mathcal{O}(\alpha_s)$

$$\begin{aligned} r_3 &= \frac{\alpha_s}{2\pi} C_F \left(2\ln(2)^2 - \frac{5}{4}\ln(3) + 4\mathrm{Li}_2\left(-\frac{1}{2}\right) + \frac{\pi^2}{3} - \frac{1}{6} \right) \\ &\sim \frac{\alpha_s}{2\pi} C_F\,(0.917)\,. \end{aligned} \qquad (4.55)$$

The thrust axis is now aligned with the gluon and the values of B_W and ρ_H are determined by the energies and angular separation of the quark and antiquark. In general B_W and ρ_H will not be small and in fact, the phase space for small B_W and ρ_H configurations is vanishingly small. Therefore, for these observables we can associate the three-jet-like contribution with $D(\lambda, \alpha_s(Q))$ in Equation (4.15). Only the two-jet configuration is logarithmically enhanced and as discussed earlier, the coherent branching algorithm has been used to resum logarithmic terms in the perturbative expansion down to $\mathcal{O}(\alpha_s^n L^n)^3$.

On the other hand, the three jet-like configuration is *not* suppressed for small values of the four-jet variables B_N and ρ_L which are generated by subsequent branching of the gluon. This type of branching engenders leading perturbative contributions of $\mathcal{O}(C_F C_A^{n-1} \alpha_s^n L^{2n-2})$ which can be resummed. Unfortunately in approximating the hard scale at the initiation of the gluon shower, we have spoiled the next-to-leading logarithm terms. This effect will introduce an uncertainty in the fourth tower of logarithms.

Let us first focus on the hemisphere masses. The fraction of events with heavy hemisphere mass less than ρ_H i.e. $k_1^2 < \rho_H Q^2$ and $k_2^2 < \rho_H Q^2$ is given entirely by

---

[3]We note that in solving the integral equations for the jet functions, certain approximations may need to be made that may limit the number of logarithmic terms that are actually resummed. For example, if the coefficient G_{22} is not determined accurately, then terms of $\mathcal{O}(\alpha_s^n L^{2n-2})$ are not exactly resummed. Dokshitzer et al [93] have recently re-studied the wide jet broadening and found that in order to obtain G_{22} correctly requires a careful treatment of quark recoil.

the two jet contribution (with $r_2 = 1 + \mathcal{O}(\alpha_s)$)

$$R_H(\rho_H, \alpha_s(Q)) \underset{\rho_H \ll 1}{=}$$

$$r_2 \Bigg(\int\limits_0^\infty dk_1^2 \int\limits_0^\infty dk_2^2 \, J^q(Q^2, k_1^2) \, J^q(Q^2, k_2^2) \, \Theta(\rho_H Q^2 - k_1^2) \, \Theta(k_1^2 - k_2^2)$$

$$+ \int\limits_0^\infty dk_1^2 \int\limits_0^\infty dk_2^2 \, J^q(Q^2, k_1^2) \, J^q(Q^2, k_2^2) \, \Theta(\rho_H Q^2 - k_2^2) \, \Theta(k_2^2 - k_1^2) \Bigg), \quad (4.56)$$

and where the constraint that $\rho_H \ll 1$ has suppressed the three and more jet contributions. Following the steps of Ref. [59], we can rewrite this formula using the phase space restrictions as

$$R_H(\rho_H, \alpha_s(Q)) \underset{\rho_H \ll 1}{=} r_2 \, [\Sigma_H^q(\rho_H, \alpha_s(Q))]^2, \quad (4.57)$$

where

$$\Sigma_H^q(\rho_H, \alpha_s(Q)) = \int\limits_0^{\rho_H Q^2} dk^2 \, J^q(Q^2, k^2). \quad (4.58)$$

The $\mathcal{O}(\alpha_s)$ contribution to r_2 is fixed by requiring that when ρ_H reaches its maximum value of 1/3 for three parton configurations, $R_H = 1 + \mathcal{O}(\alpha_s^2)$.

On the other hand, the fraction of events with light hemisphere mass less than ρ_L receives contributions from both two and three-jet configurations. For the two jet case, $k_1^2 < \rho_L Q^2$ and $k_2^2 > k_1^2$ and vice versa, while the three-jet contribution arises when $k_g^2 < \rho_L Q^2$. In the small ρ_L limit, what happens in the quark-antiquark hemisphere is irrelevant and k_1^2 and k_2^2 are unbounded. Altogether we have,

$$R_L(\rho_L, \alpha_s(Q)) \underset{\rho_L \ll 1}{=}$$

$$r_2 \Bigg(\int\limits_0^\infty dk_1^2 \int\limits_0^\infty dk_2^2 \, J^q(Q^2, k_1^2) \, J^q(Q^2, k_2^2) \, \Theta(\rho_L Q^2 - k_1^2) \, \Theta(k_2^2 - k_1^2)$$

$$+ \int\limits_0^\infty dk_1^2 \int\limits_0^\infty dk_2^2 \, J^q(Q^2, k_1^2) \, J^q(Q^2, k_2^2) \, \Theta(\rho_L Q^2 - k_2^2) \, \Theta(k_1^2 - k_2^2) \Bigg)$$

$$+ \; r_3 \; \int_0^\infty dk_g^2 J^g(Q^2, k_g^2) \Theta(\rho_L Q^2 - k_g^2) \int_0^\infty dk_1^2 J^q(Q^2, k_1^2) \int_0^\infty dk_2^2 J^q(Q^2, k_2^2) \quad (4.59)$$

where to $\mathcal{O}(\alpha_s^2)$ the two jet fraction r_2 is given by,

$$r_2 = 1 - r_3 + \mathcal{O}(\alpha_s^2). \quad (4.60)$$

Simplifying the phase space constraints and utilising the normalisation condition (4.51), we find

$$
R_L(\rho_L, \alpha_s(Q)) \underset{\rho_L \ll 1}{=} r_2 \left(2 \Sigma_H^q(\rho_L, \alpha_s(Q)) - [\Sigma_H^q(\rho_L, \alpha_s(Q))]^2 \right)
$$
$$
+ r_3 \Sigma_H^g(\rho_L, \alpha_s(Q)), \tag{4.61}
$$

where Σ_H^g is defined as an integral over the gluon jet mass distribution J^g in a similar way to Equation (4.58). The functions that resum the logarithms for the light hemisphere mass are the same as those that resum the logarithms for the heavy hemisphere mass. Now however, exponentiation in its purest form is spoiled because the final result is a sum of terms.

The analysis for the narrow jet broadening proceeds in the same way. We find that R_N, the probability of finding an event with a narrow jet broadening less than B_N, is given by [94],

$$
R_N(B_N, \alpha_s(Q)) \underset{B_N \ll 1}{=} r_2 \left(2 \Sigma_W^q(B_N, \alpha_s(Q)) - [\Sigma_W^q(B_N, \alpha_s(Q))]^2 \right)
$$
$$
+ r_3 \Sigma_W^g(B_N, \alpha_s(Q)), \tag{4.62}
$$

where the probability of obtaining a jet with summed scalar transverse momentum p_t with respect to the jet axis less than $2BQ$ starting from a parton of type a, Σ_W^a, is given by,

$$
\Sigma_W^a(B, \alpha_s(Q)) = \int_0^{2BQ} T^a(Q, 0, p_t) dp_t. \tag{4.63}
$$

4.5.4   All-Orders Resummation of Large Logarithms

In this section we discuss the all-orders resummation of leading logarithms $\mathcal{O}(\alpha_s^n L^{2n})$ as well as sub-leading logarithms down to $\mathcal{O}(\alpha_s^n L^{2n-3})$. As discussed in the previous section, a resummation of this order is achieved by considering both two-jet and three-jet configurations. From Equations. (4.61) and (4.62), we see that to determine R_L and R_N requires knowledge of Σ_H^a and Σ_W^a respectively. Both of these functions have the exponentiated form (4.15) and the exponents have been solved to single logarithmic accuracy. Σ_H^a is therefore known to $\mathcal{O}(\alpha_s^n L^n)$.

Explicit expressions for Σ_H valid to this order are given in [92] and, introducing the renormalisation scale dependence in the standard manner and dropping the

parton index, we reproduce them here for illustrative purposes,

$$
\Sigma_H(\rho, \alpha_s(\mu), \tfrac{Q^2}{\mu^2}) = \frac{\exp[\mathcal{F}(\alpha_s(\mu), L)]}{\Gamma[1 - \mathcal{S}(\alpha_s(\mu), L)]}
$$
$$
= \frac{\exp[L f_1(x) + f_2(x) + x^2 f_1'(x) \ln(\mu^2/Q^2)]}{\Gamma[1 - f_1(x) - x f_1'(x)]} + \mathcal{O}(\alpha_s^n L^{n-1})
\tag{4.64}
$$

where

$$
L = \ln(1/\rho), \qquad x = \beta_0 \alpha_s(\mu) L.
\tag{4.65}
$$

The functions f_1, f_2 and f_1' are

$$
f_1(x) = -\frac{A^{(1)}}{2\pi \beta_0 x} \left[(1 - 2x) \ln(1 - 2x) - 2(1 - x) \ln(1 - x) \right],
\tag{4.66}
$$

$$
\begin{aligned}
f_2(x) = {}& -\frac{A^{(2)}}{2\pi^2 \beta_0^2} \left[2 \ln(1 - x) - \ln(1 - 2x) \right] \\
& + \frac{B^{(1)}}{2\pi \beta_0} \ln(1 - x) - \frac{A^{(1)} \gamma_E}{\pi \beta_0} \left[\ln(1 - x) - \ln(1 - 2x) \right] \\
& - \frac{A^{(1)} \beta_1}{2\pi \beta_0^3} \left[\ln(1 - 2x) - 2 \ln(1 - x) + \frac{1}{2} \ln^2(1 - 2x) - \ln^2(1 - x) \right],
\end{aligned}
\tag{4.67}
$$

$$
f_1'(x) = \frac{A^{(1)}}{2\pi \beta_0 x^2} \left[\ln(1 - 2x) - 2 \ln(1 - x) \right],
\tag{4.68}
$$

with

$$
\beta_0 = \frac{11 C_A - 2 N_f}{12\pi}, \qquad \beta_1 = \frac{17 C_A^2 - 5 C_A N_f - 3 C_F N_f}{24\pi^2}.
\tag{4.69}
$$

For quarks,

$$
A^{(1)} = C_F, \qquad A^{(2)} = \frac{1}{2} C_F K, \qquad B^{(1)} = -\frac{3}{2} C_F,
\tag{4.70}
$$

while for gluons,

$$
A^{(1)} = C_A, \qquad A^{(2)} = \frac{1}{2} C_A K, \qquad B^{(1)} = -2\pi \beta_0,
\tag{4.71}
$$

with K given by Equation (4.50).

Altogether Equations (4.64) to (4.71) are sufficient to determine Σ_H^q and Σ_H^g to $\mathcal{O}(\alpha_s^n L^n)$. However, this does not determine R_N of Equation (4.62) to the same

order due to the approximations made in categorising two and three-jet configurations before showering. In separating these events, we have introduced an error in the resummation of the showering off the hard gluon at next-to-leading logarithm level. The expression for R_N therefore correctly sums to all orders in the strong coupling, α_s, only the leading three towers of large logarithms from $\mathcal{O}(\alpha_s^n L^{2n})$ down to $\mathcal{O}(\alpha_s^n L^{2n-2})$.

Because knowledge of Σ_H is currently limited to $\mathcal{O}(\alpha_s^n L^n)$, we can only correctly resum logarithms down to $2n - 2 \geq n$ or equivalently $n \geq 2$. The resummed formula (4.61) does not include the $\mathcal{O}(\alpha_s^2 L)$ term (just as the analogous formulae for resumming three jet variables do not include the $\mathcal{O}(\alpha_s^2 L)$ term) present in the lowest order perturbative coefficient. Similarly, it does not produce the $\mathcal{O}(\alpha_s^3 L^3)$ to $\mathcal{O}(\alpha_s^3 L)$ terms that occur in the next-to-leading order perturbative coefficient. The perturbative calculation provides the α_s^2 and α_s^3 contributions exactly and therefore the most significant omitted term is $\mathcal{O}(\alpha_s^4 L^5)$.

Precisely the same discussion applies to the narrow jet broadening. Using the coherent branching formalism, Σ_W has been determined to $\mathcal{O}(\alpha_s^n L^n)$ accuracy and Catani et al (CTW) have provided analogous expressions for Σ_W that are given in [59]. However, in doing so certain simplifying approximations concerning the recoil transverse momentum have been made. As a consequence, the terms of $\mathcal{O}(\alpha_s^n L^n)$ are incomplete. Dokshitzer and collaborators [93] have found that treating the quark recoil more carefully causes the CTW result for Σ_W to be adjusted by a multiplicative factor. This generates the correct $\alpha_s^n L^n$ terms. The final form for Σ_W is given in Appendix B. Inserting the recoil-corrected form for Σ_W in the resummed expression for R_N (4.62) again allows resummation of the first three towers of logarithms, i.e. down to $\mathcal{O}(\alpha_s^n L^{2n-2})$ [94](see Figure 4.7).

4.5.5 Numerical Results

As usual, the resummed result contains part of the fixed order perturbative contribution and the overlap must be removed by matching. This is done by expanding the resummed result as a series in the strong coupling constant and explicitly removing the terms corresponding to the fixed order calculations. This can be achieved in several ways, of which R matching and $\ln(R)$ matching are the most common. In the R matching scheme, the coefficients of each of the unsummed logarithms
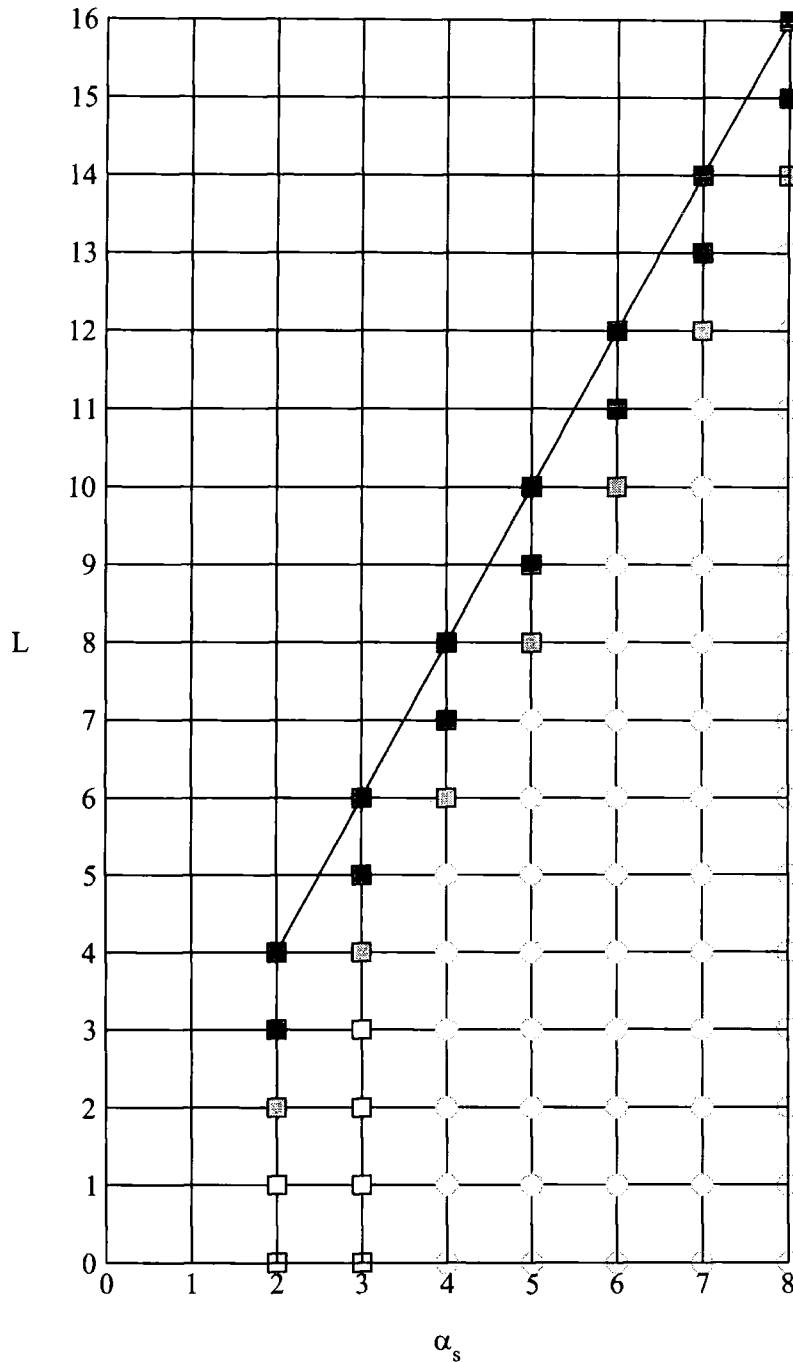
Figure 4.7: The towers of infrared logarithms appearing in the four-jet event shape rates. The resummation includes all terms down to $\mathcal{O}(\alpha_s^n L^{2n-2})$ (three towers) denoted by filled squares and complete $\mathcal{O}(\alpha_s^2, \alpha_s^3)$ contributions from fixed order denoted by the empty squares. All other terms are incomplete and denoted by empty circles. The black filled squares denote terms generated purely in the two-jet limit. The grey filled squares denote contibutions from soft gluons showering off a hard gluon.

present in the fixed order perturbative coefficients must be numerically extracted. For the four-jet event shape observables discussed here, this corresponds to determining the coefficient of $\alpha_s^2 L$ from the lowest order perturbative contribution and the coefficients of $\alpha_s^3 L^3$ to $\alpha_s^3 L$ from the next-to-leading order contribution. This is impractical. However, in the more commonly used $\ln(R)$ matching scheme, it is assumed that the fixed order result exponentiates and therefore it is not necessary to make this extraction because any logarithmic terms remaining after subtracting the overlap from the fixed order contribution are exponentially suppressed. We therefore employ the $\ln(R)$ matching procedure.

We expect that at large values of the observable λ, the resummed result is dominated by the fixed order calculation. However, the resummed expressions (4.61) and (4.62) valid in the small ρ_L and B_N limits do not contain information about the kinematic endpoints of the distributions. To ensure that the resummed result vanishes at the endpoint we make the substitution

$$\frac{1}{\lambda} \to \frac{1}{\lambda} - \frac{1}{\lambda^{\text{max}}} + 1, \tag{4.72}$$

where λ^{max} corresponds to the endpoint of the distribution at the accuracy of the fixed order calculation. We use $\rho_L^{\text{max}} = 0.167$ and $B_N^{\text{max}} = 0.204$.

Numerical results for the light hemisphere mass and for the narrow jet broadening are shown in figures 4.8 and 4.9 respectively. Throughout we set $\mu = Q = M_Z$ and use $\alpha_s(M_Z) = 0.118$ corresponding to the current world average. The next-to-leading order result which diverges at small values of the event shapes is taken from [48]. Although formally the three-jet like contribution is needed to resum terms of $\mathcal{O}(\alpha_s^n C_F C_A^{n-1} L^{2n-2})$, we find that it is numerically insignificant, mainly due to the smallness of r_3.

Figures 4.8 and 4.9 show that the resummations are extremely important for $\rho_L < 0.01$ and $B_N < 0.02$. Rather than the divergent fixed order prediction, we have the more physical resummed result that the probability of finding events with no radiation (very small values of ρ_L and B_N) is vanishingly small. For ρ_L, the peak position occurs at $\rho_L = 0.01$ with a height of 0.34, while for B_N the peak occurs at $B_N = 0.02$ with a value of 0.42. At larger values, the resummation changes the NLO prediction by a more moderate amount indicating that uncalculated higher order corrections are under control. At very large values of λ, the resummed and
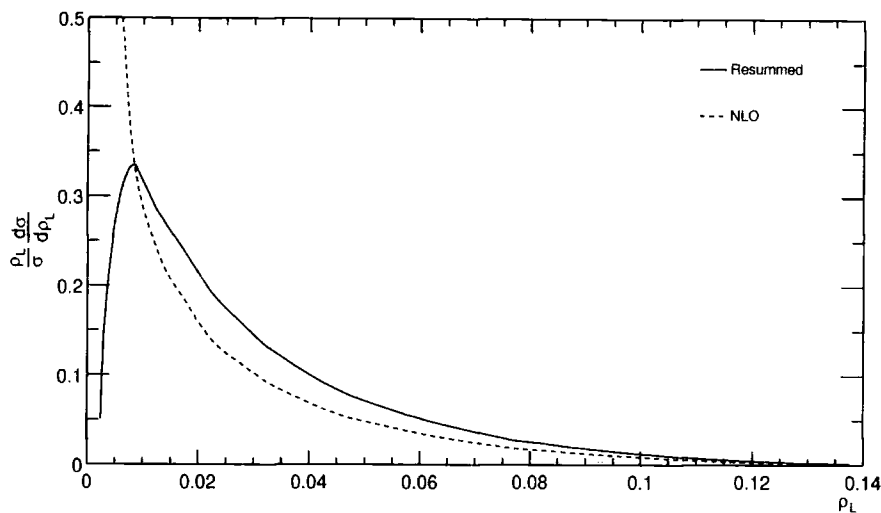
Figure 4.8: The resummed (solid) and fixed order NLO (dashed) predictions for the light hemisphere mass distribution $\frac{\rho_L}{\sigma}\frac{d\sigma}{d\rho_L}$ at $\mu = Q = M_Z$.

NLO predictions coincide because of the modification (4.72).

The infrared resummation significantly improves the perturbative prediction for the event shape observable. However, when comparing with experimental data we should be aware that important non-perturbative hadronisation corrections are present. The effect of hadronisation on the distribution is to shift the value of the observable away from the two-jet region,

$$\lambda \to \lambda + \lambda_{\mathrm{NP}}, \tag{4.73}$$

where the non-perturbative correction depends on the typical hadron scale $\mathcal{O}(1\ \mathrm{GeV})$ and is suppressed by a power of Q. In principle these power corrections can be estimated using the dispersive approach of Ref. [37, 95], where a non-perturbative parameter μ_I is introduced to describe the running of α_s in the infrared region. For the associated three jet variables, the non-perturbative corrections are typically estimated to be $\mathcal{O}(1\ \mathrm{GeV}/Q)$ for ρ_H [37, 95] and $\mathcal{O}(0.3\ \mathrm{GeV}\ln(1/B_W)/Q)$ for B_W [96] and arise through the hadronisation of one of the two jets in the event. Because the four-jet event shapes are largely related to what happens in the second jet, we might expect that the hadronisation corrections are similar. To illustrate the potential effects of hadronisation in the four-jet event shapes, we just transfer these
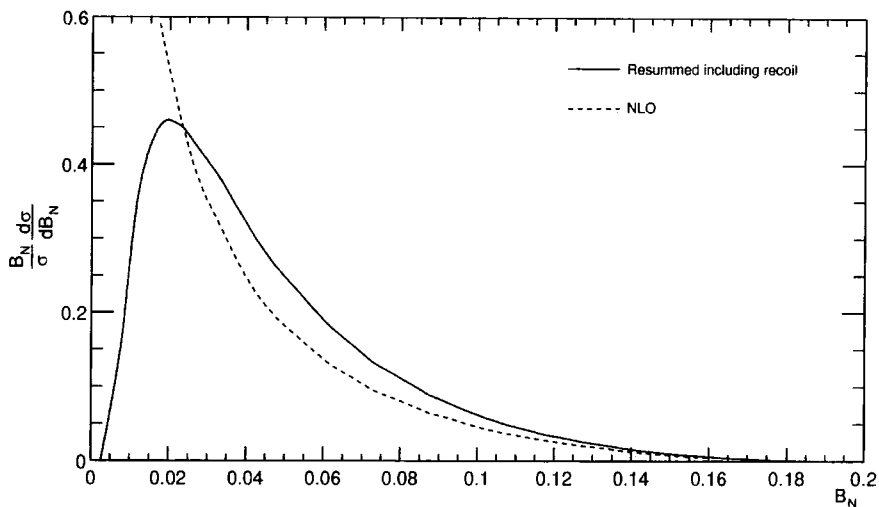
Figure 4.9: The resummed (solid) and fixed order NLO (dashed) predictions for the narrow jet broadening distribution $\frac{B_N}{\sigma}\frac{d\sigma}{dB_N}$ at $\mu = Q = M_Z$.

corrections directly so that,

$$\rho_L \;\to\; \rho_L + \frac{1\;\text{GeV}}{Q}, \tag{4.74}$$

$$B_N \;\to\; B_N + \frac{0.3\;\text{GeV}\,\ln(1/B_N)}{Q}. \tag{4.75}$$

The simplified hadronisation correction applied to the distributions for the light hemisphere mass and narrow jet broadening is shown in figures 4.10 and 4.11 respectively. There are two effects. First the distribution is shifted to the right by an amount λ_{NP} and second, the distribution is rescaled by a factor $(\lambda + \lambda_{\mathrm{NP}})/\lambda$. In the region of the turnover where λ is of the same order as λ_{NP} there is an enhancement of almost 100%. We see that the peak position of the ρ_L distribution now occurs at $\rho_L \sim 0.022$ with a height of 0.8, while the peak of the B_N distribution has a height of 0.8. The hadronisation correction is smaller at larger values of λ.

For comparison, we also show the charged hadron data collected by the DELPHI Collaboration [66] at the Z resonance. We see remarkable agreement (strikingly so in view of the simplified hadronisation correction applied here). The only discrepancy is at very small values of $\lambda < \lambda_{\mathrm{NP}}$ where individual hadrons in the light/narrow hemisphere will significantly affect the value of λ. We do not expect to successfully describe such events.
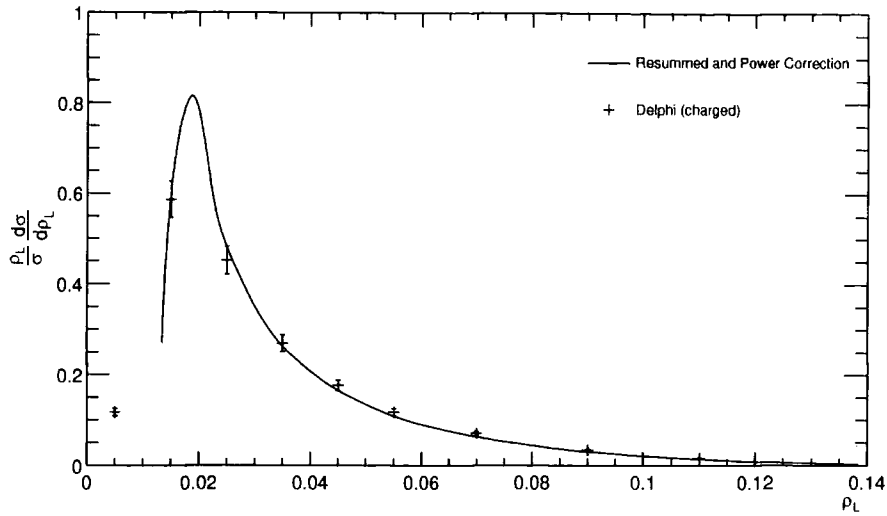
Figure 4.10: The resummed prediction for the light hemisphere mass distribution $\frac{\rho_L}{\sigma} \frac{d\sigma}{d\rho_L}$ at $Q = M_Z$ modified by a non-perturbative power correction $\rho_L \rightarrow \rho_L + 1 \text{ GeV}/Q$. For comparison, we also show the charged hadron data collected at the Z resonance by the DELPHI collaboration [66].
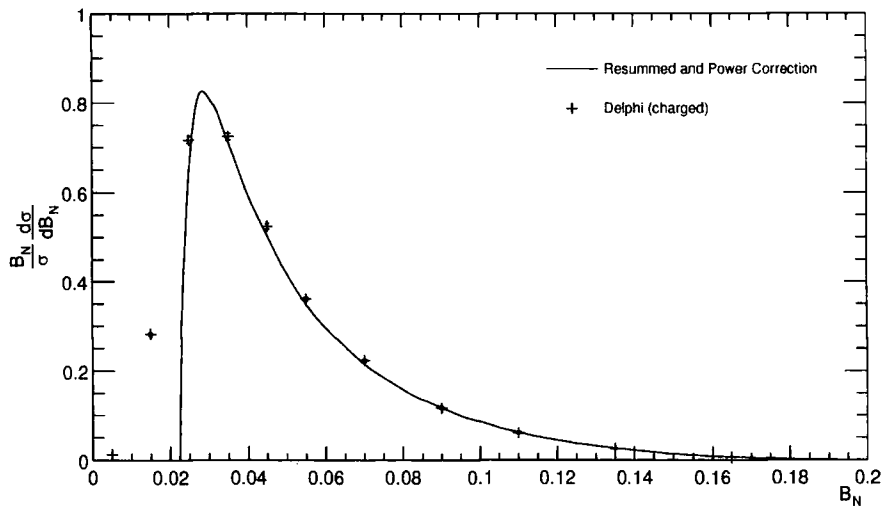

Figure 4.11: The resummed prediction for the narrow jet broadening distribution $\frac{B_N}{\sigma} \frac{d\sigma}{dB_N}$ at $Q = M_Z$ modified by a non-perturbative power correction $B_N \rightarrow B_N + 0.3 \text{ GeV} \ln(1/B_N)/Q$. For comparison, we also show the charged hadron data collected at the Z resonance by the DELPHI collaboration [66].

4.6 Renormalisation Group Improvement of Next-To-Leading Logarithm Resummations

In this section we address the problem of applying the renormalisation group improved perturbation theory to the infrared logarithm resummation. We have already witnessed the difficulties in extending the NLO analysis of Chapter 3, towards the exclusive phase space boundary where the infrared logarithms grow large. An initial attempt was made to incorporate the infrared logarithm resummation into the CORGI approach. The RG-improved perturbation theory of CORGI permits higher order terms to be incorporated via a straightforward algebraic manipulation. In contrast, the EC formalism requires the resummed formula to be inverted in order to obtain the EC scheme invariants (ρ_n) and then numerically integrated to generate the higher order contributions. Unfortunately when reformulated as a CORGI perturbation series, the final result is no longer trustworthy, displaying even erratic behaviour. This can attributed to the parameter r_1 which plays such a critical rôle in RG-improved perturbation theory. The first step is always to rewrite the series in the form of a dimensionless quantity, requiring r_1 to become a ratio of terms. While it is true that the tree-level coefficient will not be renormalisation scale dependent, it will in general have a dependence on the infrared parameter of the semi-inclusive quantity. This is effectively an additional scale corresponding to $Q_0 = \sqrt{(y_{cut})}Q$ for jet rates, $M_x = \sqrt{(\rho_x)}Q$ for jet masses, etc. When the behaviour of the fixed order coefficients is weakly dependent on the variation of the infrared cut, we may safely approximate it as a constant. This was performed in the analysis of Chapter 3 by imposing the flatness criterion upon r_1. In infrared logarithm resummations, the behaviour of the coefficients upon the cut is crucial in order to ensure the so-called "turn-over" of perturbation theory in the large logarithm limit. Meanwhile RG-improvement attempts to include the predictable contributions of r_1 appearing in all higher order coefficients. In resumming the r_1 terms we must ensure that we do not resultantly impact upon the infrared logarithm resummation. An alternative to the CORGI formalism, is to resum all the logarithms inside the $\mathcal{G}$ function of Equations (2.65) and (2.66). This was performed for the simple case of the two-jet rate in [28].

4.7 Summary

We began this chapter by illustrating the source of the large infrared logarithms, anticipated earlier, through the simple example of the 1-thrust distribution. We demonstrated how it is possible to calculate the dominating terms as we approach the exclusive boundary, then providing the phase space factorises in the appropriate manner, perform an all-orders resummation. This was practically applied to the four-jet rate where all logarithms to a next-to-leading approximation were calculated and an analytic expression given. We then considered the case of two four-jet event shape variable distributions, the "light hemisphere mass" and the "narrow jet broadening". In these cases we detailed the procedure to resum the first three towers of logarithms and matched these results via a "ln-R matching prescription" to the fixed order NLO calculation. We then applied a very simplistic model for power corrections to the event shape variables and for illustration compared with the LEP data of the DELPHI collaboration. A remarkably good agreement was found.

We anticipate that this improved theoretical description of the four-jet event shape distributions can be combined with a more sophisticated hadronisation correction based on the dispersive approach of References [37, 95]. This will yield a theoretical description of the ρ_L and B_N distributions that is on a similar footing with the well studied three-jet event shape variables, $1 - T$, ρ_H, B_W etc. The data from LEP can then be used to further test the structure of QCD.

Chapter 5

Conclusions

In this thesis we have focused on a number of aspects of Quantum Chromodynamics. Renormalisation scale and scheme dependence, large kinematic logarithms and to a lesser extent non-perturbative power corrections, have all been considered. Underpinning this study has been the attempt to provide a better understanding of QCD through a measurement of the single fundamental parameter, $\Lambda_{\overline{MS}}$ or $\alpha_s(M_z)$. A non-perturbative description of QCD is currently beyond our grasp, forcing us to resort to perturbative techniques and attempts at modeling non-perturbative effects. In doing so, we encounter numerous complexities, not least of which is the difficulty in calculating terms beyond the first few orders of perturbation theory. In most cases a NLO approximation is the extent of our current knowledge. Termination of the perturbation series brings its own problems in the guise of a renormalisation scale and scheme dependence. We saw that in order to correctly treat the energy dependence of observables, we *must* resum the μ logarithms to all orders in the coupling. Analysing the Q-dependence we see that it is even possible to eliminate the unphysical coupling parameter altogether linking the fundamental scale, Λ directly with experimentally measured quantities through a perturbative calculation.

We have demonstrated a procedure for resumming the unphysical renormalisation scale dependence to all-orders enabling the extraction of $\Lambda_{\overline{MS}}$ from jet rates, event shape variable distributions and energy-weighted cross sections when considered away from the kinematic extremes. The influence of hadronisation was seen to be significant and the modeling of its effects reduced the scatter of extracted $\Lambda_{\overline{MS}}$ values appreciably. We found values that ranged from $\sim 50\text{MeV}$ to $\sim 200\text{MeV}$. The scatter in these values should then be attributed to the uncalculated higher order

corrections.

With the availability of experimental data at different centre-of-mass energies we may then test the "RG-Improved Perturbation Theory". We would expect to see a convergence of the $\Lambda_{\overline{MS}}$ values as we approach asymptotic energy limits. The distribution of 1-thrust was investigated and reflects this behaviour as expected. We also provided a framework for incorporating higher order contributions (N^nNLO) and power corrections in a renormalisation scheme invariant manner. This permitted an investigation of the NNLO and leading power correction terms to the 1-thrust distribution. Before any reliable quantitative conclusions may be drawn, it is necessary to obtain accurate data samples at a wide range of energies. This mechanism can be used for estimating the importance of higher order corrections, taking the place of varying the unphysical renormalisation scale μ by an arbitrary amount.

It is possible to extend the ideology of complete renormalisation group improvement to other areas of perturbative QCD where an unphysical scale enters. An example already realised is in the arbitrary factorisation scale dependence of moments of structure functions in deep inelastic leptoproduction [34]. Here an analogous situation takes place where in addition to the μ and c_n renormalisation scheme parameters there will be a set of factorisation scheme parameters, M and d_n. Once again, a resummation of the ultraviolet logarithms results in the dependence on the unphysical scales disappearing.

Throughout this thesis we have taken the massless approximation for light quarks and made use of the decoupling theorem to analyse the intermediate energy region, in particular at a centre of mass energy of M_Z. A natural extension to this work is to consider the effect of non-zero quark masses. In this case, there will still be a fundamental quantity, $\Lambda_{\overline{MS}}$ of the theory, defined in the usual manner by integrating the β-function, but this will now have an additional dependence on the quark masses.

Furthermore, in considering higher order corrections to semi-inclusive quantities, we have seen how the coupling is enhanced by large infrared logarithms in the proximity of the exclusive boundary in phase space. A fixed order approximant is then no longer reliable and a resummation of the dominant logarithms must be performed to all orders. New results were obtained in this thesis of an analytic expression for the four-jet rate calculated to next-to-leading logarithm level in the perturbative expansion. We also presented a resummed calculation of the distribution of

the four-jet observables "light hemisphere mass" and "narrow jet broadening". Finally, we considered the prospects for combining the infrared resummations with the RG-improvement.

Appendix A

Splitting Functions

Altarelli-Parisi Splitting Kernels

We quote the Altarelli-Parisi Splitting Kernels at NLO.

Unregularised

$$\hat{P}_{q \to gq} = \hat{P}_{gq}[\alpha_s(k), z] = C_F \frac{\alpha_s(k)}{2\pi} \left[\frac{1 + (1-z)^2}{z} \right] + \frac{C_F K}{2} \left(\frac{\alpha_s(k)}{\pi} \right)^2 \left[\frac{1}{z} \right] \quad (A.1)$$

$$\hat{P}_{g \to q\bar{q}} = \hat{P}_{qg}[\alpha_s(k), z] = T_R N_f \frac{\alpha_s(k)}{2\pi} \left[z^2 + (1-z)^2 \right] \quad (A.2)$$

$$\hat{P}_{q \to qg} = \hat{P}_{qq}[\alpha_s(k), z] = C_F \frac{\alpha_s(k)}{2\pi} \left[\frac{1 + z^2}{1 - z} \right] + \frac{C_F K}{2} \left(\frac{\alpha_s(k)}{\pi} \right)^2 \left[\frac{1}{1 - z} \right] \quad (A.3)$$

$$\hat{P}_{g \to gg} = \hat{P}_{gg}[\alpha_s(k), z] = 2 C_A \frac{\alpha_s(k)}{2\pi} \left[\frac{z}{1 - z} + \frac{1 - z}{z} + z(1 - z) \right] \quad (A.4)$$
$$+ \frac{C_A K}{2} \left(\frac{\alpha_s(k)}{\pi} \right)^2 \left[\frac{1}{z(1 - z)} \right]$$

where the coefficient, K is dependent on the renormalisation sheme and in the $\overline{\text{MS}}$ scheme is given by

$$K = C_A \left(\frac{67}{18} - \frac{\pi^2}{6} \right) - \frac{5}{9} N_f.$$

Note that the factor of N_f is included in $\hat{P}_{qg}$ since a sum is always taken over parton splittings.

Regularised

$$P_{q \to gq} = P_{gq}[\alpha_s(k), z] = C_F \left[\frac{1 + (1 - z)^2}{z} \right] = P_{g\bar{q}}[\alpha_s(k), z] \qquad (A.5)$$

$$P_{g \to q\bar{q}} = P_{qg}[\alpha_s(k), z] = T_R \left[z^2 + (1 - z)^2 \right] \qquad (A.6)$$

$$P_{q \to qg} = P_{qq}[\alpha_s(k), z] = C_F \left[\frac{1 + z^2}{(1 - z)_+} + \frac{3}{2} \delta(1 - z) \right] \qquad (A.7)$$

$$P_{g \to gg} = P_{gg}[\alpha_s(k), z] = 2C_A \left[\frac{z}{(1 - z)_+} + \frac{1 - z}{z} + z(1 - z) \right] \qquad (A.8)$$
$$+ \frac{1}{6}(11C_A - 4n_f T_R) \, \delta(1 - z)$$

where

$$\int_0^1 dx \, \frac{f(x)}{(1 - x)_+} = \int_0^1 dx \, \frac{f(x) - f(1)}{1 - x}$$

for a sufficiently smooth function, $f(x)$.

Appendix B

Σ_W: The Resummed Expression for the Wide Jet Broadening

The final form for Σ_W is given by [93]

$$\Sigma_W(B_W, \alpha_s(\mu^2), \tfrac{Q^2}{\mu^2}) = \left(\frac{2}{\lambda}\right)^{2R'} \cdot \frac{\exp(\mathcal{F}(\alpha_s(\mu^2), L))}{(\Gamma[1 - \mathcal{S}(\alpha_s(\mu^2), L)])^2} \tag{B.1}$$

where $L = \ln(B_W)$,

$$\left(\frac{2}{\lambda}\right)^{2R'} = \left[\int_1^\infty \frac{\mathrm{d}x}{x}\left(\frac{1+x}{4}\right)^{-R'}\right]^2, \tag{B.2}$$

$$\begin{aligned}
\mathcal{F}(\alpha_s(\mu^2), L) = {} & \frac{A^{(1)}}{\pi\beta_0^2\alpha_s}[\ln(1+\omega) - \omega] \\
& + \frac{1}{\pi^2\beta_0^2}\left[C_F\pi\beta_0\ln(\tfrac{Q^2}{\mu^2}) - A^{(2)}\right]\left[\ln(1+\omega) - \frac{\omega}{1+\omega}\right] \\
& - \frac{B^{(1)}}{\pi\beta_0}\ln(1+\omega) + \frac{2A^{(1)}\gamma_E}{\pi\beta_0}\left(\frac{\omega}{1+\omega}\right) \\
& + \frac{A^{(1)}\beta_1}{\pi\beta_0^3}\left[\tfrac{1}{2}\ln^2(1+\omega) + \frac{\ln(1+\omega)}{1+\omega} - \frac{\omega}{1+\omega}\right] \\
& + \mathcal{O}(\alpha_s^{m+1}L^m),
\end{aligned} \tag{B.3}$$

with

$$R' = -\frac{2C_F\alpha_s L}{\pi}\frac{1}{1+2\beta_0\,\alpha_s L} \tag{B.4}$$

$$\mathcal{S}(\alpha_s, L) = \frac{A^{(1)}}{\pi\beta_0}\left[\frac{\omega}{1+\omega}\right] \tag{B.5}$$

and

$$\omega = 2\beta_0\,\alpha_s L \tag{B.6}$$

$$A^{(1)} = C_F, \quad A^{(2)} = \frac{C_F K^{(RS)}}{2}, \quad B^{(1)} = -\frac{3C_F}{2} \tag{B.7}$$

$$\beta_0 = \frac{11C_A - 2N_f}{12\pi}, \quad \beta_1 = \frac{153 - 19N_f}{24\pi^2}, \quad K^{\overline{\text{MS}}} = \left(\tfrac{67}{6} - \tfrac{1}{2}\pi^2 - \tfrac{5}{9}N_f\right) \tag{B.8}$$

Bibliography

[1] J. D. Bjorken, Phys. Rev. **179**, 1547 (1969).

[2] M. E. Peskin and D. V. Schroeder, *An Introduction to Quantum Field Theory*, Reading, USA: Addison-Wesley (1995) 842 p.

[3] T. Muta, *Foundations of Quantum Chromodynamics: An Introduction to Perturbative Methods in Gauge Theories* , Singapore, Singapore: World Scientific (1987) 409 P. (World Scientific Lecture Notes In Physics, 5).

[4] R. K. Ellis, W. J. Stirling, and B. R. Webber, *QCD and Collider Physics* , Cambridge, UK: Univ. Pr. (1996) 435 p. (Cambridge Monographs on Particle Physics, Nuclear Physics and Cosmology: 8).

[5] M. Gell-Mann, Phys. Lett. **8**, 214 (1964).

G. Zweig, CERN-TH-412.

[6] D. E. Groom *et al.*, Eur. Phys. J. **C15**, 1 (2000).

[7] Y. L. Dokshitzer, D. Diakonov, and S. I. Troian, Phys. Rept. **58**, 269 (1980).

[8] W. Bernreuther and W. Wetzel, Zeit. Phys. **C11**, 113 (1981).

[9] T. Kinoshita, J. Math. Phys. **3**, 650 (1962).

T. D. Lee and M. Nauenberg, Phys. Rev. **133**, B1549 (1964).

[10] G. 't Hooft and M. Veltman, Nucl. Phys. **B44**, 189 (1972).

[11] P. M. Stevenson, Phys. Rev. **D23**, 2916 (1981).

[12] Y. L. Dokshitzer, V. A. Khoze, A. H. Mueller, and S. I. Troian, *Basics of Perturbative QCD* , Gif-sur-Yvette, France: Ed. Frontieres (1991) 274 p.

[13] G. 't Hooft, Nucl. Phys. **B61**, 455 (1973).

[14] W. A. Bardeen, A. J. Buras, D. W. Duke, and T. Muta, Phys. Rev. **D18**, 3998 (1978).

[15] W. Celmaster and R. J. Gonsalves, Phys. Rev. **D20**, 1420 (1979).

[16] W. Celmaster and D. Sivers, Phys. Rev. **D23**, 227 (1981).

[17] A. J. Buras, E. G. Floratos, D. A. Ross, and C. T. Sachrajda, Nucl. Phys. **B131**, 308 (1977).

[18] E. Gardi, G. Grunberg, and M. Karliner, JHEP **07**, 007 (1998), hep-ph/9806462.

[19] B. A. Magradze, (1998), hep-ph/9808247.

B. A. Magradze, (1999), hep-ph/9911456.

[20] R. M. Corless, G. H. Gonnet, D. E. G. Hare, D. J. Jeffrey, and D. E. Knuth, Advances in Computational Mathematics **5**, 329 (1996).

[21] S. J. Brodsky, G. P. Lepage, and P. B. Mackenzie, Phys. Rev. **D28**, 228 (1983).

[22] S. J. Brodsky and H. J. Lu, Phys. Rev. **D51**, 3652 (1995), hep-ph/9405218.

[23] G. Grunberg, Phys. Lett. **B95**, 70 (1980).

[24] G. Grunberg, Phys. Rev. **D29**, 2315 (1984).

[25] C. J. Maxwell and J. A. Nicholls, Phys. Lett. **B213**, 217 (1988).

[26] J. Chyla, A. Kataev, and S. Larin, Phys. Lett. **B267**, 269 (1991).

[27] P. M. Stevenson, Ann. Phys. **132**, 383 (1981).

[28] D. T. Barclay, C. J. Maxwell, and M. T. Reader, Phys. Rev. **D49**, 3480 (1994).

[29] S. J. Burby and C. J. Maxwell, In preparation.

[30] V. Gupta, D. V. Shirkov, and O. V. Tarasov, Int. J. Mod. Phys. **A6**, 3381 (1991).

[31] C. J. Maxwell, Phys. Lett. **B409**, 450 (1997), hep-ph/9706365.

[32] C. J. Maxwell, (1998), hep-ph/9809270.

[33] C. J. Maxwell, (1999), hep-ph/9908463.

[34] C. J. Maxwell and A. Mirjalili, Nucl. Phys. **B577**, 209 (2000), hep-ph/0002204.

[35] A. H. Mueller, QCD: 20 Years Later, Aachen.

[36] V. I. Zakharov, Nucl. Phys. **B385**, 452 (1992).

[37] Y. L. Dokshitzer, G. Marchesini, and B. R. Webber, Nucl. Phys. **B469**, 93 (1996), hep-ph/9512336.

[38] W. Bernreuther and W. Wetzel, Nucl. Phys. **B197**, 228 (1982).

[39] K. G. Chetyrkin, B. A. Kniehl, and M. Steinhauser, Phys. Rev. Lett. **79**, 2184 (1997), hep-ph/9706430.

[40] TASSO, R. Brandelik *et al.*, Phys. Lett. **B86**, 243 (1979).

[41] R. K. Ellis, D. A. Ross, and A. E. Terrano, Nucl. Phys. **B178**, 421 (1981). K. Fabricius, I. Schmitt, G. Kramer, and G. Schierholz, Zeit. Phys. **C11**, 315 (1981).

[42] Z. Kunszt, P. Nason, G. Marchesini, and B. R. Webber, Proceedings of the 1989 LEP Physics Workshop, Geneva, Swizterland, Feb 20, 1989.

[43] L. Dixon and A. Signer, Phys. Rev. **D56**, 4031 (1997), hep-ph/9706285.

[44] Z. Nagy and Z. Trocsanyi, Phys. Rev. **D57**, 5793 (1998), hep-ph/9712385.

[45] S. Weinzierl and D. A. Kosower, Phys. Rev. **D60**, 054028 (1999), hep-ph/9901277.

[46] Z. Bern, L. Dixon, D. A. Kosower, and S. Weinzierl, Nucl. Phys. **B489**, 3 (1997), hep-ph/9610370.

[47] Z. Bern, L. Dixon, and D. A. Kosower, Nucl. Phys. **B513**, 3 (1998), hep-ph/9708239.

[48] J. M. Campbell, M. A. Cullen, and E. W. N. Glover, Eur. Phys. J. **C9**, 245 (1999), hep-ph/9809429.

[49] E. W. N. Glover and D. J. Miller, Phys. Lett. **B396**, 257 (1997), hep-ph/9609474.

[50] J. M. Campbell, E. W. N. Glover, and D. J. Miller, Phys. Lett. **B409**, 503 (1997), hep-ph/9706297.

[51] S. Moretti, L. Lonnblad, and T. Sjostrand, JHEP **08**, 001 (1998), hep-ph/9804296.

[52] JADE, S. Bethke *et al.*, Phys. Lett. **B213**, 235 (1988).

[53] N. Brown and W. Stirling, Z. Phys. **C53**, 629 (1992).

[54] S. Catani, Y. L. Dokshitzer, M. Olsson, G. Turnock, and B. R. Webber, Phys. Lett. **B269**, 432 (1991).

[55] S. Bethke, Z. Kunszt, D. E. Soper, and W. J. Stirling, Nucl. Phys. **B370**, 310 (1992).

S. Bethke, Z. Kunszt, D. E. Soper, and W. J. Stirling, (1998), hep-ph/9803267.

[56] S. Brandt, C. Peyrou, R. Sosnowski, and A. Wroblewski, Phys. Lett. **12**, 57 (1964).

E. Farhi, Phys. Rev. Lett. **39**, 1587 (1977).

[57] D. P. Barber *et al.*, Phys. Rev. Lett. **43**, 830 (1979).

[58] L. Clavelli, Phys. Lett. **B85**, 111 (1979).

[59] S. Catani, G. Turnock, and B. R. Webber, Phys. Lett. **B295**, 269 (1992).

[60] G. Parisi, Phys. Lett. **B74**, 65 (1978).

J. F. Donoghue, F. E. Low, and S.-Y. Pi, Phys. Rev. **D20**, 2759 (1979).

[61] C. L. Basham, L. S. Brown, S. D. Ellis, and S. T. Love, Phys. Rev. Lett. **41**, 1585 (1978).

C. L. Basham, L. S. Brown, S. D. Ellis, and S. T. Love, Phys. Rev. **D19**, 2018 (1979).

C. L. Basham, L. S. Brown, S. D. Ellis, and S. T. Love, Phys. Rev. **D17**, 2298 (1978).

[62] Y. Ohnishi and H. Masuda, SLAC-PUB-6560.

[63] SLD, K. Abe *et al.*, Phys. Rev. **D51**, 962 (1995), hep-ex/9501003.

[64] ALEPH, R. Barate *et al.*, Phys. Rept. **294**, 1 (1998).

[65] DELPHI, P. Abreu *et al.*, Eur. Phys. J. **C14**, 557 (2000), hep-ex/0002026.

[66] DELPHI, P. Abreu *et al.*, Z. Phys. **C73**, 11 (1996).

[67] L3, B. Adeva *et al.*, Z. Phys. **C55**, 39 (1992).

[68] OPAL, P. D. Acton *et al.*, Z. Phys. **C55**, 1 (1992).

[69] W. T. Giele and E. W. N. Glover, Phys. Rev. **D46**, 1980 (1992).

[70] T. Sjostrand, Comput. Phys. Commun. **82**, 74 (1994).

[71] G. Marchesini *et al.*, Comput. Phys. Commun. **67**, 465 (1992), hep-ph/9912396.

[72] Private Communication. We are grateful to Phil Burrows (SLD), Siggi Hahn (DELPHI) and Otmar Biebel (OPAL) for generously providing hadronisation corrections for their experimental collaboration's respective data sets.

[73] M. Schmelling, Phys. Scripta **51**, 676 (1995).

[74] TASSO, W. Braunschweig *et al.*, Z. Phys. **C47**, 187 (1990).

[75] MARK-II, A. Petersen *et al.*, Phys. Rev. **D37**, 1 (1988).

[76] AMY, Y. K. Li *et al.*, Phys. Rev. **D41**, 2675 (1990).

[77] S. Bethke, (2000), hep-ex/0004021.

[78] S. Catani, L. Trentadue, G. Turnock, and B. R. Webber, Nucl. Phys. **B407**, 3 (1993).

[79] S. Catani, G. Turnock, and B. R. Webber, Phys. Lett. **B272**, 368 (1991).

[80] S. Catani, G. Turnock, B. R. Webber, and L. Trentadue, Phys. Lett. **B263**, 491 (1991).

[81] B. R. Webber, Phys. Lett. **B339**, 148 (1994), hep-ph/9408222.

G. P. Korchemsky and G. Sterman, Nucl. Phys. **B437**, 415 (1995), hep-ph/9411211.

R. Akhoury and V. I. Zakharov, Phys. Lett. **B357**, 646 (1995), hep-ph/9504248.

R. Akhoury and V. I. Zakharov, Nucl. Phys. **B465**, 295 (1996), hep-ph/9507253.

P. Nason and M. H. Seymour, Nucl. Phys. **B454**, 291 (1995), hep-ph/9506317.

[82] G. Dissertori, Nucl. Phys. Proc. Suppl. **65**, 43 (1998), hep-ex/9705016.

[83] G. Dissertori, Nucl. Phys. Proc. Suppl. **64**, 46 (1998).

[84] A. Bassetto, M. Ciafaloni, and G. Marchesini, Phys. Rept. **100**, 201 (1983).

[85] D. Amati, A. Bassetto, M. Ciafaloni, G. Marchesini, and G. Veneziano, Nucl. Phys. **B173**, 429 (1980).

[86] A. H. Mueller, Phys. Lett. **B104**, 161 (1981).

[87] Ed. A. H. Mueller, *Perturbative Quantum Chromodynamics* , Singapore, Singapore: World Scientific (1989) 614 P. (Advanced Series On Directions In High Energy Physics, 5).

[88] Y. L. Dokshitzer, V. S. Fadin, and V. A. Khoze, Zeit. Phys. **C15**, 325 (1982).

[89] C. N. Lovett-Turner, Phys. Lett. **B329**, 361 (1994), hep-ph/9405211.

[90] S. J. Burby, Phys. Lett. **B453**, 54 (1999), hep-ph/9902305.

[91] J. B. Rosser, Methods of Computation, Brooklyn, US (1948).

[92] S. Catani and L. Trentadue, Phys. Lett. **B217**, 539 (1989).

S. Catani and L. Trentadue, Nucl. Phys. **B327**, 323 (1989).

S. Catani, B. R. Webber, and G. Marchesini, Nucl. Phys. **B349**, 635 (1991).

[93] Y. L. Dokshitzer, A. Lucenti, G. Marchesini, and G. P. Salam, JHEP **01**, 011 (1998), hep-ph/9801324.

[94] S. J. Burby and E. W. N. Glover, In preparation.

[95] Y. L. Dokshitzer and B. R. Webber, Phys. Lett. **B404**, 321 (1997), hep-ph/9704298.

[96] Y. L. Dokshitzer, G. Marchesini, and G. P. Salam, Eur. Phys. J. direct **C3**, 1 (1999), hep-ph/9812487.